FINAL REPORT OF STATISTICAL ANALYSIS

OPTIMIZATION OF LONG TERM OPERATIONS/ LONG TERM MONITORING (LTO/LTM) AT SELECTED GROUNDWATER PLUMES AT THE MASSACHUSETTS MILITARY RESERVATION, CAPE COD, MASSACHUSETTS

CONTRACT NUMBER: DAHA90-94-D-0007
DELIVERY ORDER: TG09
DATA ITEM NO.: 4.3B

Revised
15 January 2000

Submitted to:

HQ AFCEE/ERC
3207 North Road
Brooks AFB TX 78235

Submitted by:

Science Applications International Corporation
1710 Goodridge Drive
McLean, VA 22102

SAIC Project No. 06-5140-04-1510-043

Final Report on the Statistical Analysis of Ground-Water Monitoring Data at the Massachusetts Military Reservation

Kirk Cameron, Ph.D.
MacStat Consulting, Ltd.
December 3, 1999

Project No. SPBN19987806
Contract No. DAHA90-94-D-0007
Delivery No. TG09

Section 1. Background

This document serves as the final report on the statistical analysis of ground-water long-term monitoring (LTM) data at the Massachusetts Military Reservation (MMR) on Cape Cod. The United States Air Force Center for Environmental Excellence (AFCEE) has requested development of a spatial and temporal optimization algorithm for possible use at LTM networks located at MMR, and perhaps other sites around the country.

This report summarizes the analyses conducted and the methodology employed, and includes detailed results from applying the proposed optimization scheme at MMR. Two ground-water plumes at MMR were tested in the current effort to develop statistical approaches for optimizing long-term monitoring networks: FS-12 and Eastern Briarwood. One LTM network (FS-12) monitors a known plume of contamination for which a remediation system has been in place for more than 2 years. The other network (Eastern Briarwood) monitors a low-level plume for which no remediation has yet been required. Both plumes have a moderate to large number of ground-water monitoring wells that have been sampled over a period of years.

Successful application of the optimization algorithm (leading to potentially significant savings in monitoring costs) at the MMR plumes may lead to its use at other Air Force installations. AFCEE has stipulated that the optimization algorithm must be reasonably simple to implement, yet effective in identifying temporal and spatial redundancy. The algorithm must also be structured in terms of a decision logic flowchart that would be useful more generally at additional sites.

At FS-12, two primary constituents of concern were utilized, ethylene dibromide (EDB) and benzene. Other contaminants are contained in the available data record, but these either rarely or never exceed applicable drinking water standards (MCLs) and so were excluded from further analysis. Given the extensive list of historically-monitored wells located either within or near the boundaries of the FS-12 contaminant plume, it is noteworthy that almost 90% of the measurements are non-detect for both EDB and benzene. Of course, some of the remaining data values are very high for one or both of these contaminants. But the “hits” tend to be concentrated in a small subset of the wells being monitored at the site.

At Eastern Briarwood, two other constituents of concern were used, trichloroethene (TCE) and perchloroethene (PCE), both volatile organics (VOCs). Like FS-12, both contaminants exceeded applicable MCLs only a small fraction of the time, the "hits" being concentrated in a fairly small subset of the known monitoring wells.

The key question of interest to AFCEE is: how can an LTM network be optimized so that unnecessary resources and expense are not wasted for sampling, laboratory analysis, and/or well construction? Optimization in this context is mostly a "one-way street" — little attention is paid to whether more sampling or additional wells might be needed. Rather, the assumption here is that, if anything, too much sampling and/or too many wells have led to a waste of monitoring resources. The primary objective is to determine to what degree these resources can be pared without losing key statistical information about the plumes being monitored.

In particular, it is assumed that the goal of any LTM effort is to provide an accurate assessment over time of ground-water quality, with the ultimate objectives of enabling one to 1) construct an interpolated map of the current concentration levels across the site area, and 2) accurately assess trends or other changes in individual monitoring wells. Interpolated maps are used to assess whether or not a plume of contaminated ground water exists, and, if so, its extent and characteristics (e.g., intensity). Changes in such maps over time can indicate either improvement or decline in ground-water quality across the plume area. Changes in concentration patterns or the identification of trends at individual "sentinel" wells can also serve the same purpose.

The optimization algorithm itself has been divided into two separate components: 1) temporal redundancy, and 2) spatial redundancy. Temporal redundancy refers to whether or not certain wells are being sampled too frequently. Are samples collected so often that there is a significant degree of autocorrelation between closely spaced measurements? If so, can this redundancy be reduced or eliminated by decreasing the frequency of sampling and/or lengthening the time between collection of samples? Spatial redundancy refers to whether or not too many wells are being monitored. That is, are there wells that provide essentially redundant information and could be eliminated from the network without sacrificing resolution of ground-water quality?

At the root level, the optimization algorithm presented below consists of three basic steps: 1) Identification of temporal redundancies in currently monitored wells; 2) identification of spatially redundant wells; and 3) projection of cost savings gained by eliminating wells and/or reducing sampling frequencies.

Section 2. Temporal Optimization Algorithm

The temporal algorithm is divided into two non-overlapping pieces: A) computation of the composite temporal variogram, and B) "iterative thinning" of sampling events at selected wells.

The first approach allows time series data from many wells to be combined together into a single measure of temporal autocorrelation known as a variogram. As opposed to spatial autocorrelation, which considers the distance between points in space, temporal autocorrelation takes "distance" as the elapsed time between samples collected from the same location. Using time as the distance function, one-dimensional variograms can be constructed to measure the average correlation between pairs of measurements as the time lag between them increases or decreases.

The point in time at which the "sill" (i.e., upper bound) of this variogram is reached estimates the approximate lag time between sampling events for which there is no time-related dependency, and hence, no temporal redundancy. Samples taken from the same location at shorter intervals will tend to be correlated to some degree and therefore at least partially redundant in the statistical information they provide. Because data from multiple well locations are included in the composite temporal variogram, the variogram approach does not necessarily provide an optimal sampling frequency for each individual well. Rather, it estimates an "average" optimal frequency that can, if desired, be adopted on a site-wide basis.

To estimate the average temporal autocorrelation, the basic approach of Tuckfield (1994) was modified to estimate a one-dimensional variogram using time of sampling as the dimension. Instead of trying to explicitly model the temporal autocorrelation, the key steps were to 1) compute an empirical temporal variogram for each well; 2) average the empirical variograms across wells to build a composite temporal variogram; 3) locate the smallest time interval at which the approximate sill of the composite variogram was reached; 4) designate the time interval found in Step 3 as the minimum sampling interval providing essentially uncorrelated temporal data; and 5) adjust the sampling frequencies at the remaining monitoring wells so that the time lag between samples does not fall below this minimum interval.

The second approach is designed for key "sentinel" wells, wells exhibiting trends over time, or other monitoring locations for which a well-specific sampling frequency may be desirable or needed. Various methods for optimizing sampling frequencies at individual wells have been proposed (see Johnson, et al, 1996 for instance). At MMR, however, a somewhat different approach was taken. "Iterative thinning" refers to the temporary removal of randomly-selected data points from the time series of measurements at a given well. The algorithm consists of 1) estimating a trend using the entire time series, 2) thinning the time series by a fraction of the measurements, and then 3) re-estimating the trend to determine if the slope estimate is still close to the original slope. Additional thinning can occur until the "thinned" trend estimate is significantly different from the original trend.

Due to the high non-detect rates in EDB and benzene at FS-12 and in TCE and PCE at Eastern Briarwood, and the limited sampling records available for many wells, only a small subset of the wells from either plume exhibited a readily discernible trend or had enough time series data to make a well-specific analysis worthwhile. Further complicating the matter, at some of these wells the apparent trends were non-linear, or, even when the trend was fairly linear, in some cases the concentration data were much better behaved (i.e., exhibited less variation around the trend line) toward the end of the sampling record than the near the beginning.

For all these reasons, it is recommended that the iterative thinning approach be restricted to selected wells at a given site having adequate data and some indication of a trend if possible. Furthermore, to avoid statistical assumptions inherent in standard linear regression methods, trend estimation was done with a non-parametric technique known as Sen's method (Gilbert, 1986). Sen's procedure can be applied to a wide variety of datasets and is readily adapted to non-detect measurements and irregular sampling frequencies.

Using Sen's method, only the basic linear slope of the time series was estimated, along with a confidence interval around the slope estimate. The premise of the iterative thinning approach is that if fractions of the data are randomly removed from the time series, yet the same basic slope is estimated (within the bounds of the original confidence interval) on the reduced data set, temporally redundant data exists and the sampling frequency at that well can be adjusted to further lengthen the time between sampling events.

Steps in Temporal Variogram Approach

1) Pre-Process the Data

Several steps were taken with the datasets from both plumes to prepare them for optimization. First, the raw data were examined for basic characteristics, including missing data fields, laboratory qualifiers and detection limits, data inconsistencies and gaps in the historical record, number, types, and locations of wells, well screen depth information, and analytical methods. Since the electronic database was not maintained consistently by a single contractor, various data gaps existed between the years 1991, when the first samples used in this analysis were recorded, and the last quarter of 1998. These gaps were filled in with historical data records as often as possible, especially with the hopes of gauging historical trends on-site, but the final FS-12 and Eastern Briarwood datasets were still generally spotty up until late 1996.

At this point, the current remediation effort at FS-12 was begun in earnest, with several new wells sited and a great deal of additional sampling throughout FS-12. Although no remediation program has begun at Eastern Briarwood, the sampling of both sites (or at least what is recorded in the available data) is generally more intense and inclusive of a larger number of distinct well locations starting from the late part of 1996 and continuing through 1998.

More than one type of well was used to collect ground-water monitoring information. Of these, any well labeled an injection well was excluded from the analysis since such wells dilute the ground water at the point of contact and therefore do not offer reliable concentration estimates of the in-situ contaminant levels. Other wells, including extraction wells at FS-12, were kept in the analysis (even if not strictly labeled as monitoring wells) as long they provided actual concentration estimates of the constituents of concern. The final sets of well locations used for the temporal analyses are shown in **Figures 2-1** and **2-2**, representing FS-12 and Eastern Briarwood respectively. The total number of locations used for the spatial analyses was 147 at FS-12 and 273 at Eastern Briarwood. These are listed by Well ID in **Tables 2-1** and **2-2**.

One should note that while all the well locations in **Figures 2-1** and **2-2** have distinct easting and northing coordinates, some of these wells represent well clusters screened at different depths but with boring locations in close proximity to one another. For purposes of this report, any well location with a distinct Well ID and distinct coordinates was treated as a separate well. Essentially the same algorithm could be performed considering well clusters as single locations if desired, but that was not the approach taken in this case.

Since the analytical methods and detection limits used at MMR varied somewhat from sample to sample and across the years of data collection, yet the vast majority of the data were non-detect (regardless of contaminant), it was impractical to fit standard parametric distributional models to the concentration data. Instead the data were simplified by transforming each reported value into an "indicator value" (IV), that is, a zero or one respectively, depending on whether the value exceeded a fixed concentration cutoff for the contaminant.

With an indicator transformation, information about extreme concentration levels is lost (other than knowing the value exceeds the cutoff). However, it is often easier using indicators to fit the kinds of geostatistical covariance models (discussed later) needed to gauge the degree of spatial redundancy and to determine an approximate "sill" for measuring the lowest point of temporal redundancy. Furthermore, non-detect concentrations need not be known or imputed (at least if the detection/quantitation limit is at or below the cutoff), since any concentration presumably less than the detection/quantitation limit also will not exceed the chosen cutoff. It is therefore possible to unambiguously classify a dataset into indicator values without resorting to complicated imputation schemes or tenuous statistical models.

While the concentration cutoff used to form the indicator values is somewhat arbitrary, "natural" options would include the highest detection or quantitation limit, an applicable MCL or regulatory limit, or perhaps an already established background level (e.g., a mean or upper confidence limit). At FS-12, the indicator cutoff was taken as the MCL: 5 ppb for benzene and .02 ppb for EDB. At Eastern Briarwood, the cutoffs for TCE and PCE were selected equal to their respective detection limits. For the latter plume, a sill was more readily identified for both contaminants using the detection limit as the cutoff instead of the MCL of 5 ppb. In practice, more than one cutoff may need to be examined to ensure that the least amount of statistical information is lost when forming either the temporal variogram or the spatial variograms to be discussed later.

2) Compute Composite Temporal Variogram

Once the data were converted to indicators, a sample estimate of the time-dependency between sampling events was computed known as the composite temporal variogram. A temporal variogram is a measure of correlation over time between two sampling events (at the same well), roughly equal to the average squared difference in indicator values for all pairs of measurements separated by a given "lag" (i.e., defined here as the time between sampling events).

To form the composite temporal variogram, separate variograms were first calculated using the time series from each individual well. First, a base lag spacing was chosen to represent increasing periods of time. For example, one set of lags might be taken as 0 months (1st lag), 2 months (2nd lag), 4 months (3rd lag), 6 months (4th lag), and so on, using a lag spacing of 2 months. Then, at each distinct well location, the squared differences between indicators from all possible pairs of sampling events were computed and grouped by nearest lag. After averaging the squared differences associated with each distinct lag, a sample variogram for each well was born. Finally, a composite temporal variogram was computed by averaging the individual well variograms across wells for each common lag to get a typical measure of temporal correlation applicable to the site as a whole.

One complication encountered in constructing the composite temporal variogram was that the historical records at many wells were quite limited, with less than a handful of separate sampling events at many locations and very tight temporal spacing at others (e.g., all samples collected over a two-to-three week period). Because of this, many wells contributed only a small number of data pairs to the composite variogram, at perhaps one or two lags. Fortunately, other wells contributed longer data records, allowing the composite variogram to be "filled out" with additional time lags.

Since the actual times between sampling event pairs often did not correspond exactly to a given set of lags, the same calculations explained above were made for three different base lag spacings. Then the variograms from all three spacings were amalgamated together to get the final composite variogram. This tends to ensure that the resulting temporal variogram is not biased due to an artifact of choosing one particular set of lags.

Another point to note is that for multipoint wells (i.e., wells with multiple screens at different depths but along the same bore hole), concentration values from different depths were converted to separate indicator values and used independently in forming the temporal variograms. That is, the well data were not stratified by depth. One consequence of this simplifying step was that some pairs of indicators represented data from the same sampling event but at different depths within a given well. To the extent that a contaminant plume has a narrow vertical width and differentially impacts distinct well screens along a given bore hole, the variation measured by the temporal variogram could be somewhat overestimated, especially at the smallest lags. However, the degree of overestimation should be partially offset by the use of indicator values instead of the actual concentrations in the variogram computations.

3) Adjust Global Sampling Frequency

With a composite temporal variogram in hand for each contaminant of concern, a non-linear smoothing technique was applied to each graph to determine an approximate sill. The composite variograms and the smoothed overlay are presented in **Figures 2-3** through **2-6**. The sill represents the highest *stable* numerical level on a variogram. It first occurs at the smallest lag time where there is no discernible correlation between a pair of sampling events. That is, if a sill has been reached when reading a variogram from left to right, any pair of sampling events that are separated by lag times at least as long as those associated with the sill should be uncorrelated in a statistical sense.

Given the fact that some information is lost by converting the actual concentration data to indicators, it might be tempting to use the actual concentrations when forming the temporal variogram. However, it must be remembered that the composite variogram is an average of the temporal variation from all wells at the site. The same precise temporal pattern is not likely to hold for each and every well. Indeed, the composite variogram is designed to be a parsimonious way to determine a typical or "average" global sampling frequency that can be applied more or less to all the wells uniformly. As a consequence, though, one should not expect to see simple, smooth patterns when examining the points on a composite temporal variogram.

At the MMR plumes, using the indicator values to form the temporal variograms resulted in substantial variation in the estimated values at neighboring lags, as seen in **Figures 2-3** through **2-6**. The same variograms computed on the raw concentration data resulted in even greater variation, so this avenue was not pursued further. What was done, however, was to apply a non-linear smoothing algorithm to each composite variogram, in order to estimate a smooth pattern consistent with the data. A variety of non-linear smoothers are available in standard statistical software packages, including moving window averages, geostatistical variogram fitters, the

Levenberg-Marquardt algorithm, etc. In this case, a lowess procedure (lowess denoting a **lo**cally-**we**ighted regre**ss**ion) was applied to the variograms, giving the results seen in **Figures 2-3** through **2-6**.

The lowess procedure is akin to a moving window average, but instead of a simple arithmetic average a weighted regression is performed on the data points included in each moving window. Like all moving window algorithms, the resulting smooth depends on the size of the window used, so alternate window widths must typically be tried to properly balance the degree of smoothness in the fit and how quickly the fit responds to changes in the data.

The purpose for using any smoother on the composite temporal variograms is to try and identify an approximate sill, and to determine at what approximate lag time the sill first occurs. At FS-12, the lowess fit for EDB first levels off in the approximate range of 400-500 days, while the fit for benzene is more problematic. In the latter case, a definite plateau is not evident in the range of data available, though what possibly might be a sill starts in the range of 350-400 days.

To some extent, the difficulty in ascertaining a sill for benzene may be related to the use of an MCL of 5 ppb as the indicator cutoff for this contaminant. Although an MCL cutoff was also utilized for EDB, the cutoff value of .02 ppb was not hugely different from the detection limits used to classify each measurement as detected or non-detected. By comparison, the cutoffs for both TCE and PCE at Eastern Briarwood were set to the highest detection limits, and the sills for these contaminants are more readily discernible. For TCE, the sill appears to begin in the range of 400-450 days, while for PCE, the sill starts roughly in the range of 450-500 days.

Remembering that the sill on a temporal variogram represents the point of lowest correlation between sampling events (actually the point of zero correlation), the smallest lag time associated with the sill for a given contaminant can be taken as a kind of optimal sampling interval, optimal in the sense of indicating the shortest time between samples with zero statistical correlation. Any shorter interval is associated with some temporal redundancy, since the correlation for such lag times is positive. Consequently, the results of this approach suggest that the general lag time between samples at FS-12 should be at least a year (approximating to the nearest quarter for operational simplicity), while that for Eastern Briarwood should be at least five quarters or 1.25 years.

The projected cost savings from using this lengthened sampling schedule are detailed in a separate report, but it is worth noting that application of the proposed optimized schedule to the current sampling frequencies at Eastern Briarwood — without removing any of the current monitoring wells — would result in a 36% annual reduction in the total sampling and analysis budget. Even greater cost reductions are projected for the FS-12 plume; however, the savings are based on reduction in sampling frequencies as well as removal of certain currently monitored wells.

Note that this approach does not adjust the sampling frequencies of individual wells. Rather, the composite temporal variogram offers a "broad brush" view of temporal autocorrelation on-site and provides an impartial method to set uniform, optimal sampling frequencies based on minimizing the degree of temporal autocorrelation. Of course, selected wells may need to sampled more often for other reasons (e.g., new well installations, hydrogeologic factors, etc.). And there may be some wells with well-defined trends that can be adjusted/optimized individually using the other approaches above. However, for most of the wells at MMR, locating a discernible trend in the contaminants of concern was difficult, either due to high proportions of non-detects or a limited sampling record. In these cases, the composite temporal variogram holds the promise of estimating a typical (albeit rough) temporal pattern that can facilitate sampling decisions.

Steps in Iterative Thinning Approach

1) Establish Baseline Trend

To establish an initial trend estimate for a given well, the slope was estimated using a non-parametric technique known as Sen's method. Sen's procedure involves forming all possible pairs of the raw data measurements (note that indicator values are not used in this portion of the optimization scheme) and computing a pairwise slope value for each pair. This involved subtracting the concentration value of the earlier measurement from the concentration value of the later one, and then dividing by the elapsed time between the sampling events. Once a list of all the possible pairwise slopes was created, the list was sorted and Sen's estimate was taken as the median slope value on the list.

To account for sampling and measurement fluctuations/variability, basic formulas involving the same list of pairwise slope values were used to compute a confidence interval around Sen's slope estimate (Gilbert, 1987). Essentially, the lower and upper confidence bounds were set equal to slope values in the sorted list less than and greater than, respectively, the median (which was Sen's estimate). By constructing a confidence interval around the initial trend, re-estimates of the trend after "thinning" the data series could be compared to the confidence bounds to determine whether the slope value had changed in a significant way.

As noted earlier, Sen's method can be adapted to the presence of non-detects, although some choice must be made to impute the non-detect concentration values. Perhaps the easiest tack is set all non-detects equal to zero for purposes of estimating the trend. Other values might be chosen, such as half the detection or quantitation limit. However, if multiple detection/quantitation limits exist in the data, one should be careful not to estimate a positive or negative pairwise slope between two non-detects just because their detection limits are different. At MMR, all non-detects were treated as zeros, so that any pairwise slope calculated between two non-detects was necessarily zero as well.

One other issue with Sen's method is the possibility of irregular sampling intervals. If a given well is intensely sampled for a period of time (say during initial installation), but then the frequency drops significantly, many more of the pairwise slopes will arise between samples collected during the intense phase than from other portions of the sampling record, potentially biasing the median pairwise slope estimate. To remedy this possibility, the data at irregularly sampled wells should be grouped into equally-spaced, non-overlapping time periods. No pairs are then formed between samples *within a given time period*, but only between samples located in *distinct* time periods. Sen's slope estimate is again the median of the list of pairwise slopes so formed, but the confidence interval bounds are changed slightly to account for multiple sample points in each time period.

2) “Thin” the Data Series and Assess Accuracy

Once Sen’s slope estimate and the confidence interval around the trend were in hand, the data series was “thinned.” To do this, a column of random numbers between 0 and 1 was generated alongside the time-ordered concentration data. Then, in iterative fashion, increasing percentages of the data were randomly “removed” from each time series. For example, at 20% censoring, from each successive group of five measurements one was removed, simply by flagging the lowest random number from the corresponding column in that group of five. At 33% censoring, one of every three successive values was removed, and so on. Flagging the values in this way ensured that the random removals would not be “bunched” at one end or the other of the time series; rather, the series was simply “thinned out” in a practical way.

After thinning each time series, Sen’s slope (but not the confidence interval) was recomputed to see if it fell within the original confidence bounds and to make sure the sign of the slope had not changed. The highest censoring level for which the re-computed slope was still comparable to the original trend estimate was then used to adjust the sampling frequency at that well and to determine the degree of temporal redundancy that existed.

3) Adjust the Well-Specific Sampling Frequency

To optimize the sampling frequency at a given well, the fraction of data points removed in the thinning process was considered. For instance, if the highest level of thinning was 50% before the slope changed, half the data could be removed and yet still provide a comparable slope estimate. In this case, the optimized sampling interval would essentially double in length. If only 20% of the data were removable, the optimized sampling interval would increase by roughly 25%.

More fundamentally, the optimized sampling interval for wells sampled on a fairly regular schedule can be computed as the total length time in the sampling record divided by the number of points remaining after thinning. For wells with irregular sampling histories (including most of those at MMR), it was important to avoid biasing the sampling frequency by early periods of intense sampling. Consequently, the optimized sampling interval was computed by dividing the most recent sampling interval (i.e., the lag between the two most recent, distinct sampling dates) by one minus the fraction of data points thinned. This step avoided the problem of creating an optimized sampling interval that might actually be *shorter* than the current one based on the most recent monitoring schedule. However, some caution must be used when performing such a step on an automated basis. Ideally, the interval from the most current sampling schedule ought to be utilized before dividing by the complement of the fraction thinned, rather than just assuming that the last two sampling events adequately define the sampling interval, as in this report.

Results of these analyses at FS-12 and Eastern Briarwood suggested that temporal redundancies do indeed exist at MMR, at least for selected wells with sufficient data. Data at these wells can be “thinned” without losing the ability to estimate the basic trend in concentration levels over time. The iterative thinning approach is fairly easy to implement and does not require more sophisticated non-linear fitting of the trend function. However, it does presuppose a sufficient number of data values (say at least 8 to 10) with which to perform the random subsetting and to estimate the slope of the trend.

Specific lists of wells at which sampling events/results were thinned in this manner are included in **Tables 2-3** to **2-6** (note that iterative thinning as defined in this algorithm presupposes that the selected wells will continue to be sampled, only at a reduced frequency). The tables present the shorthand well number, the sample size used, the fraction of non-detects, the grouping interval used (in days; >1 for cases of highly irregular or skewed sampling, =1 when no multi-day grouping was deemed necessary), Sen's slope estimate and lower and upper 80% confidence bounds on the slope for the original data set, the average fraction that could be thinned from each data set without significantly altering the slope (algorithm was repeated 10 times for each well), the current sampling interval (based as noted above on the most recent two sampling dates), and the optimized sampling interval (after adjusting for the fraction of points thinned).

The last two entries in **Tables 2-3** to **2-6** are shown for illustrative purposes primarily. Some wells that met the minimum data requirements had very few distinct sampling events and so had intervals of 0 or 1 day. Such cases would not be practical candidates for this kind of optimization. At other wells, a case-by-case examination of the sampling history may be needed to determine the typical current sampling interval prior to adjusting by the thinning fraction. Of particular interest are the average fractions thinned. Here a variety of values were computed, including many in the range of 40 to 70 percent. Such thinning percentages would translate into significant cost savings in reduced sampling at the impacted wells.

Section 3. Spatial Optimization Algorithm

The spatial side of the optimization algorithm is predicated on the notion that well locations are redundant if nearby wells offer nearly the same information about the underlying plume. Specifically, a well is considered redundant if its removal does not significantly change an interpolated map of the plume; that is, essentially the same iso-concentration contours result.

The path taken in identifying potentially redundant wells included the following steps: 1) generate an initial plume map via a geostatistical interpolation method known as kriging; 2) assign numerical weights (denoted *global kriging weights*) to the well locations in the monitoring network to gauge their relative contribution to the plume map; 3) temporarily remove that subset of wells with the lowest global kriging weights and re-estimate the plume map; and 4) assess whether the plume map has changed in any significant way and gauge via the kriging variance whether the spatial uncertainty has substantially increased. If not, try removing some additional wells and repeating the process. But if significant changes are evident, do not remove that subset of well locations.

Key Steps

1) Pre-Process the Data

Many of the same initial steps used to form the composite temporal variogram were taken to prepare the data for spatial optimization. In particular, the raw data were examined to resolve inconsistencies and to fill-in data gaps where possible. The data at both plumes were also converted from concentration values into indicators (IV), using the same cutoffs as selected for the temporal optimization.

As a side note, to keep the statistical algorithm as operationally feasible as possible, only a single indicator cutoff (e.g., MCL, detection/quantitation limit, etc.) was used to convert the raw data. To better represent the actual distribution of contaminant concentrations, one could potentially use a multiple indicator approach with multiple cutoffs set at increasing concentration levels. Less detail about the extreme portions of the plume would be lost. However, the steps needed to geostatistically model the data would be multiplied. Unless rather detailed information about the plume is needed, the added complexity will probably not provide much in the way of useful information on spatial redundancy over the approach taken here.

As another simplifying step, a subset of the well locations at FS-12 and Eastern Briarwood was labeled in the database as multipoint wells, meaning they were screened at multiple depths along a single bore hole. Other wells were screened at a single depth, but given that the MMR plumes tend to move at oblique angles relative to the ground surface plane, these depths varied. Since the number of data points at any given depth was fairly limited, the three-dimensional nature of each plume was collapsed into a two-dimensional problem by “averaging” indicator values over depth for a given well location. “Averaging” in this context refers to labeling the sampling at a particular well on any given date/event as a “hit” (i.e., exceeding the indicator cutoff, so that IV = 0) if any one or more of the samples with depth was a “hit.” Well locations where all values did not exceed the indicator cutoff were assigned indicator values of IV = 1.

A final pre-processing step was necessary to accommodate the irregular sampling schedules observed at FS-12 and Eastern Briarwood. Since different types of wells were included in the database and since many of these wells were installed at different times, some of the wells were sampled more often than others. In fact, it is not uncommon for newly installed wells to be sampled fairly frequently at first, followed by a gradual reduction in the sampling schedule. To avoid giving more statistical weight to some well locations than others simply by the volume of data points available at frequently sampled wells, each dataset was divided arbitrarily into a series of quarterly "snapshots" or time slices.

For a given three-month time span, a well with *any* "hits" was labeled as a "hit" for that quarter, regardless of the number of times it was sampled. This meant that as long as a well was sampled even once during that quarter, it was given the same relative statistical weight as a well sampled more frequently. Again, collapsing the problem in this way "loses" or ignores some information about the temporal pattern of contaminant concentrations. But the gain in simplicity is significant, especially when it is recognized that 1) the number of sample measurements available on any given day/event was typically limited, and 2) kriging (as described below) must be performed for each time slice. The greater the number of time slices, the greater the number of statistical calculations necessary.

A related decision was made to limit the number of time slices included in the spatial analysis to those with a relatively large number of wells sampled (typically 30 or more). Modeling a spatial covariance pattern and kriging a dataset both work best if the number of available data points is moderate to large. In addition, limiting the number of time slices reduced the amount of statistical calculations necessary. Accordingly, 10 quarterly time slices were utilized at FS-12 and 9 quarterly time slices were included for Eastern Briarwood, in both cases covering the time period from late 1996 through 1998, but also including some earlier data for FS-12.

2) Model the Spatial Covariance

Once the data were collapsed into a single horizontal plane and grouped by quarter of sample collection, the indicator data from each quarterly time slice were fit to standard geostatistical spatial covariance models. This involved two basic steps. First, a sample estimate of the spatial correlation function known as the empirical variogram was computed. A variogram is a measure of correlation with distance between two sampling locations, roughly equal to the average squared difference in indicator values for all pairs of locations separated by a given "lag" (i.e., distance between locations).

To account for possible changes in the plumes over time, the empirical variogram for each quarterly slice of data was examined to see if that pattern also changed with time. If substantial differences are evident in the empirical variograms, a separate spatial covariance model should be fit to each time slice, since the data from each slice are kriged separately. At both MMR plumes, the correlation pattern was fairly similar for the bulk of the quarterly time slices (**Figures 3-1** through **3-4**). Occasionally, one or two quarters exhibited a somewhat different (non-parallel) pattern from the rest, but the differences were not great enough to necessitate separate variance modeling. Consequently, the quarterly variograms were averaged across the time slices (weighted by the number of pairs contributed to the variogram estimate in each time slice) to form a single, time-averaged variogram.

Another typical step is to compute the empirical variograms with different base lag spacings (e.g., separations between successive lags of 100 ft, 300 ft, 1000 ft, etc) to ensure that the choice of lag does not overly influence the appearance of the resulting variogram. At MMR, the basic pattern was similar regardless of the base lag spacing employed. So, the empirical variograms at three different lag spacings were amalgamated to form a final variogram prior to modeling.

Once the empirical variogram for each contaminant was estimated, a non-linear fitting program (utilizing the Levenberg-Marquardt algorithm) was used to determine an appropriate positive-definite spatial covariance model. Four such models are common in the geostatistical literature: spherical, exponential, gaussian, and power. The fitting algorithm was set up to either fit a combination of up to three spherical, exponential, and/or gaussian components (termed "nested structures" in geostatistical lingo) or a combination of up to three power model components.

At FS-12 (**Figures 3-5** and **3-6**), EDB was best fit with essentially a spherical model, while the variogram for benzene was best described by a power model (with a nearly quadratic power coefficient). At Eastern Briarwood (**Figures 3-7** and **3-8**), TCE was best fit with a power model (using a nearly quadratic power coefficient), while for PCE, no standard model was entirely adequate. Instead, the variation with distance for PCE fluctuated more or less around a constant level, suggesting that a constant "nugget" variance term be used as the variogram model. Such a model implies that there is no correlation with distance between neighboring well locations. Lack of spatial correlation does occur in practice, but might be related in this setting to the indicator cutoff used for PCE and/or the "averaging" of the indicators across depths within wells or across sampling events within time slices. In any event, the results of spatial redundancy analysis at Eastern Briarwood when comparing TCE and PCE, as discussed below, were surprisingly consistent despite the difference in spatial model used.

On a final note, as with many non-linear fitting algorithms, the one utilized with the MMR data features a weighted least squares fitting criterion. Essentially, lags with variogram values based on larger numbers of data pairs were weighted more heavily than lags with fewer data pairs. This helps to avoid placing undue weight to anomolous or outlier data points in the fitting of the spatial covariance model.

3) Krige the Indicator Data

To actually determine which wells might be spatially redundant, remember that a monitoring well should be considered redundant if other (nearby) wells provide much the same information concerning the plume being monitored. More specifically, a well is redundant if it provides little independent or additional information when generating a map of the plume.

To generate a plume map, estimates of concentration are needed at unsampled locations, not just the installed wells. These estimates typically involve an interpolation of the known concentrations at already existing wells. Most often the interpolation is computed as a weighted linear combination of the sample data from a series of (n) fixed locations.

One way to define spatial redundancy is when one or more wells are assigned very small weights in the interpolation process compared to other wells. For only those wells with larger weights contribute significantly to the estimation at unsampled locations.

While many methods for linear interpolation exist, the approach adopted at MMR is a widely used method for linear interpolation over a spatial area known in the geostatistical literature as *kriging*. Not only does kriging offer a kind of "best" unbiased linear interpolation, but it alone among common interpolation schemes explicitly accounts for the statistical redundancy at nearby sample locations, through its estimate (i.e., model) of the spatial covariance function.

Although there exist a variety of kriging methods, the most common is known as *ordinary kriging* (OK). OK generally works well for concentrations or other measurement data that are mostly detected or quantified. For chemical parameters with low detection rates, however, OK can be difficult to apply for three reasons: 1) the spatial covariance model is often hard to model due to the unknown concentrations of non-detects and the fact that some type of imputation must be made for these unknown values; 2) the linear interpolation at unsampled locations must again rely on combinations of imputed non-detect values; 3) if the detected values are additionally quite skewed, both the empirical variograms and kriged estimates can fluctuate in unpredictable and anomalous ways.

At the MMR plumes, empirical variograms of the raw concentration data (simply taking non-detects as zeros) were quite jagged and impossible to fit using the standard spatial covariance models. Because of this and the reasons outlined above, an alternative procedure known as *indicator kriging* (IK) was employed. In simple IK, all the sample data are re-classified as ones or zeros depending on whether or not the actual concentration is below or above a fixed threshold (i.e., the indicator cutoff). While detail concerning the intensity of the plume is lost, there is also no need to know the exact concentrations of non-detects. Furthermore, the algorithm is exactly the same as OK except that the indicator data are used in place of the raw concentrations.

Because the data are transformed into indicator values, the results of IK interpolation at unsampled locations do not represent concentration estimates. What they do represent are probabilities of exceeding or not exceeding the indicator cutoff. That is, assuming for instance that the MCL is the cutoff, a *low* IK estimate denotes a *low probability* that the true concentration at that estimated location is *below* the MCL, while a *high* IK estimate denotes a *high probability* that the true concentration *does not exceed* the MCL. Low IK values therefore represent probable MCL exceedances, while high IK values represent the opposite.

The basic IK algorithm used at MMR was to first divide the plume area into a series of non-overlapping blocks. At each block a simple search algorithm was used to locate a set of sampled locations closest to the block. Then, using the modeled spatial covariance function, local kriging or interpolation weights were computed based on the spatial configuration of the known indicator values (that is, the data from known surrounding wells) relative to the block and the spatial correlation between the average block location and each known indicator. These local weights were then combined with the known indicator values to generate a block indicator estimate (consisting of a weighted average of the indicators). The block indicator estimates taken as a whole produce an estimated indicator plume map. **Figures 3-9** through **3-12** display examples of these initial plume maps, representing the 4th Quarter of 1998.

4) Compute Global Kriging Weights

Though the indicator plume maps resulting from indicator kriging do not provide explicit concentration estimates for the plume, two intermediary computations from the kriging exercise are extremely useful: 1) the local kriging weights assigned to sampled locations near each block can be accumulated and averaged to generate a "global" interpolation weight for each well (see Isaaks & Srivastava, 1989); 2) at each block, the local kriging estimation variance indicates the relative uncertainty of the local block estimate compared to estimates at other blocks.

Since the search algorithm described above when kriging individual blocks locates known wells nearest to the block being estimated, some wells, depending on their location (and particularly those toward the middle of the plume), are used in the local estimation of many different blocks. These wells will potentially receive a different local kriging weight each time they are tagged by the search algorithm, since the geometric position of a fixed well relative to the block being estimated will change with each new block. The global interpolation weights were thus formed by averaging all of the local kriging weights for each given well, in order to estimate the well's overall contribution to the estimation process. Note that to assess the average contribution of a given well not only across the site spatially, but also over time, the local kriging weights for each time slice were further averaged across the slices. The final global kriging weights for each contaminant are listed in **Tables 3-1** and **3-2**.

The global interpolation weights offer a relative ranking of the well locations in terms of the amount of independent spatial information provided. Those wells that are spatially redundant will tend to have the lowest global weights since their local kriging weights will frequently be small. By choosing a threshold value of, for instance, .01 or .02, and eliminating all those wells with global weights no greater than the threshold, an impartial decision criterion can be established for removing spatially redundant well locations.

At FS-12, six different thresholds were tested for both EDB and benzene. The thresholds used were specific to each contaminant, with the lowest threshold designed to eliminate close to the lowest ranking 10% of the well locations, and successively larger thresholds chosen to roughly capture an additional 10% of the wells remaining at each stage. For EDB, the thresholds were .0008, .001, .0015, .002, .003, and .0035. For benzene, the thresholds included .0005, .0012, .002, .0025, .003, and .004.

When multiple chemical parameters are being monitored, it may be that the most spatially redundant well for one parameter is not the most redundant for others. The goal is then to remove only those wells that exhibit spatial redundancy *across* the monitored parameters. One possible strategy is to compute a separate set of global interpolation weights for each parameter and then average these sets across the parameters. That way, the final ranking for selecting candidate wells for removal will account for all the parameters of interest.

Another strategy, and the one used at MMR, is to simply compare the lists of tentatively removed wells for each parameter and only remove those that appear on each list. Remarkably, even though different spatial covariance models were fit to EDB and benzene, the lists of spatially redundant wells were very similar for the two parameters at each of the weight thresholds tested. The close correspondence offers additional confidence that the wells targeted as candidates for removal do indeed provide redundant spatial information.

Like FS-12, at Eastern Briarwood six distinct thresholds were tested with TCE and PCE. The thresholds for TCE were set at .0002, .0004, .0005, .0008, .0011, and .0014. For PCE, the thresholds included .0003, .0005, .0007, .001, .0013, and .0016. Again it was the case that despite the use of different spatial covariance models for the two chemicals, the lists of potentially redundant wells were very similar, exhibiting a high degree of overlap. Once again, the wells ultimately tagged for potential removal included only those flagged as redundant for *both* TCE and PCE.

5) Assess Relative Uncertainty

Although the weight thresholds provide an impartial way to identify potentially spatially redundant wells, the thresholds are arbitrary. Ultimately it must be determined whether removing those wells has any measurable impact on the estimation of the indicator plume maps. One useful measure that is part of any standard kriging output is the local kriging variance, which, in the case of block kriging, is a separate number associated with each estimated local block. As with any statistical variance estimate, large local kriging variances suggest that the estimated value for a given block is much less precise than estimated blocks with small local kriging variances.

Since the size of the local kriging variance for a given block depends on the spatial covariance model, the number and configuration of the sampled locations, and the position of the estimated block relative to nearby samples (i.e., known well locations), the local kriging variance also provides a measure of relative spatial redundancy. In fact, by averaging the local kriging variances *across blocks* as suggested by Bertolino, et al (1983), the overall uncertainty using one configuration of well locations can be compared to the uncertainty derived from alternate configurations. This quantity — after further averaging across all the time slices — is denoted as the *global kriging variance* in the proposed optimization scheme.

In particular, if all wells with global kriging weights smaller than a particular threshold are eliminated from the mix, and the site is re-kriged on the same blocks, the new global kriging variance can be checked against the original measure to examine whether or not too much spatial information has been lost. Used in an iterative fashion, this algorithm allows the set of well locations to be narrowed to those that are most helpful as statistical estimators of ground-water quality. For instance, it might be agreed that a subset of wells can be removed from monitoring as long as the increase in global kriging variance is no more than, say, 5% of the original value. While a 5% increase may seem at first glance to be less than consequential, remember that the local kriging variances are being averaged across blocks and across time slices. Any increase in the overall average will necessarily entail a number of blocks with significant jumps in the local kriging variance, indicative of a loss of spatial information. So even small increases in the global kriging variance are likely to have significance.

Values of the global kriging variance for each weight threshold and its relative change with respect to the initial global kriging variance are provided in **Table 3-3**. Using a relative increase of 5% as a target and *based on this criterion alone*, wells would only be tagged as potentially redundant up to threshold #4 for EDB (relative increase of 4.2%), threshold #3 for benzene (relative increase of 3%), threshold #3 For TCE (relative increase of 2.2%), and threshold #6 for PCE (relative increase of 4.2%).

Unfortunately, despite the simplicity of the global kriging variance, it must usually be supplemented by other uncertainty measures. In particular, it is quite helpful to compute ratios — on a block-by-block basis — of the local kriging variance at a given threshold and the initial local kriging variance before any well locations have been removed. By further averaging these ratios across time slices, it is possible to create maps of the time-averaged local kriging variance ratios. Such maps are displayed for FS-12 in **Figures 3-13** through **3-24**, and for Eastern Briarwood in **Figures 3-25** through **3-36**.

Maps of the local kriging variance ratios indicate what parts of the estimated plume map are associated with the largest change in relative uncertainty, after removing a subset of the well locations. Presumably, by removing a subset of wells from the analysis, the kriging variances will tend to increase at some of the estimated blocks. Large ratios in particular sectors of the plume will then suggest that a significant amount of spatial information has been lost in those sectors. This allows further refining of the criteria used to remove wells, providing an indication of when the weight threshold has been set too high. In fact, by examining these maps, the initial thresholds targeted via the global kriging variance for EDB, benzene, and TCE were deemed reasonable, but the threshold for PCE was lowered to #3 since too many local areas of Eastern Briarwood had high kriging variance ratios at higher thresholds.

As a final check of uncertainty, note that the final goal of the optimization is to ensure that reasonably consistent plume maps can be constructed even after removing a set of spatially redundant wells. Any weight threshold or targeted increase in the kriging variance is to some extent arbitrary. One should therefore examine before-and-after indicator plume maps to determine if the basic pattern and features of the map estimates have been fundamentally altered. If so, it suggests that too many wells may have been removed from the mix. Examples of these maps from the 4^{th} Quarter of 1998 are presented for EDB in **Figures 3-37** to **3-42** (corresponding to each of the six weight thresholds), for benzene in **Figures 3-43** to **3-48**, for TCE in **Figures 3-49** to **3-54**, and for PCE in **Figures 3-55** to **3-60**.

Though the changes are subtle for some of the maps, a significant loss of detail for benzene in the southeast area of FS-12 is seen particularly in the transition from threshold #x to threshold #x. Even subtle changes in contour lines indicate some loss of spatial information, since the map estimates are then no longer fully consistent with those gotten using all the well locations. However, examining such maps takes some practice and can be more subjective in nature than the checks on the local and global kriging variances outlined above.

6) Finalize List of Redundant Wells

After determining an appropriate threshold for each contaminant of concern, the lists of potentially redundant wells for each plume were compared. As noted earlier, there was a high degree of overlap in the lists resulting from the EDB and benzene analyses at FS-12, and in the lists generated from the TCE and PCE analyses at Eastern Briarwood. Ultimately, only those well locations tagged on the lists of both contaminants at each plume were judged to be spatially redundant. The particular well locations for each plume are given in **Tables 3-4** and **3-5**.

Of interest, the datasets for each plume at MMR were finalized for analysis in early 1999. Because of changes in engineering contractors, on-site data management, and remediation efforts, and the fact that these databases purposely included as much historical data from the past decade as possible, the list of currently monitored well locations at the two plumes does not coincide entirely with the lists supplied to the optimization algorithm. On the basis of the spatial analysis, 38 of 173 distinct locations were tagged as spatially redundant at FS-12. Of these 38, only 21 locations are still being monitored under the current regime as of Fall 1999. At Eastern Briarwood, 71 of 363 well locations were tagged as spatially redundant. None of these 71 are still being monitored according to information supplied by the latest contractor.

Despite the fact that many of the redundant well locations are no longer being regularly sampled, removing those that still exist and applying the recommended global sampling frequency (from the composite temporal variograms in Section 2) leads to significant potential cost reductions at FS-12 and Eastern Briarwood. The separate report on estimated cost savings indicates that the sampling and analysis budget at FS-12 could potentially be reduced by 42% from the current expenditure of $403,925 for a savings of $167,722 per year. At Eastern Briarwood, the potential reduction is 36% of a current budget of $212,348 for an annual savings of $76,009.

It must be noted that the lists of spatially redundant wells in **Tables 3-4** and **3-5** are proposed for removal *strictly on the basis* of the present statistical analysis. Before such a recommendation is implemented, the specific well locations should be examined by hydrogeologists familiar with the sites and by the appropriate regulators to ensure that valuable information other than the concentration data used here would not be lost. Other than a change in cost estimates, the optimization algorithm is in no way harmed or altered if someone decides for other reasons that one or more wells tagged as redundant should be kept on the monitoring list and not removed.

Section 4. Final Considerations

Regardless of cost savings realized in adopting this optimization scheme, its ability to optimize sampling schedules and monitoring well locations is strongly dependent on the quality and currency of the input data. As plumes change over time and historical data is better regarded as "out-of-date," it is highly recommended that an ongoing review be conducted, say, every three to five years after the initial implementation. At these intervals, the optimization algorithm should be re-conducted using more recent sampling information, in order to determine whether the global sampling frequency or the frequencies at individual wells need adjustment, and to determine whether or not additional wells show significant spatial redundancies. It also might happen that new wells may need to be put *into* the monitoring network, not necessarily at historically sampled locations.

To make the ongoing review as successful and efficient as possible, operational adjustments to the sampling schedule should be taken to maximize the statistical utility of the resulting measurement data. By way of example, suppose the initial analysis suggests a global sampling interval of one year, so that each distinct well is to be sampled once per annum. Rather than sampling all wells at the same time every year, a better strategy would be to divide the wells into four non-overlapping subsets and sample one-quarter of the wells (i.e., one subset) each quarter.

Such a scheme will tend to minimize biases or artifacts creeping into the data due to seasonal fluctuations, for instance.

In addition, so that enough pairs of measurements at different time lags are available to reconstruct a composite temporal variogram at the next program review, it is recommended that the rotation be determined at random as to which subset of wells gets sampled during a given quarterly sampling event. In other words, if subset #1 was sampled during the third quarter of the first year after implementing the optimization scheme, it might be sampled during the first quarter of the following year, and perhaps the fourth quarter of the year after that. The intervals between consecutive samplings of the same well will then not always be a full year (sometimes less, sometimes more), but the sampling frequency will still be yearly.

By allowing for partially randomly-determined sampling intervals, data pairs can be formed at a variety of different lag times, thus enabling re-examination of the temporal variogram and whether or not the optimal sampling interval has changed. Otherwise, if a given well was sampled at precisely the same time from year to year, only pairs with a one-year lag time or greater could be formed.

On the spatial side of the algorithm, one way to determine whether new wells should be *added* to the network is to examine maps of the local kriging variances. Specific areas of the site with very high kriging variances represent parts of the plume where concentration estimates are likely to be rather uncertain. Often the placement of one or two wells in such areas will dramatically reduce the local kriging variances and improve the reliability of interpolated concentration maps made of the plume.

A final reminder should be made that many of the well locations (as identified by unique well IDs) designated as potentially redundant by the spatial algorithm in **Tables 3-4** and **3-5** are apparently no longer in service or being sampled as part of either monitoring network. To clarify which wells should still be sampled after applying the optimization algorithm, **Table 4-1** lists for both plumes those wells which are currently being sampled (based on the latest contractor-supplied information) *and* which were *not* tagged as spatially redundant.

Section 5. References

Bertolino, F., Luciano, A., & Racugno, W. (1983) Some aspects of detection networks optimization with the kriging procedure. *Metron*, 41(3): 91-107.

Gilbert, R.O. (1987) *Statistical Methods for Environmental Pollution Monitoring*. Van Nostrand Reinhold, New York.

Isaaks, E.H. & Srivastava, R.M. (1989) *Applied Geostatistics*. Oxford University Press, New York.

Johnson, V.M., Tuckfield, R.C., Ridley, M.N., & Anderson, R.A. (1996) Reducing the sampling frequency of ground-water monitoring wells. *Environmental Science & Technology*, 30(1): 355-358.

Tuckfield, R.C. (1994) Estimating an appropriate sampling frequency for monitoring ground water well contamination. Paper presented at International Nuclear Materials Management (INMM) Annual Meeting, Naples.

Appendix

Table 2-1. FS-12 Well Locations Used for Spatial Analysis

Well ID	Well Number	Easting	Northing
90BH0073	1	867579	252465
90EW0002	4	867448.62	252455.8
90EW0006	5	868071	252332
90EW0007	6	868225	252305
90EW0008	7	868342	252300.7
90EW0009	8	868469.31	252246.8
90EW0010	9	868596.12	252821.7
90EW0011	10	868636.38	252655.8
90EW0012	11	868630.81	252505.91
90EW0013	12	868601	252415.8
90EW0014	13	868543.31	252256.41
90EW0015	14	868532.69	252050.2
90EW0016	15	868539.38	251933.41
90EW0017	16	868617.81	251793.3
90EW0018	17	868811.38	251717
90EW0019	18	868923.5	251408.8
90EW0020	19	868784	250494.41
90EW0021	20	868890	250568.8
90EW0022	21	869020.69	250621.41
90EW0023	22	869133.69	250678.5
90EW0024	23	869255.12	250728.59
90EW0025	24	869400	250795.41
90EW0026	25	869557.88	250866.5
90EW0027	26	869687.31	250926.59
90EW0028	27	869818.69	250999
90EW0029	28	869916.38	251112.59
90EW0030	29	870043.12	251155.2
90JB0001B	30	869662.31	250130.59
90JB0001C	31	869662.88	250135.5
90JB0001D	32	869657.5	250137
90JB0004A	33	870035.69	250041.59
90JB0004C	34	870042.12	250054.7
90JB0006B	35	869005.88	250271.59
90MP0060D	40	868100.38	251174.59
90MW0001	43	868194	253687
90MW0002	44	868186	253695
90MW0003	45	868600.31	252861.59
90MW0004	46	867294.81	253314.5
90MW0005	48	868602.38	252853.41
90MW0006	49	868420.38	252285.2
90MW0007	50	868181.62	253701.09
90MW0008	51	868177.62	253707.7
90MW0009	52	868157.38	252314.3
90MW0010	53	867959	251902
90MW0011	54	867958	251907
90MW0012	55	868626.69	252162.3
90MW0013	56	867839	254731
90MW0014	57	867351	254509
90MW0015	58	867956.69	251912.91
90MW0016	59	868620.12	252165.41
90MW0017	60	868414	252288
90MW0018	61	868912	252091
90MW0019	62	868025.12	253982.3
90MW0020	63	869057	251880
90MW0021	64	867576.62	254657.2
90MW0022	65	867113	254101
90MW0023	68	867930	254760
90MW0024	69	869268	251765.09
90MW0025	70	868877	251335
90MW0026	71	869111.31	251305.59

90MW0027	72	868480.5	251376.3
90MW0028	73	869429.88	251262.59

Table 2-1. FS-12 Well Locations Used for Spatial Analysis

Well ID	Well Number	Easting	Northing
90MW0029B	74	867937	255042
90MW0033	75	869914	252110
90MW0034	76	868645	253868
90MW0035	77	867392	252463
90MW0040	79	869028.62	250984.91
90MW0042	80	870394	251163
90MW0047	81	868811	250486
90MW0048	82	868493.31	251370.59
90MW0049	83	868008.12	251365.41
90MW0050	84	868343.88	250978.8
90MW0053	85	869430.81	250840.91
90MW0054	86	866999.81	252663.5
90MW0055	87	869417.81	250870.2
90MW0056	88	868821.12	250476.59
90MW0057	89	869000.62	250268.91
90MW0058	90	868487.31	250369.09
90MW0060	91	869562	252128
90MW0061	92	867965	254429.3
90MW0063	93	867495.31	252977.91
90MW0064	94	870280.38	250673.91
90MW0064A	95	870286.81	250668.09
90MW0065	96	870709	251100.3
90MW0066	97	869438.31	250478.5
90MW0066A	98	869443.81	250473.2
90MW0067	99	870166.5	251148.41
90MW0068	100	869837.38	250521.59
90MW0069	101	867187	252391
90MW0070	102	867726.81	253039.3
90MW0071	103	867890.38	253039.3
90MW0072A	104	867428	252519
90MW0076	105	869021.19	250979.7
90MW0077	106	870269.12	250683.3
90MW0078	107	869195.62	250677.91
90MW0079A	108	869754.88	250936.91
90MW0079B	109	869758.62	250932.3
90MW0079C	110	869762.38	250920.2
90MW0080	111	867908	252359.8
90MW0081	112	869428.62	251267
90MW0083	113	869448.81	250477.5
90MW0084A	114	869838.5	250533.91
90MW0084B	115	869844.12	250533.8
90MW0085A	116	868552.69	250328.3
90MW0085B	117	868552.69	250328.2
90MW0086A	118	870189.5	251651.91
90MW0086B	119	870189.19	251651.91
90MW0086C	120	870185.38	251645.41
90MW0086D	121	870185.5	251645.59
90MW0087A	122	870406.31	250946.09
90MW0087B	123	870406.12	250945.8
90MW0088A	124	870401.69	250701
90MW0088B	125	870401.5	250700.8
90MW0089A	126	870330.19	250398.2
90MW0089B	127	870330.31	250397.91
90MW0089C	128	870338.38	250399.3
90MW0089D	129	870338.69	250398.91
90MW0089E	130	870345.31	250400.2
90MW0089F	131	870345.62	250400.3
90MW0090A	132	870194	250159.91
90MW0090B	133	870193.88	250159.59
90MW0090C	134	870192.12	250153

90MW0090D	135	870191.88	250153.09
90MW0090E	136	870190	250146.2

Table 2-1. FS-12 Well Locations Used for Spatial Analysis

Well ID	Well Number	Easting	Northing
90MW0090F	137	870190.19	250146.5
90MW0091A	138	870190	249993.59
90MW0091B	139	870190.19	249993.8
90MW0091C	140	869198.5	249986.5
90MW0091D	141	869198.38	249986
90MW0091E	142	869196.88	249979.59
90MW0091F	143	869196.81	249979.41
90WT0001	144	868669	252489
90WT0002	145	869383	254876
90WT0003	146	868021	254790
90WT0004	147	867403	254543
90WT0005	148	866891.62	253392.3
90WT0006	149	868406	255096
90WT0013	154	868411	254735
ECPZSNP01A	206	868027.88	251147.5
ECPZSNP01B	207	868027.88	251147.59
ECPZSNP02B	208	866553	249864.59
ECPZSNP03B	209	867774.38	251900
ECPZSNP03C	210	867774.38	251900
ECPZSNP04B	211	867564.19	251608.09
ECPZSNP05B	212	867252.81	251095.7
ECPZSNP06D	213	866657.62	250830.09
ECPZSNP09B	214	867635.62	251055.41

Table 2-2. Eastern Briarwood Well Locations Used for Spatial Analysis

Well ID	Well Number	Easting	Northing
00BH0596	1	866993.4	232153.6
00BW0582	5	865768	230847.6
00BW0586	7	867177.9	232854.4
00BW0588	9	870005.4	226494.2
00BW0589	10	863783.3	229647.6
00MP0571A	13	869979	233205
00MW0524A	24	866023.8	232685.3
00MW0524B	25	866023.5	232678.9
00MW0524C	26	866021	232672.8
00MW0525A	29	866878.3	232847.6
00MW0525B	30	866879.2	232841.9
00MW0526A	32	866411.9	232504.4
00MW0526B	33	866407.6	232512
00MW0526X	34	866387.9	232514.3
00MW0526Z	35	866380.7	232498.5
00MW0527	36	864159.9	235065.9
00MW0528A	37	864498.8	234302.3
00MW0528B	38	864493.2	234304.1
00MW0530	39	866722	236583
00MW0531	40	867657	237110
00MW0536A	43	867799	235170
00MW0536C	44	867791	235189
00MW0537A	46	868288	235243
00MW0537B	47	868293	235249
00MW0538A	48	869499	235753
00MW0539A	50	868118.5	233600.3
00MW0539B	51	868112.7	233606.1
00MW0539C	52	868109.9	233609.4
00MW0539D	53	868115.4	233602.9
00MW0539E	54	868104.9	233615.6
00MW0541A	57	867204.6	232832
00MW0541B	58	867200.1	232834.4
00MW0541C	59	867197	232836.8
00MW0541D	60	867194.5	232838.5
00MW0542A	61	868819	234137
00MW0542C	63	868818	234131
00MW0543	64	869232.3	233644.2
00MW0544A	65	869848.4	233455.1
00MW0544B	66	869844.2	233452.7
00MW0544C	67	869839.7	233450.3
00MW0544D	68	869834.9	233447.8
00MW0545	69	867668	234817
00MW0547A	71	865546.9	233699
00MW0547B	72	865539.5	233701
00MW0548A	73	865219.7	233426.1
00MW0548B	74	865230.1	233420.2
00MW0549	75	866254	232304.1
00MW0550A	76	869666	231816
00MW0550B	77	869670	231835
00MW0550C	78	869667	231825
00MW0555A	83	869292.3	231251.1
00MW0555B	84	869295.8	231246.9
00MW0555C	85	869306.8	231240.6
00MW0555D	86	869306.8	231240.7
00MW0557	87	871337	231014
00MW0561	90	869459	234553
00MW0562A	92	869522.3	233158.6
00MW0562B	93	869513.6	233161.8
00MW0562C	94	869517.6	233160
00MW0564	95	866074.9	231916.6

00MW0565	96	865915.8	231625.1

Table 2-2. Eastern Briarwood Well Locations Used for Spatial Analysis

Well ID	Well Number	Easting	Northing
00MW0567	97	868445	235487
00MW0568	98	869802	233910
00MW0569	99	869238	233971
00MW0570A	100	868951	234618
00MW0570B	101	868941	234608
00MW0572A	103	869436.6	233553.3
00MW0572B	104	869436.3	233553.2
00MW0572C	105	869435.4	233560.4
00MW0572D	106	869435.7	233560.3
00MW0573A	107	869992.2	233638.3
00MW0573B	108	869991.9	233638.2
00MW0573C	109	869992.9	233651.4
00MW0573D	110	869992.7	233651.4
00MW0574A	111	869791.9	233904.2
00MW0574B	112	869795.9	233914.2
00MW0574C	113	869791.8	233904.1
00MW0574D	114	869795.9	233914
00MW0575A	115	869295.2	234001.1
00MW0575B	116	869295.1	234001
00MW0576A	117	868451.8	235489.7
00MW0576B	118	868451.5	235489.6
00MW0576C	119	868457	235501.9
00MW0580B	121	864599.7	230160.3
00MW0580C	122	864595.6	230164.1
00MW0580D	123	864599.7	230160.2
00MW0583A	128	868211.5	229136.9
00MW0584A	131	869057.4	230335.5
00MW0584B	132	869061.7	230339
00MW0584C	133	869057.4	230335.4
00MW0586A	134	867177.9	232854.4
00MW0586B	135	867177.9	232854.3
00MW0587A	136	870295.5	228166
00MW0589A	140	863783.3	229647.6
00MW0591B	146	868010.2	225507.5
00MW0592A	148	864304.1	226576.2
00MW0593	150	866619.3	232374.9
03BH0003	153	863918.4	235133.3
03MP0092A	165	862798.2	233346.3
03MW0054A	171	863056.7	234642.1
03MW0054B	172	863068.2	234662.9
03MW0057A	173	862866.6	235378.6
03MW0057Z	175	862852.7	235391.1
03MW0058	176	863271.8	235420.4
03MW0059	177	863704.7	235203
03MW0060	178	864235.5	234679.1
03MW0061	179	863586.3	234405.3
03MW0064	180	863279.9	233685.1
03MW0065	181	863051	236848
03MW0073	183	863592	236328
03MW0104A	185	862625.6	234502.8
03MW0104B	186	862625.5	234502.5
03MW0105A	187	863887.6	235497.4
03MW0105B	188	863880.9	235496.7
03MW0114A	189	862703.6	236189.8
03MW0114B	190	862703.4	236189.4
03MW0202G	198	862824	235424.1
03MW0203E	200	862849.6	235412.5
03MW0204C	202	862870.3	235401.8
03MW0204D	203	862866.5	235397.9
03MW0204F	204	862870.1	235402.1

03MW0206F	209	862909.7	235382.3
03MW0206G	210	862904.7	235384.9

Table 2-2. Eastern Briarwood Well Locations Used for Spatial Analysis

Well ID	Well Number	Easting	Northing
03MW0211C	223	863037.6	234825.4
03MW0211E	224	863037.9	234825.5
03MW0212B	225	863056	234818.3
03MW0212C	226	863061	234815.9
03MW0212F	228	863061.2	234815.6
03MW0213E	230	863084.3	234804.4
03MW0219C	239	863156.5	234854.1
03MW0219E	240	863156.3	234854.3
03MW0220D	241	863147.7	234726
03MW0220E	242	863148	234726
03MW0221F	244	862926.8	235287.6
03MW0222F	246	862967.2	235418.1
03MW0223D	247	862805.6	235548.9
03MW0223F	248	862805.6	235549.2
03MW0224C	249	862971.1	235003.3
03MW0224E	250	862970.8	235003.4
03RW0001EF	251	862832	235436.5
03RW0001IN	252	862831.9	235436.5
03RW0002EF	253	862913.6	235397.2
03RW0002IN	254	862913.5	235397.1
03RW0003EF	255	863020.3	234847.6
03RW0003IN	256	863020.2	234847.5
03RW0004EF	257	863112.5	234809.2
03RW0004IN	258	863112.4	234809.1
28BH0036	261	866361.2	232526.1
28BH0576	262	865682.8	236025.4
28BH0578	263	864194.6	237708
28BH0581	264	864910	236322
28BH0582	265	864679	236240
28EW0001	266	865379	236161
28EW0002	267	865308	236186
28EW0003	268	865250	236205
28EW0004	269	865197	236227
28EW0005	270	865138	236256
28EW0006	271	865056	236273
28EW0007	272	864976	236298
28EW0008	273	864910	236340
28EW0009	274	864839	236359
28EW0010	275	864769	236391
28IW0100	276	865138.4	236255.5
28MW0018C	284	865455	236170
28MW0019A	285	864874	236346
28MW0020	287	864748.5	236642.4
28MW0020A	288	864741	236647.9
28MW0020B	289	864747.5	236650.4
28MW0021	290	864574.9	236707.8
28MW0022	291	863963	237103
28MW0023	292	864213	236929
28MW0026A	294	864297.3	237188.9
28MW0026B	295	864297.1	237188.7
28MW0027A	296	864412.3	236303.2
28MW0027B	297	864412.6	236303.1
28MW0032A	298	865132.8	233697
28MW0032B	299	865132.7	233697.2
28MW0032C	300	865130	233711.7
28MW0033A	301	865643.4	233205.7
28MW0033B	302	865643.2	233205.5
28MW0033C	303	865636.7	233216.4
28MW0034A	304	865905.8	232813.9
28MW0034B	305	865906.2	232813.7

28MW0035A	306	866245	232256.1

Table 2-2. Eastern Briarwood Well Locations Used for Spatial Analysis

Well ID	Well Number	Easting	Northing
28MW0035B	307	866244.7	232256.2
28MW0035C	308	866241.7	232249.4
28MW0037A	309	866502.7	232729.7
28MW0037B	310	866503.1	232730
28MW0571	314	866775	233079
28MW0572	315	865371.4	232860.5
28MW0573	316	864552.2	236273.8
28MW0574	317	864960.2	236786.3
28MW0575	318	864511.4	235807.6
28MW0577B	319	864783	237308
28MW0579A	320	865319	237889
28MW0580	321	864717	238370
28MW0587	322	865135	236244
28MW0588	323	865146	236216
28MW0589	324	865109	236258
28MW0590	325	865141	236171
28MW0591A	326	865316	236162
28MW0591E	327	865316.2	236161.8
28MW0591F	328	865316	236160.8
28MW0592A	329	864855.1	236303.5
28MW0592B	330	864855.1	236303.1
28MW0592C	331	864859.3	236310.8
28MW0593A	332	865046.7	236229.8
28MW0593B	333	865046.7	236229
28MW0593C	334	865050.9	236238.1
28MW0594A	335	865054.3	236152.4
28MW0594B	336	865054.3	236152.1
28MW0594C	337	865047.8	236155.3
28MW0595A	338	864659	236138.8
28MW0595B	339	864659	236138.6
28MW0595C	340	864663.4	236144.1
28MW0596	341	865006.5	236770.9
28MW0602F	347	865996.9	232682.8
28PZ0583	348	865142	236242
28PZ0584	349	865062	236254
28PZ0585	350	865147	236171
28PZ0586	351	865142	236217
30MW0583A	352	862782	231438
30MW0583B	353	862776	231447
30MW0583C	354	862779	231442
30MW0583D	355	862784	231442
30MW0583E	356	862782	231446
30MW0591	357	862693	230134
37MW0002	358	867543	236492
37MW0004	359	867265	235982
39MW0002	360	864230.5	238521.9
39MW0004	361	864258.8	238090.1
39MW0005A	363	864238.5	237924.4
91MW0315A	367	865468.9	235216.9
91MW0315B	368	865470.5	235222.6
91MW0317	369	865116	236253
91MW0522A	370	864833.1	234002.3
91MW0522B	371	864831.6	234006.7
91MW0522C	372	864829.6	234009.1
91MW0522D	373	864828.5	234012.6
91MW0522Y	374	864827	234019
91WT0004	375	867848	235548
95MW0214A	376	863100.3	228842.4
95MW0215A	377	863096.6	228834.4
98MW0001	378	867596	237670

ECMWAMP05A	381	863567	234405.4

Table 2-2. Eastern Briarwood Well Locations Used for Spatial Analysis

Well ID	Well Number	Easting	Northing
ECMWAMP05B	382	863567.2	234405.2
ECMWEAP01	383	865059.6	235552.6
ECMWEAP02	384	865063.5	235556.7
ECPZAMP02A	385	863410.1	233464.2
ECPZAMP02C	386	863509.6	233380
ECPZAMP02D	387	863563.2	233341.7
ECPZEAP01	388	864930.7	235434.3
ECPZJNP01A	389	866615.6	232407
ECPZJNP01C	390	866767.4	232459.6
ECPZJNP01D	391	866831.6	232453.8
ECPZVP101	392	864222.6	235185.9
ECPZVP102	393	864225.5	235187.5
ECPZVP301	394	866209.6	226198
H3WT0017	395	871318	231028
H3WT0020	396	869804	228928
MAMW0196D	397	868275	225479
MAMW0296I	398	868280	225485
MAMW0396S	399	868285	225490
MAMW0512D	402	867325	235466
MAMW0513A	404	865676	235838
MAMW0514C	406	863747.6	235366
MAMW0514D	407	863751.5	235368.8
MAMW0515A	408	868766	235409
MAMW0515B	409	868766	235409
MAMW0518A	412	865617.7	234276.5
MAMW0518C	413	865620.6	234286.5
MAMW0519B	414	865225.4	234245.8
USFW348078	415	862672	230099.1

Table 3-1. FS-12 Global Kriging Weights

Well Number	Easting	Northing	EDB wgt	BZ wgt
1	867579	252465	0.00167	0.00153
4	867448.62	252455.8	0.00132	0.00138
5	868071	252332	0.00338	0.00454
6	868225	252305	0.0016	0.00161
7	868342	252300.7	0.00109	0.00041
8	868469.31	252246.8	0.00095	0.00045
9	868596.12	252821.7	0.0041	0.00567
10	868636.38	252655.8	0.00304	0.00346
11	868630.81	252505.91	0.00179	0.00207
12	868601	252415.8	0.00135	0.00109
13	868543.31	252256.41	0.00432	0.00429
14	868532.69	252050.2	0.00123	0.00101
15	868539.38	251933.41	0.00147	0.00116
16	868617.81	251793.3	0.00182	0.00171
17	868811.38	251717	0.00311	0.00366
18	868923.5	251408.8	0.00619	0.00814
19	868784	250494.41	0.00415	0.00538
20	868890	250568.8	0.00258	0.00304
21	869020.69	250621.41	0.00181	0.00191
22	869133.69	250678.5	0.00172	0.00106
23	869255.12	250728.59	0.00166	0.00155
24	869400	250795.41	0.00153	0.00158
25	869557.88	250866.5	0.00175	0.00145
26	869687.31	250926.59	0.00404	0.00412
27	869818.69	250999	0.00203	0.00227
28	869916.38	251112.59	0.00347	0.00342
29	870043.12	251155.2	0.00442	0.006
30	869662.31	250130.59	0.00432	0.00424
31	869662.88	250135.5	0.00478	0.00476
32	869657.5	250137	0.00461	0.00596
33	870035.69	250041.59	0.00803	0.01057
34	870042.12	250054.7	0.00816	0.01012
35	869005.88	250271.59	0.0084	0.00902
40	868100.38	251174.59	0.01267	0.01536
43	868194	253687	0.00383	0.00186
44	868186	253695	0.00394	0.00222
45	868600.31	252861.59	0.03752	0.03919
46	867294.81	253314.5	0.06036	0.05924
48	868602.38	252853.41	0.03745	0.03805
49	868420.38	252285.2	0.00252	0.00089
50	868181.62	253701.09	0.00392	0.00211
51	868177.62	253707.7	0.00395	0.00205
52	868157.38	252314.3	0.0063	0.00393
53	867959	251902	0.00492	0.00248
54	867958	251907	0.00489	0.00266
55	868626.69	252162.3	0.00246	0.00134
56	867839	254731	0.0035	0.00177
57	867351	254509	0.00541	0.00269
58	867956.69	251912.91	0.02327	0.02316
59	868620.12	252165.41	0.00577	0.0054
60	868414	252288	0.00254	0.00085
61	868912	252091	0.00517	0.00284
62	868025.12	253982.3	0.00591	0.00407
63	869057	251880	0.0382	0.0428
64	867576.62	254657.2	0.00418	0.00214
65	867113	254101	0.01233	0.00742
68	867930	254760	0.0037	0.00155
69	869268	251765.09	0.00765	0.00491
70	868877	251335	0.0196	0.01497

Table 3-1. FS-12 Global Kriging Weights

Well Number	Easting	Northing	EDB wgt	BZ wgt
71	869111.31	251305.59	0.00983	0.00573
72	868480.5	251376.3	0.02421	0.02236
73	869429.88	251262.59	0.02539	0.02265
74	867937	255042	0.00345	0.00376
75	869914	252110	0.066	0.07492
76	868645	253868	0.00939	0.01064
77	867392	252463	0.00127	0.00109
79	869028.62	250984.91	0.00681	0.00791
80	870394	251163	0.02257	0.02739
81	868811	250486	0.0028	0.00251
82	868493.31	251370.59	0.00251	0.00308
83	868008.12	251365.41	0.00205	0.00189
84	868343.88	250978.8	0.00965	0.00955
85	869430.81	250840.91	0.00614	0.0041
86	866999.81	252663.5	0.00414	0.00513
87	869417.81	250870.2	0.00463	0.00296
88	868821.12	250476.59	0.00196	0.00136
89	869000.62	250268.91	0.00233	0.00316
90	868487.31	250369.09	0.00473	0.00589
91	869562	252128	0.00609	0.00708
92	867965	254429.3	0.007	0.00764
93	867495.31	252977.91	0.00217	0.00114
94	870280.38	250673.91	0.00707	0.00859
95	870286.81	250668.09	0.00695	0.00735
96	870709	251100.3	0.0041	0.00417
97	869438.31	250478.5	0.00521	0.00517
98	869443.81	250473.2	0.00519	0.00621
99	870166.5	251148.41	0.00316	0.00349
100	869837.38	250521.59	0.00561	0.00644
101	867187	252391	0.0031	0.00371
102	867726.81	253039.3	0.04735	0.05274
103	867890.38	253039.3	0.00341	0.00455
104	867428	252519	0.00126	0.00123
105	869021.19	250979.7	0.00684	0.00717
106	870269.12	250683.3	0.00707	0.00781
107	869195.62	250677.91	0.00612	0.00618
108	869754.88	250936.91	0.00593	0.00623
109	869758.62	250932.3	0.00592	0.00769
110	869762.38	250920.2	0.00224	0.00299
111	867908	252359.8	0.04428	0.04949
112	869428.62	251267	0.01102	0.01521
113	869448.81	250477.5	0.0038	0.0046
114	869838.5	250533.91	0.00367	0.00201
115	869844.12	250533.8	0.00369	0.00278
116	868552.69	250328.3	0.01976	0.02392
117	868552.69	250328.2	0.01479	0.0166
118	870189.5	251651.91	0.00334	0.00345
119	870189.19	251651.91	0.00334	0.00356
120	870185.38	251645.41	0.00333	0.00313
121	870185.5	251645.59	0.00333	0.00325
122	870406.31	250946.09	0.00205	0.00266
123	870406.12	250945.8	0.00086	0.00106
124	870401.69	250701	0.00141	0.00053
125	870401.5	250700.8	0.00057	0.00012
126	870330.19	250398.2	0.00086	0.00147
127	870330.31	250397.91	0.00029	0.00052
128	870338.38	250399.3	0.00031	0.00038
129	870338.69	250398.91	0.00083	0.0013
130	870345.31	250400.2	0.00094	0.00162

Table 3-1. FS-12 Global Kriging Weights

Well Number	Easting	Northing	EDB wgt	BZ wgt
131	870345.62	250400.3	0.00094	0.00158
132	870194	250159.91	0.00096	0.00082
133	870193.88	250159.59	0.00035	0.00005
134	870192.12	250153	0.00031	0.00043
135	870191.88	250153.09	0.00032	0.00038
136	870190	250146.2	0.00028	0.00036
137	870190.19	250146.5	0.00028	0.00036
138	870190	249993.59	0.00089	0.00079
139	870190.19	249993.8	0.00089	0.00079
140	869198.5	249986.5	0.0014	0.00149
141	869198.38	249986	0.0014	0.00138
142	869196.88	249979.59	0.00054	0.00049
143	869196.81	249979.41	0.00054	0.00049
144	868669	252489	0.00434	0.00162
145	869383	254876	0.01524	0.00845
146	868021	254790	0.00391	0.00214
147	867403	254543	0.00456	0.00243
148	866891.62	253392.3	0.01086	0.00597
149	868406	255096	0.00498	0.00312
154	868411	254735	0.00563	0.00641
206	868027.88	251147.5	0.00685	0.00729
207	868027.88	251147.59	0.00446	0.0051
208	866553	249864.59	0.0028	0.00308
209	867774.38	251900	0.00234	0.00251
210	867774.38	251900	0.00613	0.00741
211	867564.19	251608.09	0.00326	0.00391
212	867252.81	251095.7	0.00474	0.00549
213	866657.62	250830.09	0.00534	0.00604
214	867635.62	251055.41	0.00355	0.00379

Table 3-2. Eastern Briarwood Global Kriging Weights

Well Number	Easting	Northing	TCE wgt	PCE wgt
1	866993.38	232153.59	0.00447	0.0042
5	865768	230847.59	0.00515	0.00515
7	867177.88	232854.41	0.00458	0.00429
9	870005.38	226494.2	0.00608	0.00608
10	863783.31	229647.59	0.00655	0.00655
13	869979	233205	0.00483	0.00426
24	866023.81	232685.3	0.00036	0.00051
25	866023.5	232678.91	0.00036	0.00051
26	866021	232672.8	0.00034	0.00048
29	866878.31	232847.59	0.00066	0.00082
30	866879.19	232841.91	0.00065	0.00082
32	866411.88	232504.41	0.00108	0.00108
33	866407.62	232512	0.00446	0.00469
34	866387.88	232514.3	0.00474	0.0049
35	866380.69	232498.5	0.00431	0.00437
36	864159.88	235065.91	0.02422	0.02382
37	864498.81	234302.3	0.00381	0.00337
38	864493.19	234304.09	0.0028	0.00266
39	866722	236583	0.04521	0.04484
40	867657	237110	0.0321	0.03244
43	867799	235170	0.00385	0.00364
44	867791	235189	0.00388	0.00441
46	868288	235243	0.00147	0.00141
47	868293	235249	0.00893	0.00854
48	869499	235753	0.00538	0.00538
50	868118.5	233600.3	0.01824	0.01824
51	868112.69	233606.09	0.00113	0.00116
52	868109.88	233609.41	0.01666	0.01657
53	868115.38	233602.91	0.00394	0.00397
54	868104.88	233615.59	0.00148	0.00151
57	867204.62	232832	0.00102	0.00102
58	867200.12	232834.41	0.00086	0.00086
59	867197	232836.8	0.00086	0.00087
60	867194.5	232838.5	0.00694	0.00684
61	868819	234137	0.00761	0.00808
63	868818	234131	0.01215	0.01231
64	869232.31	233644.2	0.01186	0.01054
65	869848.38	233455.09	0.00094	0.00148
66	869844.19	233452.7	0.00126	0.00188
67	869839.69	233450.3	0.00357	0.00457
68	869834.88	233447.8	0.0027	0.0035
69	867668	234817	0.02146	0.02062
71	865546.88	233699	0.00297	0.00272
72	865539.5	233701	0.00934	0.00915
73	865219.69	233426.09	0.00229	0.00242
74	865230.12	233420.2	0.00213	0.0023
75	866254	232304.09	0.00071	0.00076
76	869666	231816	0.00725	0.00702
77	869670	231835	0.002	0.00199
78	869667	231825	0.00198	0.00199
83	869292.31	231251.09	0.00498	0.00517
84	869295.81	231246.91	0.00146	0.00146
85	869306.81	231240.59	0.00511	0.00517
86	869306.81	231240.7	0.0051	0.00517
87	871337	231014	0.00317	0.00316
90	869459	234553	0.02453	0.02292
92	869522.31	233158.59	0.00861	0.00845
93	869513.62	233161.8	0.00164	0.00144
94	869517.62	233160	0.00809	0.0081
95	866074.88	231916.59	0.00167	0.00144

Table 3-2. Eastern Briarwood Global Kriging Weights

Well Number	Easting	Northing	TCE wgt	PCE wgt
96	865915.81	231625.09	0.00061	0.00058
97	868445	235487	0.01124	0.01182
98	869802	233910	0.00991	0.00862
99	869238	233971	0.01085	0.0107
100	868951	234618	0.01333	0.014
101	868941	234608	0.01257	0.01295
103	869436.62	233553.3	0.0005	0.00064
104	869436.31	233553.2	0.0005	0.00062
105	869435.38	233560.41	0.00122	0.00144
106	869435.69	233560.3	0.00122	0.00144
107	869992.19	233638.3	0.00072	0.0008
108	869991.88	233638.2	0.00123	0.00135
109	869992.88	233651.41	0.00123	0.00127
110	869992.69	233651.41	0.00068	0.00072
111	869791.88	233904.2	0.00056	0.00062
112	869795.88	233914.2	0.00051	0.00056
113	869791.81	233904.09	0.00132	0.00131
114	869795.88	233914	0.00125	0.00125
115	869295.19	234001.09	0.00068	0.00075
116	869295.12	234001	0.0019	0.00186
117	868451.81	235489.7	0.00105	0.0012
118	868451.5	235489.59	0.00159	0.00178
119	868457	235501.91	0.0016	0.00178
121	864599.69	230160.3	0.00008	0.00008
122	864595.62	230164.09	0.00008	0.00008
123	864599.69	230160.2	0.00008	0.00008
128	868211.5	229136.91	0.00023	0.00023
131	869057.38	230335.5	0.00321	0.00318
132	869061.69	230339	0.00711	0.00707
133	869057.38	230335.41	0.00321	0.00318
134	867177.88	232854.41	0.00081	0.00084
135	867177.88	232854.3	0.00081	0.00084
136	870295.5	228166	0.00609	0.00608
140	863783.31	229647.59	0.00641	0.0064
146	868010.19	225507.5	0.00005	0.00012
148	864304.12	226576.2	0.00655	0.00655
150	866619.31	232374.91	0.00184	0.00203
153	863918.38	235133.3	0.00142	0.00153
165	862798.19	233346.3	0.00404	0.00398
171	863056.69	234642.09	0.00253	0.0025
172	863068.19	234662.91	0.00058	0.00058
173	862866.62	235378.59	0.0003	0.00037
175	862852.69	235391.09	0.00018	0.00018
176	863271.81	235420.41	0.0014	0.00123
177	863704.69	235203	0.00127	0.00136
178	864235.5	234679.09	0.00622	0.0061
179	863586.31	234405.3	0.00526	0.00466
180	863279.88	233685.09	0.01127	0.01119
181	863051	236848	0.00608	0.00608
183	863592	236328	0.00903	0.00857
185	862625.62	234502.8	0.00035	0.00035
186	862625.5	234502.5	0.00217	0.00178
187	863887.62	235497.41	0.00278	0.00291
188	863880.88	235496.7	0.00118	0.00131
189	862703.62	236189.8	0.00412	0.00402
190	862703.38	236189.41	0.00155	0.00144
198	862824	235424.09	0.00045	0.00052
200	862849.62	235412.5	0.00043	0.00048
202	862870.31	235401.8	0.00036	0.00048
203	862866.5	235397.91	0.00035	0.00037

204	862870.12	235402.09	0.00037	0.0005

Table 3-2. Eastern Briarwood Global Kriging Weights

Well Number	Easting	Northing	TCE wgt	PCE wgt
209	862909.69	235382.3	0.0004	0.00047
210	862904.69	235384.91	0.00043	0.00052
223	863037.62	234825.41	0.00041	0.00051
224	863037.88	234825.5	0.00038	0.00049
225	863056	234818.3	0.00043	0.00062
226	863061	234815.91	0.00046	0.00064
228	863061.19	234815.59	0.00045	0.00061
230	863084.31	234804.41	0.00042	0.00056
239	863156.5	234854.09	0.00034	0.00035
240	863156.31	234854.3	0.00036	0.00036
241	863147.69	234726	0.00075	0.00093
242	863148	234726	0.00076	0.00093
244	862926.81	235287.59	0.00036	0.00039
246	862967.19	235418.09	0.0007	0.0006
247	862805.62	235548.91	0.00106	0.00095
248	862805.62	235549.2	0.00104	0.00091
249	862971.12	235003.3	0.00048	0.0004
250	862970.81	235003.41	0.00052	0.00044
251	862832	235436.5	0.00053	0.00063
252	862831.88	235436.5	0.00053	0.00063
253	862913.62	235397.2	0.00039	0.00049
254	862913.5	235397.09	0.00039	0.00049
255	863020.31	234847.59	0.00037	0.00044
256	863020.19	234847.5	0.00016	0.00021
257	863112.5	234809.2	0.0002	0.00029
258	863112.38	234809.09	0.00023	0.00034
261	866361.19	232526.09	0.0056	0.0057
262	865682.81	236025.41	0.00057	0.00058
263	864194.62	237708	0.00216	0.00214
264	864910	236322	0.00029	0.00045
265	864679	236240	0.00113	0.00103
266	865379	236161	0.0001	0.00011
267	865308	236186	0.00007	0.00011
268	865250	236205	0.00004	0.00011
269	865197	236227	0.00009	0.00011
270	865138	236256	0.00014	0.0002
271	865056	236273	0.00013	0.00026
272	864976	236298	0.00018	0.00026
273	864910	236340	0.00022	0.00036
274	864839	236359	0.00023	0.00038
275	864769	236391	0.00037	0.00045
276	865138.38	236255.5	0.00089	0.00111
284	865455	236170	0.00229	0.00225
285	864874	236346	0.00132	0.00207
287	864748.5	236642.41	0.00379	0.00454
288	864741	236647.91	0.00382	0.00456
289	864747.5	236650.41	0.0009	0.00087
290	864574.88	236707.8	0.00618	0.00624
291	863963	237103	0.02427	0.02259
292	864213	236929	0.00958	0.00949
294	864297.31	237188.91	0.00213	0.00193
295	864297.12	237188.7	0.00414	0.00383
296	864412.31	236303.2	0.00075	0.00068
297	864412.62	236303.09	0.00186	0.00154
298	865132.81	233697	0.00642	0.00657
299	865132.69	233697.2	0.0007	0.00084
300	865130	233711.7	0.00069	0.00082
301	865643.38	233205.7	0.00449	0.00441
302	865643.19	233205.5	0.00077	0.00078
303	865636.69	233216.41	0.00075	0.00076

304	865905.81	232813.91	0.004	0.00414

Table 3-2. Eastern Briarwood Global Kriging Weights

Well Number	Easting	Northing	TCE wgt	PCE wgt
305	865906.19	232813.7	0.00063	0.00064
306	866245	232256.09	0.00036	0.00041
307	866244.69	232256.2	0.00035	0.00043
308	866241.69	232249.41	0.00038	0.0004
309	866502.69	232729.7	0.00153	0.00129
310	866503.12	232730	0.00153	0.00127
314	866775	233079	0.00214	0.0018
315	865371.38	232860.5	0.00626	0.00569
316	864552.19	236273.8	0.00598	0.00557
317	864960.19	236786.3	0.00656	0.00568
318	864511.38	235807.59	0.01195	0.00969
319	864783	237308	0.00079	0.00088
320	865319	237889	0.00677	0.00675
321	864717	238370	0.00478	0.00462
322	865135	236244	0.00015	0.00019
323	865146	236216	0.00009	0.00009
324	865109	236258	0.00014	0.00023
325	865141	236171	0.00036	0.00035
326	865316	236162	0.00003	0.00007
327	865316.19	236161.8	0.00012	0.00014
328	865316	236160.8	0.00012	0.00014
329	864855.12	236303.5	0.00028	0.00062
330	864855.12	236303.09	0.00029	0.00061
331	864859.31	236310.8	0.00023	0.00062
332	865046.69	236229.8	0.00021	0.00037
333	865046.69	236229	0.00021	0.00034
334	865050.88	236238.09	0.00019	0.00032
335	865054.31	236152.41	0.00026	0.00031
336	865054.31	236152.09	0.00026	0.00032
337	865047.81	236155.3	0.0003	0.00037
338	864659	236138.8	0.00081	0.00103
339	864659	236138.59	0.00081	0.00103
340	864663.38	236144.09	0.00073	0.00093
341	865006.5	236770.91	0.00313	0.0027
347	865996.88	232682.8	0.00597	0.00597
348	865142	236242	0.00101	0.00124
349	865062	236254	0.00015	0.00027
350	865147	236171	0.00035	0.00032
351	865142	236217	0.00104	0.00124
352	862782	231438	0.00099	0.00098
353	862776	231447	0.00106	0.00106
354	862779	231442	0.00098	0.00098
355	862784	231442	0.00106	0.00106
356	862782	231446	0.00105	0.00106
357	862693	230134	0.00468	0.00468
358	867543	236492	0.03015	0.03018
359	867265	235982	0.01234	0.01271
360	864230.5	238521.91	0.00897	0.00864
361	864258.81	238090	0.01588	0.01667
363	864238.5	237924.41	0.01824	0.01815
367	865468.88	235216.91	0.0017	0.00163
368	865470.5	235222.59	0.00169	0.00163
369	865116	236253	0.00016	0.00026
370	864833.12	234002.3	0.00189	0.002
371	864831.62	234006.7	0.0057	0.00585
372	864829.62	234009.09	0.0057	0.00585
373	864828.5	234012.59	0.00097	0.00094
374	864827	234019	0.00567	0.00585

Table 3-2. Eastern Briarwood Global Kriging Weights

Well Number	Easting	Northing	TCE wgt	PCE wgt
375	867848	235548	0.00108	0.00104
376	863100.31	228842.41	0.00652	0.00651
377	863096.62	228834.41	0.00649	0.00651
378	867596	237670	0.03779	0.03744
381	863567	234405.41	0.00166	0.00162
382	863567.19	234405.2	0.00167	0.00162
383	865059.62	235552.59	0.00129	0.00152
384	865063.5	235556.7	0.00129	0.00152
385	863410.12	233464.2	0.00283	0.00277
386	863509.62	233380	0.00238	0.00242
387	863563.19	233341.7	0.00274	0.00277
388	864930.69	235434.3	0.00249	0.00224
389	866615.62	232407	0.00145	0.00144
390	866767.38	232459.59	0.00152	0.00164
391	866831.62	232453.8	0.00181	0.00199
392	864222.62	235185.91	0.00241	0.00279
393	864225.5	235187.5	0.00239	0.00279
394	866209.62	226198	0.00632	0.00632
395	871318	231028	0.00339	0.00339
396	869804	228928	0.00561	0.00562
397	868275	225479	0.00044	0.00043
398	868280	225485	0.00045	0.00043
399	868285	225490	0.0007	0.00066
402	867325	235466	0.00369	0.00359
404	865676	235838	0.01637	0.01593
406	863747.62	235366	0.0062	0.0063
407	863751.38	235368.8	0.01042	0.01005
408	868766	235409	0.00339	0.00324
409	868766	235409	0.00272	0.0024
412	865617.69	234276.5	0.00192	0.00188
413	865620.62	234286.5	0.00194	0.00188
414	865225.38	234245.8	0.00173	0.00164
415	862672	230099.09	0.00468	0.00468

Table 3-3. Changes in Global Kriging Variance by Threshold

	Global KV	Relative Change	Global KV	Relative Change
	EDB (FS-12)		Benzene (FS-12)	
Baseline	.18618	—	.01902	—
Threshold 1	.18690	+0.4%	.01890	–0.2%
Threshold 2	.18814	+1.1%	.01920	+0.9%
Threshold 3	.19005	+2.1%	.01959	+3.0%
Threshold 4	.19395	+4.2%	.02021	+6.3%
Threshold 5	.19617	+5.4%	.02064	+8.5%
Threshold 6	.19572	+5.1%	.02208	+10.8%
	TCE (Eastern Briarwood)		PCE (Eastern Briarwood)	
Baseline	.05995	—	.28010	—
Threshold 1	.06123	+2.1%	.27387	–2.2%
Threshold 2	.06121	+2.1%	.27517	–1.8%
Threshold 3	.06127	+2.2%	.27999	–0.0%
Threshold 4	.06336	+5.7%	.28318	+1.1%
Threshold 5	.06447	+7.5%	.28745	+2.6%
Threshold 6	.06609	+10.2%	.29184	+4.2%

Table 3-4. Spatially Redundant Wells at FS-12

Well ID	Well Number	Easting	Northing	EDB Wgt	Benzene Wgt
90BH0073	1	867579	252465	0.00167	0.00153
90EW0002	4	867448.62	252455.8	0.00132	0.00138
90EW0007	6	868225	252305	0.0016	0.00161
90EW0008	7	868342	252300.7	0.00109	0.00041
90EW0009	8	868469.31	252246.8	0.00095	0.00045
90EW0013	12	868601	252415.8	0.00135	0.00109
90EW0015	14	868532.69	252050.2	0.00123	0.00101
90EW0016	15	868539.38	251933.41	0.00147	0.00116
90EW0017	16	868617.81	251793.3	0.00182	0.00171
90EW0022	21	869020.69	250621.41	0.00181	0.00191
90EW0023	22	869133.69	250678.5	0.00172	0.00106
90EW0024	23	869255.12	250728.59	0.00166	0.00155
90EW0025	24	869400	250795.41	0.00153	0.00158
90EW0026	25	869557.88	250866.5	0.00175	0.00145
90MW0035	77	867392	252463	0.00127	0.00109
90MW0056	88	868821.12	250476.59	0.00196	0.00136
90MW0072A	104	867428	252519	0.00126	0.00123
90MW0087B	123	870406.12	250945.8	0.00086	0.00106
90MW0088A	124	870401.69	250701	0.00141	0.00053
90MW0088B	125	870401.5	250700.8	0.00057	0.00012
90MW0089A	126	870330.19	250398.2	0.00086	0.00147
90MW0089B	127	870330.31	250397.91	0.00029	0.00052
90MW0089C	128	870338.38	250399.3	0.00031	0.00038
90MW0089D	129	870338.69	250398.91	0.00083	0.0013
90MW0089E	130	870345.31	250400.2	0.00094	0.00162
90MW0089F	131	870345.62	250400.3	0.00094	0.00158
90MW0090A	132	870194	250159.91	0.00096	0.00082
90MW0090B	133	870193.88	250159.59	0.00035	0.00005
90MW0090C	134	870192.12	250153	0.00031	0.00043
90MW0090D	135	870191.88	250153.09	0.00032	0.00038
90MW0090E	136	870190	250146.2	0.00028	0.00036
90MW0090F	137	870190.19	250146.5	0.00028	0.00036
90MW0091A	138	870190	249993.59	0.00089	0.00079
90MW0091B	139	870190.19	249993.8	0.00089	0.00079
90MW0091C	140	869198.5	249986.5	0.0014	0.00149
90MW0091D	141	869198.38	249986	0.0014	0.00138
90MW0091E	142	869196.88	249979.59	0.00054	0.00049
90MW0091F	143	869196.81	249979.41	0.00054	0.00049

Table 3-5. Spatially Redundant Wells at Eastern Briarwood

Well ID	Well Number	Easting	Northing	TCE Wgt	PCE Wgt
00MW0524A	24	866023.81	232685.3	0.00036	0.00051
00MW0524B	25	866023.5	232678.91	0.00036	0.00051
00MW0524C	26	866021	232672.8	0.00034	0.00048
00MW0572A	103	869436.62	233553.3	0.0005	0.00064
00MW0572B	104	869436.31	233553.2	0.0005	0.00062
00MW0580B	121	864599.69	230160.3	0.00008	0.00008
00MW0580C	122	864595.62	230164.09	0.00008	0.00008
00MW0580D	123	864599.69	230160.2	0.00008	0.00008
00MW0583A	128	868211.5	229136.91	0.00023	0.00023
00MW0591B	146	868010.19	225507.5	0.00005	0.00012
03MW0057A	173	862866.62	235378.59	0.0003	0.00037
03MW0057Z	175	862852.69	235391.09	0.00018	0.00018
03MW0104A	185	862625.62	234502.8	0.00035	0.00035
03MW0202G	198	862824	235424.09	0.00045	0.00052
03MW0203E	200	862849.62	235412.5	0.00043	0.00048
03MW0204C	202	862870.31	235401.8	0.00036	0.00048
03MW0204D	203	862866.5	235397.91	0.00035	0.00037
03MW0204F	204	862870.12	235402.09	0.00037	0.0005
03MW0206F	209	862909.69	235382.3	0.0004	0.00047
03MW0206G	210	862904.69	235384.91	0.00043	0.00052
03MW0211C	223	863037.62	234825.41	0.00041	0.00051
03MW0211E	224	863037.88	234825.5	0.00038	0.00049
03MW0212B	225	863056	234818.3	0.00043	0.00062
03MW0212C	226	863061	234815.91	0.00046	0.00064
03MW0212F	228	863061.19	234815.59	0.00045	0.00061
03MW0213E	230	863084.31	234804.41	0.00042	0.00056
03MW0219C	239	863156.5	234854.09	0.00034	0.00035
03MW0219E	240	863156.31	234854.3	0.00036	0.00036
03MW0221F	244	862926.81	235287.59	0.00036	0.00039
03MW0224C	249	862971.12	235003.3	0.00048	0.0004
03RW0002EF	253	862913.62	235397.2	0.00039	0.00049
03RW0002IN	254	862913.5	235397.09	0.00039	0.00049
03RW0003EF	255	863020.31	234847.59	0.00037	0.00044
03RW0003IN	256	863020.19	234847.5	0.00016	0.00021
03RW0004EF	257	863112.5	234809.2	0.0002	0.00029
03RW0004IN	258	863112.38	234809.09	0.00023	0.00034
28BH0581	264	864910	236322	0.00029	0.00045
28EW0001	266	865379	236161	0.0001	0.00011
28EW0002	267	865308	236186	0.00007	0.00011
28EW0003	268	865250	236205	0.00004	0.00011
28EW0004	269	865197	236227	0.00009	0.00011
28EW0005	270	865138	236256	0.00014	0.0002
28EW0006	271	865056	236273	0.00013	0.00026
28EW0007	272	864976	236298	0.00018	0.00026
28EW0008	273	864910	236340	0.00022	0.00036
28EW0009	274	864839	236359	0.00023	0.00038
28EW0010	275	864769	236391	0.00037	0.00045
28MW0035A	306	866245	232256.09	0.00036	0.00041
28MW0035B	307	866244.69	232256.2	0.00035	0.00043
28MW0035C	308	866241.69	232249.41	0.00038	0.0004
28MW0587	322	865135	236244	0.00015	0.00019
28MW0588	323	865146	236216	0.00009	0.00009
28MW0589	324	865109	236258	0.00014	0.00023
28MW0590	325	865141	236171	0.00036	0.00035
28MW0591A	326	865316	236162	0.00003	0.00007
28MW0591E	327	865316.19	236161.8	0.00012	0.00014
28MW0591F	328	865316	236160.8	0.00012	0.00014
28MW0592A	329	864855.12	236303.5	0.00028	0.00062
28MW0592B	330	864855.12	236303.09	0.00029	0.00061

Table 3-5. Spatially Redundant Wells at Eastern Briarwood

Well ID	Well Number	Easting	Northing	TCE Wgt	PCE Wgt
28MW0592C	331	864859.31	236310.8	0.00023	0.00062
28MW0593A	332	865046.69	236229.8	0.00021	0.00037
28MW0593B	333	865046.69	236229	0.00021	0.00034
28MW0593C	334	865050.88	236238.09	0.00019	0.00032
28MW0594A	335	865054.31	236152.41	0.00026	0.00031
28MW0594B	336	865054.31	236152.09	0.00026	0.00032
28MW0594C	337	865047.81	236155.3	0.0003	0.00037
28PZ0584	349	865062	236254	0.00015	0.00027
28PZ0585	350	865147	236171	0.00035	0.00032
91MW0317	369	865116	236253	0.00016	0.00026
MAMW0196D	397	868275	225479	0.00044	0.00043
MAMW0296I	398	868280	225485	0.00045	0.00043

Table 2-3. Sampling Events/Results Thinned from EDB Wells at FS-12

Well Number	N	ND Fraction	Group Interval	Sen's Slope (M)	M Lower Bnd	M Upper Bnd	Thin Fraction	Current Interval	Optimal Interval
4	32	0.875	1.00	0.00000	0.00000	0.00000	0.562	1.00	2.29
13	25	0.560	1.00	0.88648	-2.59459	1.40541	0.800	63.00	315.00
18	20	0.250	1.00	76.00000	0.00000	96.00000	0.565	202.00	464.37
26	20	0.750	1.00	0.00000	0.00000	0.00355	0.705	202.00	684.75
40	26	0.846	1.00	0.00000	0.00000	0.00000	0.769	28.00	121.33
45	25	0.240	78.00	-0.08593	-0.13543	-0.00586	0.372	35.00	55.73
48	23	0.000	78.00	-0.07522	-0.10648	-0.04072	0.291	35.00	49.39
63	24	0.042	146.00	-0.05263	-0.10169	0.01897	0.204	35.00	43.98
70	20	0.400	70.00	-0.00001	-0.00098	0.00000	0.315	34.00	49.64
72	24	0.167	74.00	-0.01009	-0.04284	-0.00434	0.579	35.00	83.17
79	26	0.000	1.00	-0.00990	-0.23214	0.07018	0.035	35.00	36.25
84	23	0.435	1.00	-0.00007	-0.00018	0.00000	0.296	78.00	110.74
85	22	0.409	61.00	0.00033	0.00001	0.00107	0.364	40.00	62.86
100	44	0.909	69.00	0.00000	0.00000	0.00000	0.782	41.00	187.92
109	18	0.833	1.00	0.00000	0.00000	0.00000	0.606	49.00	124.23
162	8	0.125	1.00	0.06645	-1.76471	0.16387	0.113	17.00	19.15

Table 2-4. Sampling Events/Results Thinned from Benzene Wells at FS-12

Well Number	N	ND Fraction	Group Interval	Sen's Slope (M)	M Lower Bnd	M Upper Bnd	Thin Fraction	Current Interval	Optimal Interval
3	10	0.600	1.00	0.00000	0.00000	0.00000	0.800	0.00	0.00
4	16	0.812	1.00	-0.06000	-0.12000	0.00000	0.100	1.00	1.11
13	13	0.538	1.00	1.18919	0.00000	2.54098	0.615	63.00	163.80
45	12	0.000	74.00	-0.76923	-1.09375	-0.27778	0.458	35.00	64.62
48	12	0.000	69.00	-0.92531	-1.35593	-0.64815	0.383	35.00	56.76
58	9	0.333	1.00	0.00049	-0.00138	0.00056	0.278	104.00	144.00
63	13	0.077	146.00	0.00000	-0.61810	0.36574	0.177	35.00	42.52
103	10	0.700	1.00	0.00000	0.00000	-3.28767	0.000	49.00	49.00

Table 2-5. Sampling Events/Results Thinned from TCE Wells at EBW

Well Number	N	ND Fraction	Group Interval	Sen's Slope (M)	M Lower Bnd	M Upper Bnd	Thin Fraction	Current Interval	Optimal Interval
5	21	0.667	1.00	0.00000	0.00000	0.28000	0.495	1.00	1.98
10	29	0.862	1.00	0.00000	0.00000	0.00000	0.797	5.00	24.58
24	12	0.167	1.00	-0.00116	-0.00396	0.00092	0.250	436.00	581.33
25	10	0.000	1.00	0.01108	-0.02795	0.05008	0.320	436.00	641.18
33	15	0.000	1.00	-0.01005	-0.01290	-0.00651	0.387	160.00	260.87
39	10	0.100	92.00	-0.00227	-0.00396	-0.00118	0.540	90.00	195.65
67	17	0.588	176.00	-0.00266	-0.00531	-0.00103	0.524	102.00	214.07
74	12	0.083	1.00	0.00449	-0.00591	0.01280	0.208	456.00	576.00
75	8	0.000	1.00	0.00228	-0.00509	0.00490	0.113	460.00	518.31
90	13	0.077	1.00	-0.00072	-0.00189	-0.00046	0.315	94.00	137.30
97	15	0.000	1.00	-0.00683	-0.01569	-0.00160	0.473	82.00	155.70
99	25	0.280	1.00	0.00780	0.00521	0.01149	0.376	82.00	131.41
100	24	0.833	1.00	0.00000	0.00000	0.00000	0.733	82.00	307.50
101	10	0.200	1.00	0.01298	0.00894	0.01515	0.360	82.00	128.13
103	19	0.632	1.00	0.00000	-0.34333	0.00000	0.058	28.00	29.72
150	10	0.500	1.00	0.00000	0.00000	0.00000	0.800	0.00	0.00
171	10	0.000	1.00	0.93264	0.12077	1.15304	0.390	496.00	813.11
173	19	0.000	84.00	-1.62154	-2.40723	-0.42002	0.642	84.00	234.71
174	10	0.300	1.00	-0.00870	-0.21471	0.00908	0.110	30.00	33.71
175	48	0.188	42.00	-1.03540	-2.18072	-0.34427	0.644	502.00	1409.12
176	34	0.559	1.00	1.13889	0.39338	2.64815	0.332	543.00	813.30
177	30	0.600	1.00	0.03846	0.00203	0.11236	0.417	542.00	929.14
178	28	0.857	1.00	0.00206	0.00000	0.02143	0.564	117.00	268.52
179	34	0.647	1.00	0.11727	0.06981	0.19476	0.479	557.00	1069.94
180	30	0.233	1.00	0.14796	0.05238	0.33108	0.477	149.00	284.71
181	21	0.619	1.00	0.10458	0.00000	0.69091	0.476	184.00	351.27
185	23	0.783	1.00	0.00000	0.00000	0.00000	0.696	74.00	243.14
189	29	0.379	1.00	7.74000	1.28788	11.40000	0.479	88.00	169.01
192	25	0.640	1.00	0.00000	-0.00112	0.00000	0.464	29.00	54.10
193	16	0.000	1.00	-0.28295	-0.37424	-0.20000	0.419	30.00	51.61
194	13	0.000	1.00	-0.54573	-0.84848	-0.26923	0.477	30.00	57.35
197	12	0.000	1.00	0.26374	-0.75862	0.31746	0.058	29.00	30.80
198	18	0.000	80.00	-0.37092	-0.69357	-0.22914	0.478	80.00	153.19
199	18	0.000	1.00	-0.05621	-0.45714	-0.02155	0.428	29.00	50.68
200	21	0.000	1.00	-1.81293	-2.25806	-1.45648	0.476	87.00	166.09
202	20	0.700	1.00	0.00000	-0.13832	0.00000	0.205	85.00	106.92
203	24	0.000	1.00	-0.09282	-0.10932	-0.07296	0.496	86.00	170.58
204	20	0.000	1.00	0.00000	-1.79348	1.56946	0.040	86.00	89.58
205	14	0.714	1.00	0.00000	0.00000	0.00000	0.564	29.00	66.56
206	12	0.000	1.00	-0.83838	-3.32353	-0.43590	0.525	29.00	61.05
207	18	0.833	1.00	0.00000	0.00000	0.00000	0.544	25.00	54.88
209	46	0.000	1.00	-0.84519	-1.46429	0.33333	0.483	87.00	168.15
210	30	0.000	1.00	-0.49861	-0.54576	-0.42151	0.463	87.00	162.11
211	12	0.167	1.00	-0.05586	-0.77419	-0.00552	0.542	29.00	63.27
212	12	0.000	1.00	5.04132	3.26042	6.33333	0.550	29.00	64.44
213	14	0.286	1.00	-0.42198	-0.70968	0.03509	0.179	29.00	35.30
214	12	0.000	1.00	-1.57143	-5.17647	-0.19355	0.558	29.00	65.66
215	24	0.000	1.00	0.03252	-0.07143	0.08613	0.279	28.00	38.84
216	18	0.000	1.00	1.35593	0.54348	2.47059	0.461	29.00	53.81
217	12	0.000	1.00	-0.25974	-1.08029	-0.13636	0.483	28.00	54.19
218	14	0.000	1.00	0.04579	0.00459	0.08163	0.450	28.00	50.91
220	12	0.000	1.00	-6.31207	-7.31034	-2.86777	0.458	29.00	53.54
221	14	0.000	1.00	-0.53534	-1.03448	-0.45763	0.357	31.00	48.22
222	12	0.000	1.00	-0.06228	-0.14689	-0.04403	0.442	29.00	51.94
223	24	0.000	1.00	-0.23940	-0.27937	-0.21125	0.396	93.00	153.93

Table 2-5. Sampling Events/Results Thinned from TCE Wells at EBW

Well Number	N	ND Fraction	Group Interval	Sen's Slope (M)	M Lower Bnd	M Upper Bnd	Thin Fraction	Current Interval	Optimal Interval
224	22	0.000	1.00	0.90189	0.22581	2.16250	0.418	93.00	159.84
225	23	0.000	1.00	0.54910	-0.41935	1.05233	0.157	92.00	109.07
226	24	0.000	1.00	-0.42308	-0.93793	-0.22191	0.387	92.00	150.20
227	16	0.000	1.00	-0.47418	-3.65540	0.14800	0.100	30.00	33.33
228	20	0.000	1.00	-0.41284	-1.33929	0.15692	0.535	90.00	193.55
229	14	0.000	1.00	-1.08831	-3.00000	-0.66167	0.536	32.00	68.92
230	18	0.000	1.00	-1.07903	-4.41542	1.32196	0.322	91.00	134.26
232	14	0.143	1.00	-3.48940	-4.78431	-2.31071	0.571	28.00	65.33
233	18	0.000	1.00	1.69512	-8.21429	5.27132	0.233	35.00	45.65
234	21	0.429	1.00	-0.07708	-0.10000	-0.05313	0.610	28.00	71.71
235	12	0.000	1.00	-0.90435	-8.16287	-0.86129	0.383	30.00	48.65
236	14	0.000	1.00	-7.71134	-10.65289	-4.79839	0.536	30.00	64.62
237	14	0.000	1.00	-1.55473	-2.07941	-1.29677	0.464	34.00	63.47
238	12	0.000	1.00	-10.22917	-17.37121	-5.74725	0.450	34.00	61.82
239	20	0.000	1.00	-0.12500	-0.15203	-0.10455	0.590	90.00	219.51
240	16	0.000	1.00	-1.33628	-1.67299	-0.54839	0.425	90.00	156.52
241	16	0.000	1.00	0.02612	0.00852	0.04805	0.350	91.00	140.00
242	16	0.000	1.00	1.41935	-2.36181	3.64734	0.325	90.00	133.33
244	26	0.000	1.00	0.71239	0.48008	0.92762	0.769	87.00	377.00
246	17	0.000	1.00	-0.00086	-0.01250	0.00635	0.018	87.00	88.56
247	23	0.000	1.00	-0.11789	-0.12997	-0.10305	0.157	85.00	100.77
248	23	0.000	1.00	-5.59871	-7.18750	-4.32584	0.252	85.00	113.66
249	23	0.000	1.00	-2.06081	-2.68085	-1.71946	0.170	49.00	59.01
250	16	0.000	1.00	-5.15223	-6.52027	-4.39252	0.363	90.00	141.18
251	16	0.062	9.00	0.06897	-0.06863	0.40741	0.100	100.00	111.11
252	16	0.000	9.00	0.00000	-0.62593	4.44444	0.081	100.00	108.84
253	18	0.000	21.00	-0.06797	-0.42857	-0.04206	0.472	37.00	70.11
254	18	0.000	21.00	-0.96714	-5.23810	-0.47612	0.461	37.00	68.66
255	10	0.000	1.00	-0.05867	-0.09144	-0.02363	0.460	37.00	68.52
256	8	0.000	1.00	0.92308	0.00000	1.37019	0.400	416.00	693.33
261	18	0.389	1.00	0.00000	-0.61000	0.11040	0.211	3.00	3.80
264	17	0.824	1.00	0.00000	0.00000	0.00000	0.682	1.00	3.15
293	12	0.667	1.00	0.00000	0.00000	0.00000	0.000	98.00	98.00
298	24	0.500	1.00	-0.21120	-0.68200	0.00000	0.358	16.00	24.94
301	17	0.294	1.00	-0.88000	-2.05000	-0.07571	0.441	23.00	41.16
304	18	0.389	1.00	-0.67450	-3.41000	0.00000	0.400	26.00	43.33
306	25	0.360	1.00	0.02110	-0.03975	0.06643	0.300	19.00	27.14
317	24	0.167	92.00	0.01130	0.00112	0.01606	0.225	77.00	99.35
326	11	0.364	1.00	0.10000	-0.25000	0.16000	0.327	1.00	1.49
336	23	0.870	1.00	0.00000	0.00000	0.00000	0.691	76.00	246.20
341	18	0.333	1.00	0.03431	0.01399	0.06367	0.567	77.00	177.69
347	13	0.077	1.00	0.05000	-0.90000	0.53000	0.200	1.00	1.25
348	22	0.409	1.00	0.00000	-0.24615	0.00119	0.091	58.00	63.80
349	16	0.438	1.00	-0.94607	-39.30000	0.00000	0.250	27.00	36.00
350	16	0.375	1.00	0.00863	0.00000	0.00571	0.000	27.00	27.00
361	10	0.700	1.00	0.00000	-0.00144	0.00000	0.060	82.00	87.23
371	12	0.250	1.00	0.01058	-0.00581	0.01865	0.342	165.00	250.63
372	8	0.375	1.00	-0.02288	-0.02817	-0.01365	0.425	165.00	286.96
376	30	0.900	1.00	0.00000	0.00000	0.00000	0.800	18.00	90.00
378	10	0.100	1.00	-0.00094	-0.00200	-0.00038	0.470	83.00	156.60

Table 2-6. Sampling Events/Results Thinned from PCE Wells at EBW

Well Number	N	ND Fraction	Group Interval	Sen's Slope (M)	M Lower Bnd	M Upper Bnd	Thin Fraction	Current Interval	Optimal Interval
13	10	0.000	89.00	-0.00138	-0.00323	0.00054	0.270	91.00	124.66
24	12	0.333	1.00	0.00052	0.00000	0.00148	0.500	436.00	872.00
25	10	0.300	1.00	0.00000	-0.00071	0.00000	0.260	436.00	589.19
33	14	0.500	1.00	0.00000	-0.00058	0.00000	0.221	160.00	205.50
36	13	0.462	1.00	0.00130	0.00047	0.00220	0.438	77.00	137.12
39	10	0.500	92.00	-0.00033	-0.00115	0.00000	0.190	90.00	111.11
40	11	0.091	1.00	0.00018	-0.00022	0.00053	0.155	90.00	106.45
52	14	0.786	1.00	0.00000	0.00000	0.00000	0.650	171.00	488.57
63	11	0.182	1.00	-0.00038	-0.00146	0.00058	0.127	91.00	104.27
69	9	0.444	1.00	-0.00157	-0.00395	-0.00068	0.500	179.00	358.00
74	12	0.667	1.00	0.00000	0.00000	0.00000	0.525	456.00	960.00
75	8	0.000	1.00	-0.00360	-0.00624	0.00000	0.325	460.00	681.48
150	10	0.000	1.00	0.00000	0.00000	0.00000	0.800	0.00	0.00
171	10	0.300	1.00	0.00000	-0.00803	0.00427	0.050	496.00	522.11
173	18	0.556	84.00	0.00000	0.00000	0.01648	0.650	84.00	240.00
175	47	0.745	42.00	0.00000	0.00000	0.00000	0.764	502.00	2125.59
176	35	0.829	1.00	0.00000	0.00000	0.00000	0.571	543.00	1267.00
177	30	0.900	1.00	0.00000	0.00000	0.00000	0.800	542.00	2710.00
178	28	0.857	1.00	0.00051	0.00000	0.00071	0.461	117.00	216.95
179	34	0.912	1.00	0.00000	0.00000	0.00000	0.824	557.00	3156.33
180	30	0.867	1.00	0.00000	0.00000	0.00000	0.730	149.00	551.85
181	21	0.714	1.00	0.00000	0.00000	0.00828	0.695	184.00	603.75
189	29	0.552	1.00	0.57100	0.05615	1.36000	0.431	88.00	154.67
192	25	0.640	1.00	0.00000	-0.00110	0.00000	0.504	29.00	58.47
193	16	0.000	1.00	-0.01833	-0.01977	-0.00395	0.525	30.00	63.16
194	13	0.154	1.00	0.00025	-0.01545	0.00600	0.062	30.00	31.97
197	12	0.000	1.00	0.01959	0.00333	0.02979	0.425	29.00	50.43
198	18	0.000	80.00	-0.01387	-0.02919	-0.00545	0.467	80.00	150.00
200	21	0.286	1.00	0.01292	0.00000	0.02257	0.581	87.00	207.61
203	24	0.000	1.00	-0.00851	-0.01028	-0.00741	0.425	86.00	149.57
204	20	0.100	1.00	0.02559	-0.00393	0.04330	0.425	86.00	149.57
206	12	0.167	1.00	-0.01083	-0.09661	0.02228	0.217	29.00	37.02
209	46	0.087	1.00	0.00188	-0.01406	0.01371	0.093	87.00	95.97
210	30	0.200	1.00	0.00034	-0.00096	0.00748	0.290	87.00	122.54
212	12	0.333	1.00	0.05039	0.00628	0.06224	0.583	29.00	69.60
214	12	0.500	1.00	0.12857	0.00175	0.13235	0.550	29.00	64.44
215	24	0.750	1.00	0.00000	-0.00171	0.00000	0.392	28.00	46.03
216	18	0.167	1.00	0.03882	0.02685	0.05968	0.606	29.00	73.52
217	12	0.000	1.00	-0.00920	-0.02758	0.00781	0.342	28.00	42.53
218	14	0.143	1.00	0.00085	0.00000	0.00182	0.550	28.00	62.22
220	12	0.667	1.00	0.00000	-0.02500	0.00000	0.433	29.00	51.18
224	22	0.545	1.00	0.01094	0.00575	0.03981	0.441	93.00	166.34
225	23	0.435	1.00	0.00000	-0.00475	0.00000	0.304	92.00	132.25
226	24	0.750	1.00	0.00000	-0.00376	0.00000	0.100	92.00	102.22
228	20	0.200	1.00	-0.00396	-0.01263	0.00000	0.415	90.00	153.85
230	18	0.333	1.00	0.01038	0.00271	0.02517	0.494	91.00	180.00
232	14	0.714	1.00	0.00000	0.00000	0.00000	0.571	28.00	65.33
233	18	0.333	1.00	0.00000	-0.09780	0.06536	0.139	35.00	40.65
240	16	0.125	1.00	-0.00323	-0.00964	-0.00002	0.381	90.00	145.45
242	16	0.000	1.00	0.03864	0.03286	0.05055	0.437	90.00	160.00
244	26	0.115	1.00	0.01729	-0.01060	0.02358	0.769	87.00	377.00
246	17	0.824	1.00	0.00000	0.00000	0.00000	0.647	87.00	246.50
247	23	0.000	1.00	-0.01024	-0.01045	-0.00763	0.387	85.00	138.65
248	23	0.000	1.00	-0.04619	-0.07098	-0.03591	0.426	85.00	148.11

Table 2-6. Sampling Events/Results Thinned from PCE Wells at EBW

Well Number	N	ND Fraction	Group Interval	Sen's Slope (M)	M Lower Bnd	M Upper Bnd	Thin Fraction	Current Interval	Optimal Interval
249	23	0.043	1.00	-0.00899	-0.01406	0.00219	0.135	49.00	56.63
250	16	0.000	1.00	-0.05439	-0.06304	-0.03460	0.431	90.00	158.24
251	16	0.625	9.00	0.00000	-0.00682	0.00000	0.194	100.00	124.03
252	16	0.625	9.00	0.00000	0.00000	0.00000	0.450	100.00	181.82
253	18	0.667	21.00	0.00000	-0.00055	0.00000	0.111	37.00	41.62
254	18	0.500	21.00	-0.00255	-0.00892	0.00000	0.111	37.00	41.62
261	18	0.278	1.00	0.29000	0.00000	0.92500	0.522	3.00	6.28
264	17	0.765	1.00	0.19000	0.00000	0.93000	0.706	1.00	3.40
282	16	0.750	1.00	0.00000	-0.00014	0.00000	0.375	76.00	121.60
283	17	0.000	81.00	-0.00137	-0.00204	-0.00042	0.406	77.00	129.60
290	18	0.833	97.00	0.00000	0.00000	0.00000	0.639	84.00	232.62
293	12	0.750	1.00	0.00000	0.00000	-0.00007	0.000	98.00	98.00
298	24	0.583	1.00	0.00000	-0.05033	0.00000	0.342	16.00	24.30
301	17	0.471	1.00	0.00000	-0.18950	0.01367	0.265	23.00	31.28
304	18	0.500	1.00	0.06186	0.00000	0.58000	0.483	26.00	50.32
306	25	0.280	1.00	0.08500	0.05100	0.15917	0.536	19.00	40.95
309	14	0.214	1.00	0.04700	0.00000	0.19700	0.471	19.00	35.95
314	30	0.767	1.00	0.00000	0.00000	0.00000	0.760	353.00	1470.83
315	16	0.562	1.00	0.00072	0.00054	0.15000	0.488	459.00	895.61
316	22	0.864	1.00	0.00000	0.00000	0.00000	0.495	93.00	184.32
317	24	0.875	92.00	0.00000	0.00000	0.00000	0.808	77.00	401.74
326	11	0.364	1.00	0.10500	-0.46000	0.35000	0.127	1.00	1.15
329	19	0.579	1.00	-0.00376	-0.00769	0.00000	0.132	77.00	88.67
330	17	0.765	1.00	0.00000	0.00000	0.00000	0.629	77.00	207.78
332	20	0.100	1.00	0.00085	0.00032	0.00142	0.450	77.00	140.00
335	16	0.250	1.00	0.00182	0.00153	0.00238	0.581	76.00	181.49
341	18	0.722	1.00	0.00000	0.00000	0.00146	0.517	77.00	159.31
343	14	0.000	1.00	0.00089	0.00000	0.00383	0.614	70.00	181.48
347	13	0.385	1.00	3.00000	1.21000	4.70000	0.523	1.00	2.10
348	22	0.636	1.00	0.00341	0.00000	0.00345	0.509	58.00	118.15
349	16	0.812	1.00	0.00000	0.00000	0.00536	0.694	27.00	88.16
350	16	0.625	1.00	0.05185	0.00000	0.00556	0.000	27.00	27.00
358	10	0.100	92.00	-0.00252	-0.00585	0.00087	0.360	92.00	143.75
363	14	0.571	1.00	0.00000	-0.00190	0.00000	0.157	82.00	97.29
366	10	0.700	1.00	0.00049	0.00000	0.00118	0.560	76.00	172.73
378	10	0.000	1.00	0.00000	-0.00570	0.00116	0.100	83.00	92.22
402	8	0.000	1.00	-0.00006	-0.00127	0.00230	0.013	184.00	186.33

Table 4-1. Currently Sampled, Non-Redundant Well Locations (MMR)

EBW Wells	FS-12 Wells	
98MW0001	90JB0001B	90MW0085B
37MW0002	90JB0001C	90MW0085A
MAMW0512D	90JB0001D	90MW0086A
MAMW0515D	90JB0004A	90MW0086B
00MW0531	90JB0004C	90MW0086C
00MW0537B	90JB0006B	90MW0086D
00MW0542A	90MP0060D	90MW0087A
00MW0542C	90MW0001	96SV0004
00MW0543	90MW0002	96SV0006
00MW0544A	90MW0003	90WT0013
00MW0544B	90MW0004	
00MW0544C	90MW0005	
00MW0544D	90MW0007	
00MW0545	90MW0015	
00MW0561	90MW0020	
00MW0562A	90MW0025	
00MW0562C	90MW0027	
00MW0567	90MW0028	
00MW0568	90MW0033	
00MW0569	90MW0034	
00MW0570A	90MW0040	
00MW0570B	90MW0041	
00MP0571A	90MW0042	
00MP0571C	90MW0050	
MAMW0512C	90MW0053	
MAMW0512A	90MW0055	
MAMW0515A	90MW0064A	
00MW0576B	90MW0064	
00MW0576C	90MW0066A	
00MW0574C	90MW0066	
00MW0575B	90MW0068	
00MW0572C	90MW0070	
00MW0572D	90MW0080	
00MW0573B	90MW0081	
00MW0573C	90MW0076	
00DP0001	90MW0079A	
00DP0002	90MW0079B	
	90MW0079C	
	90MW0078	
	90MW0083	
	90MW0077	
	90MW0084B	
	90MW0084A	

Figure 3-9. EDB IK Estimates, All Wells, Q4 1998 (FS-12)

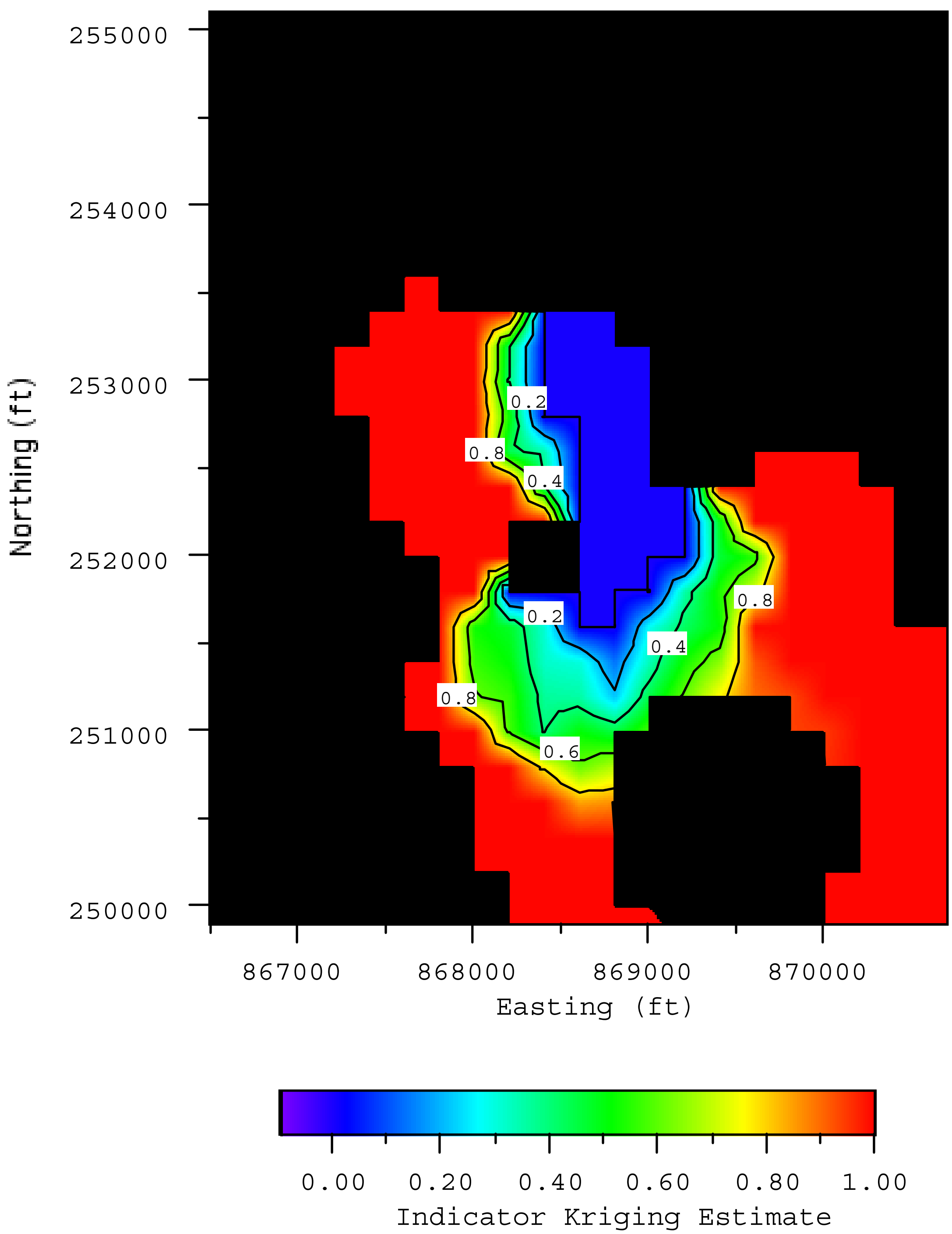

Figure 3-10. Benzene IK Estimates, All Wells, Q4 1998 (FS-12)

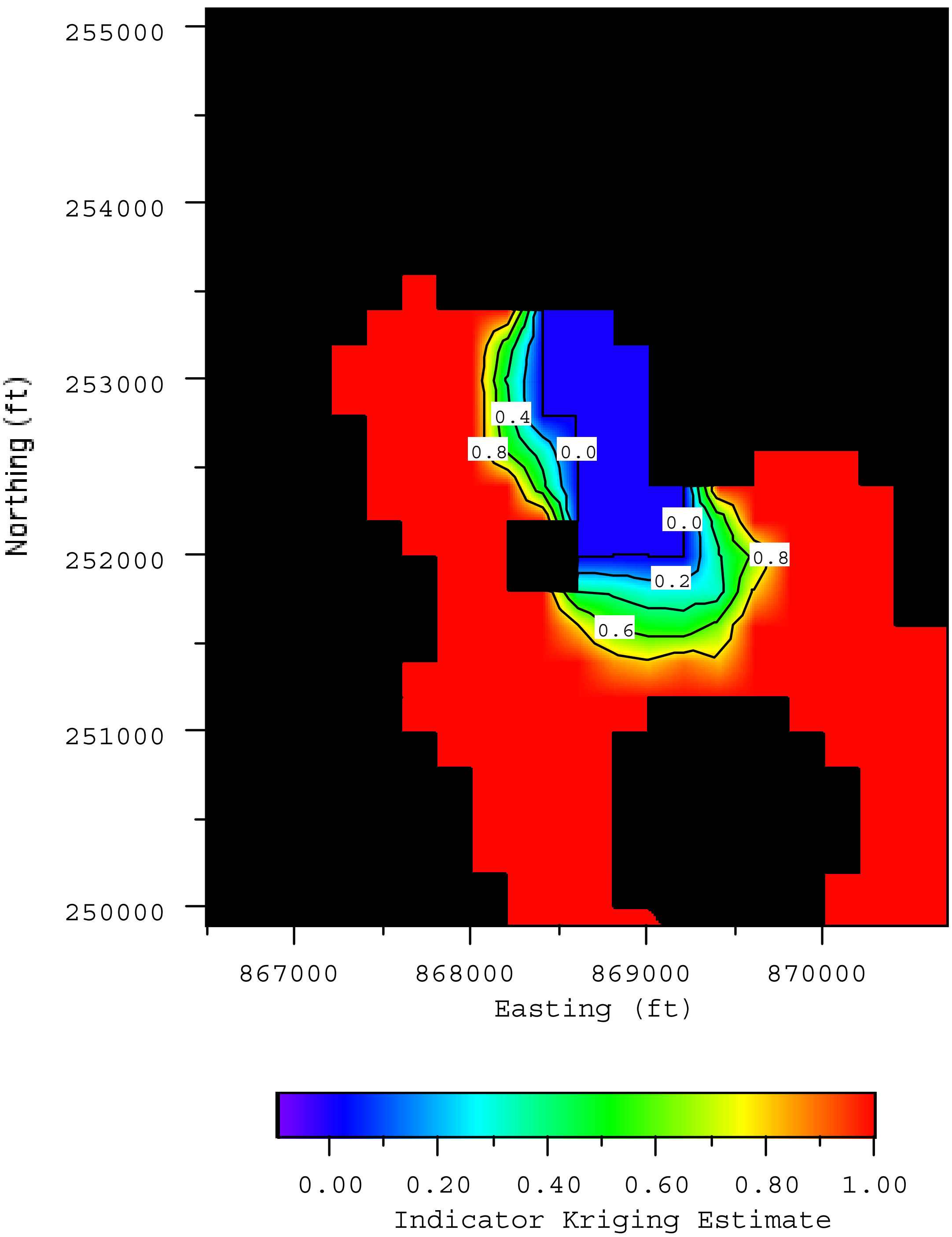

Figure 3-11. TCE IK Estimates, All Wells, Q4 1998 (EBW)

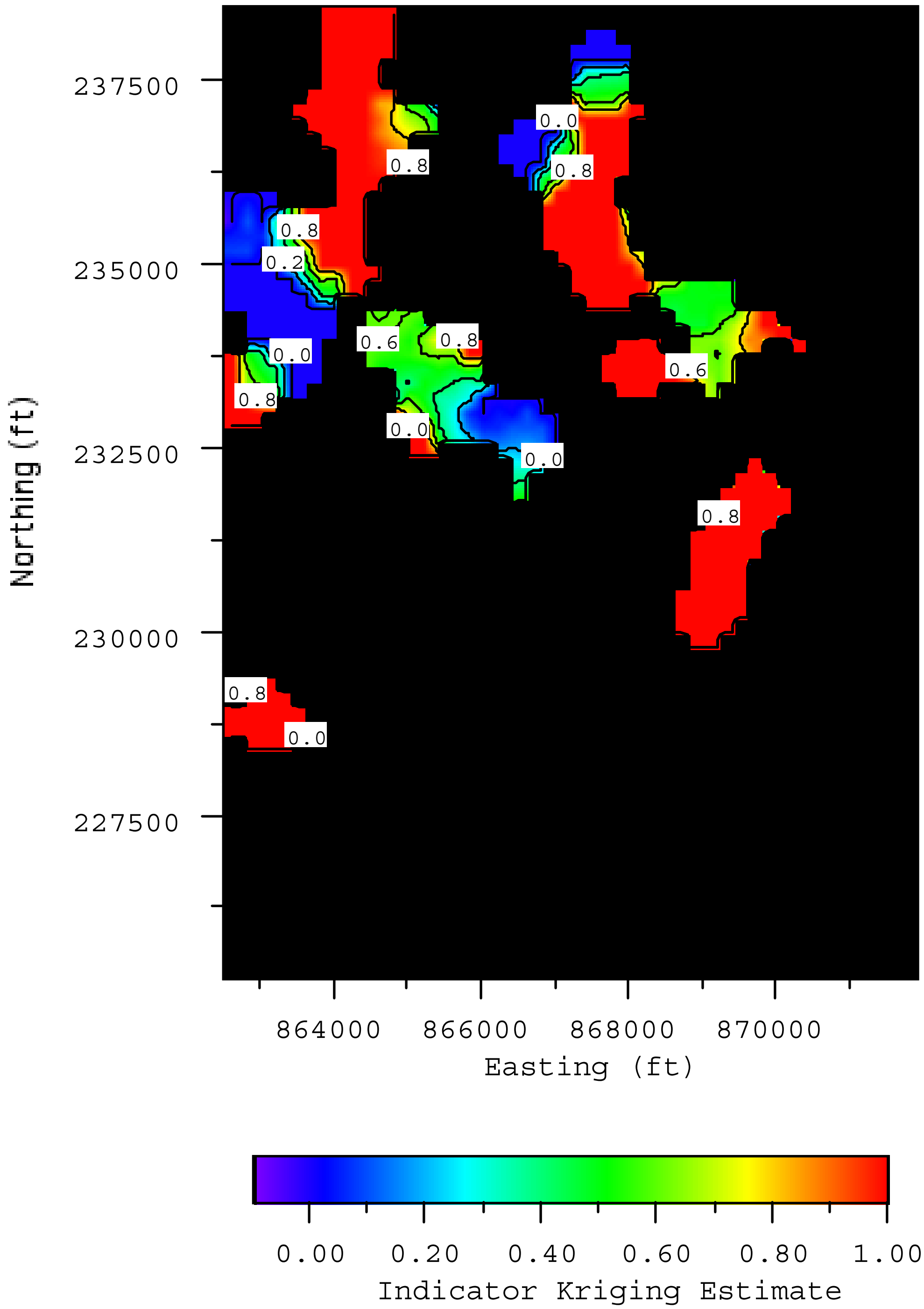

Figure 3-12. PCE IK Estimates, All Wells, Q4 1998 (EBW)

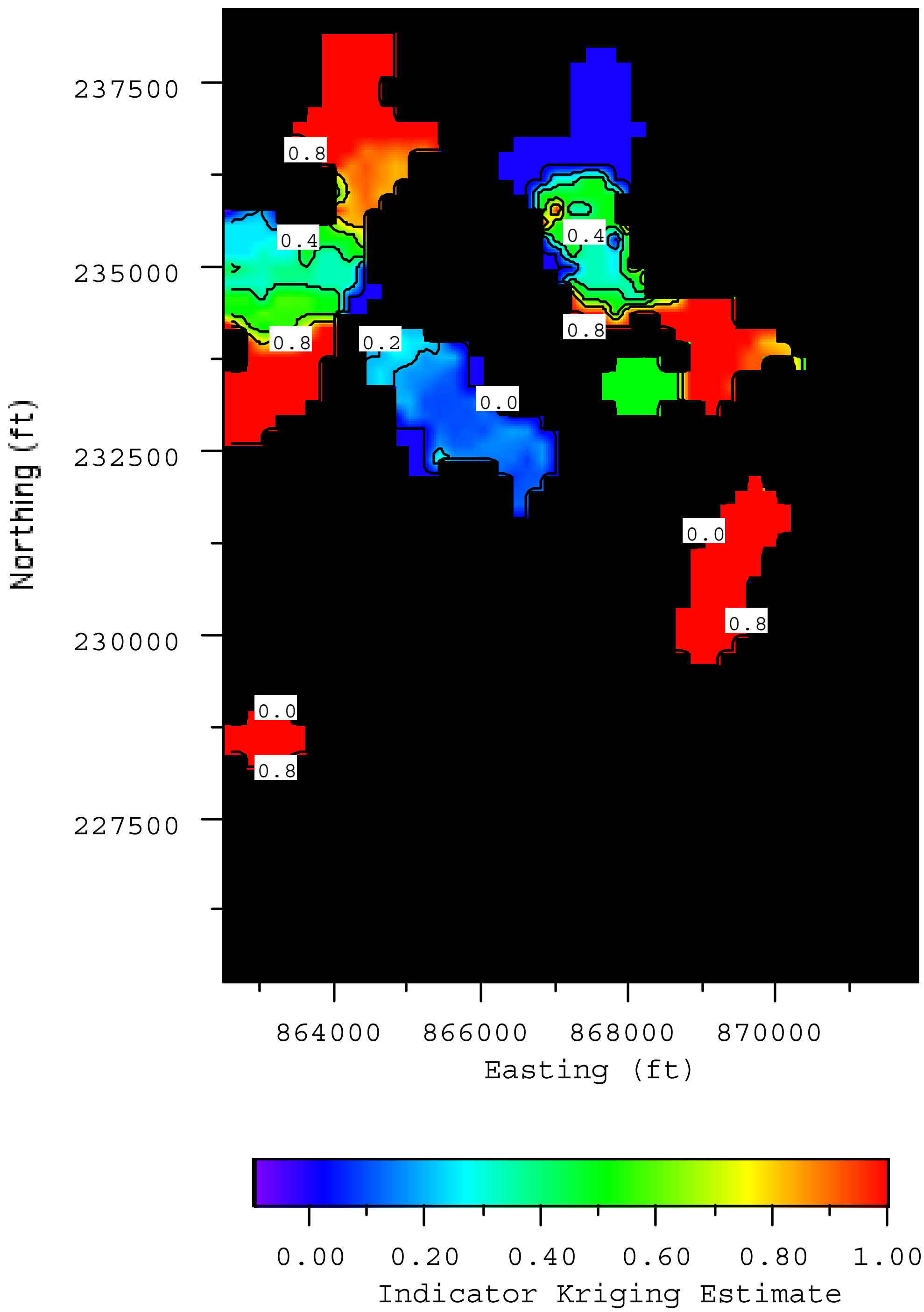

Figure 3-13. EDB KV Ratios, 1st Threshold (FS-12)

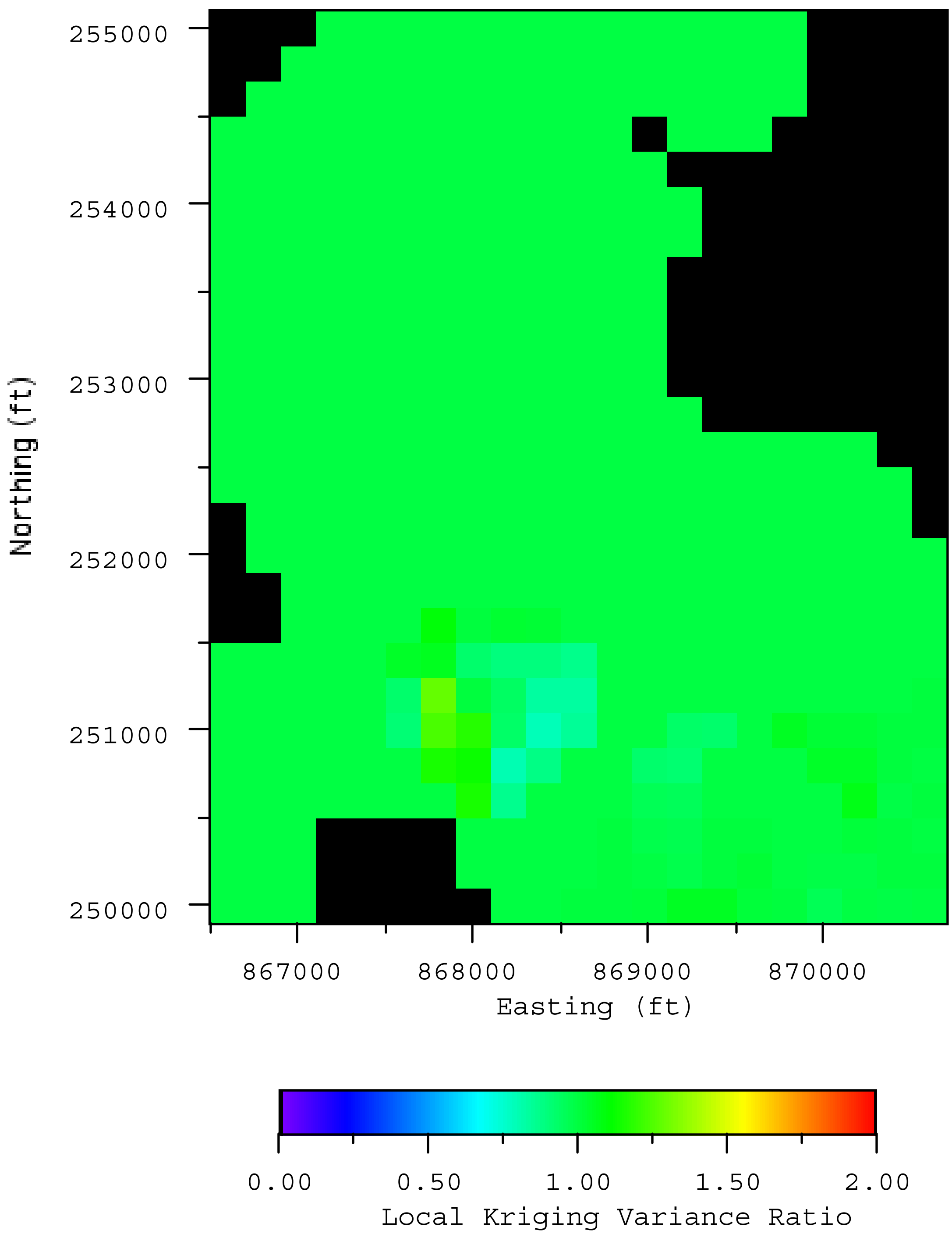

Figure 3-14. EDB KV Ratios, 2nd Threshold (FS-12)

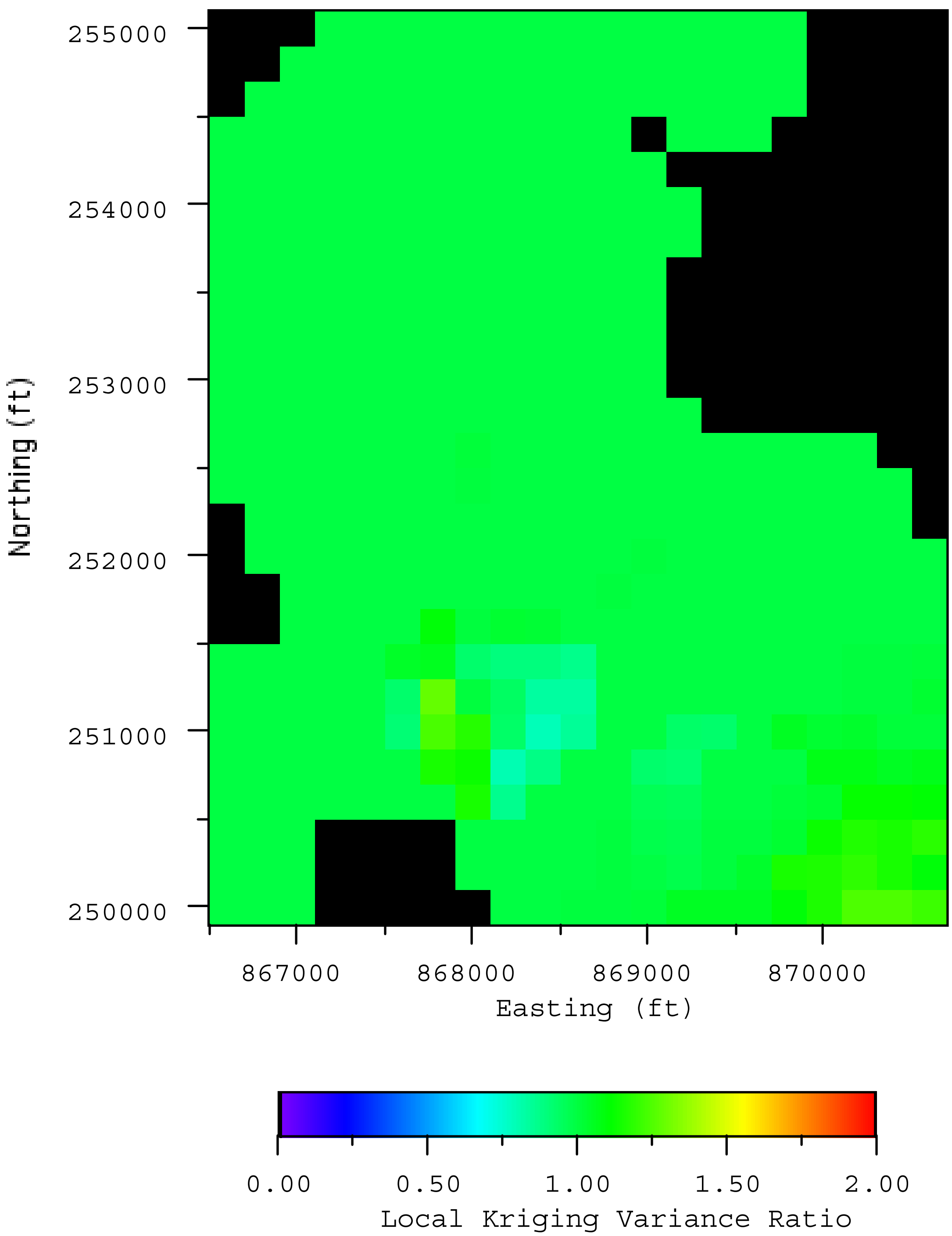

Figure 3-15. EDB KV Ratios, 3rd Threshold (FS-12)

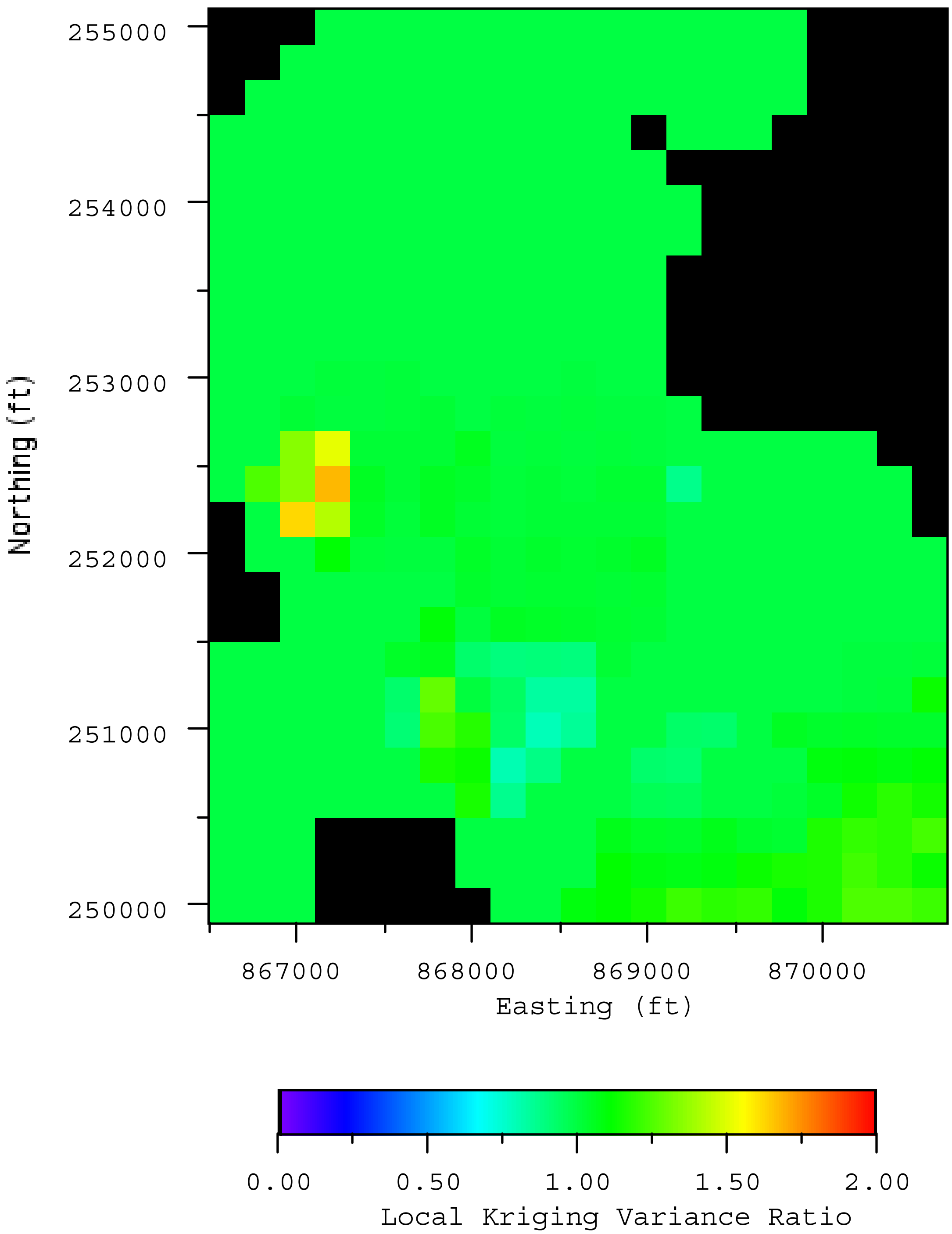

Figure 3-16. EDB KV Ratios, 4th Threshold (FS-12)

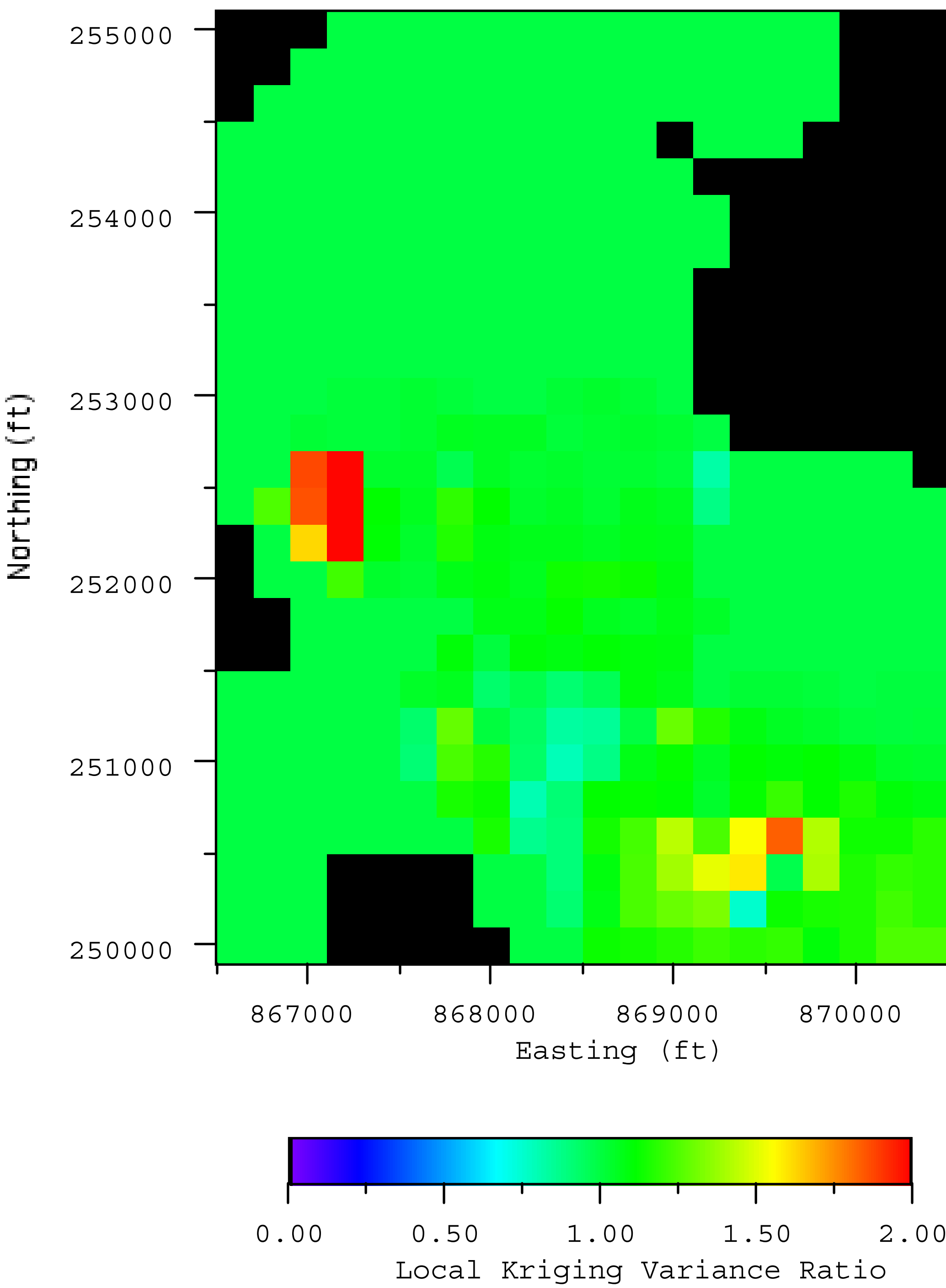

Figure 3-17. EDB KV Ratios, 5th Threshold (FS-12)

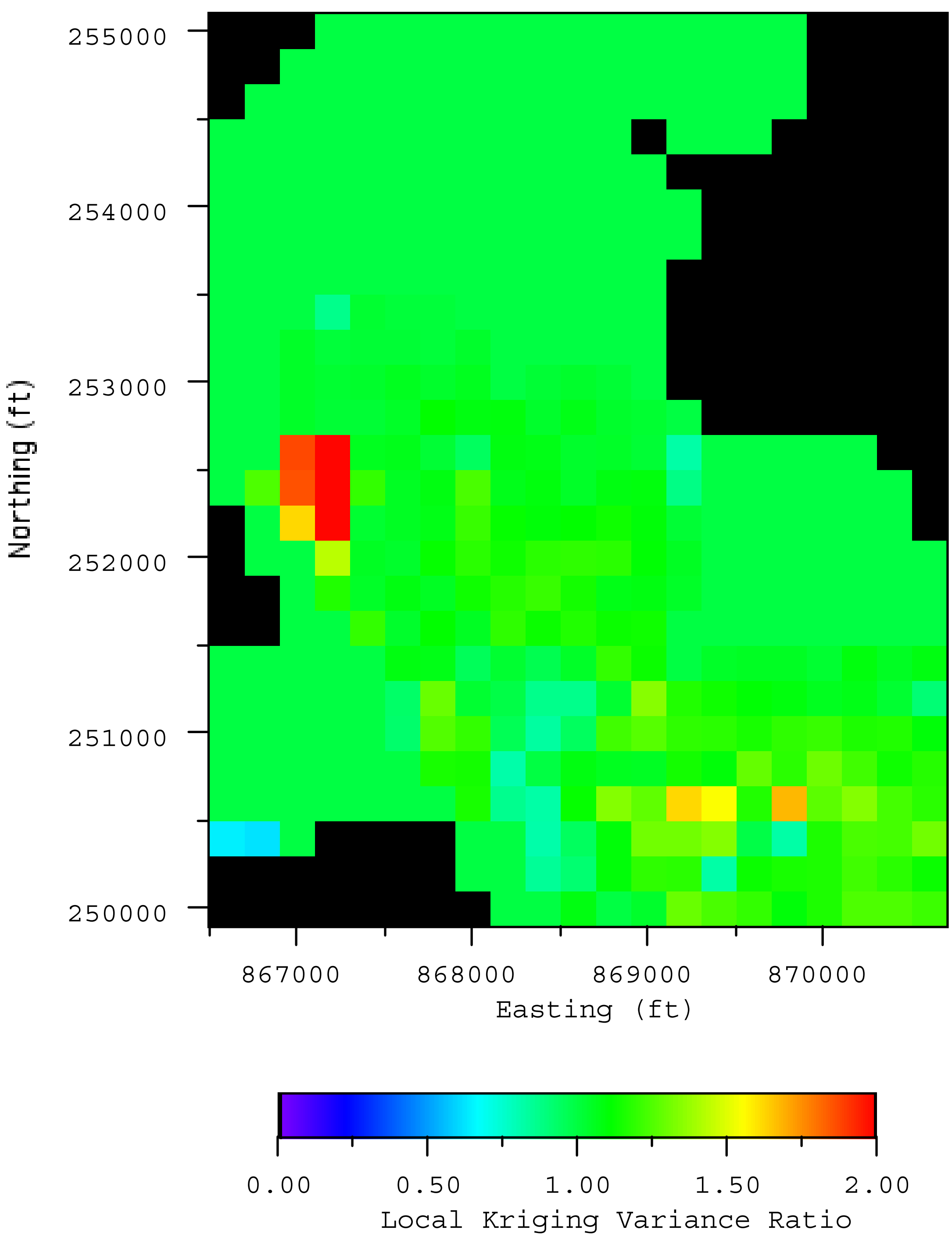

Figure 3-18. EDB KV Ratios, 6th Threshold (FS-12)

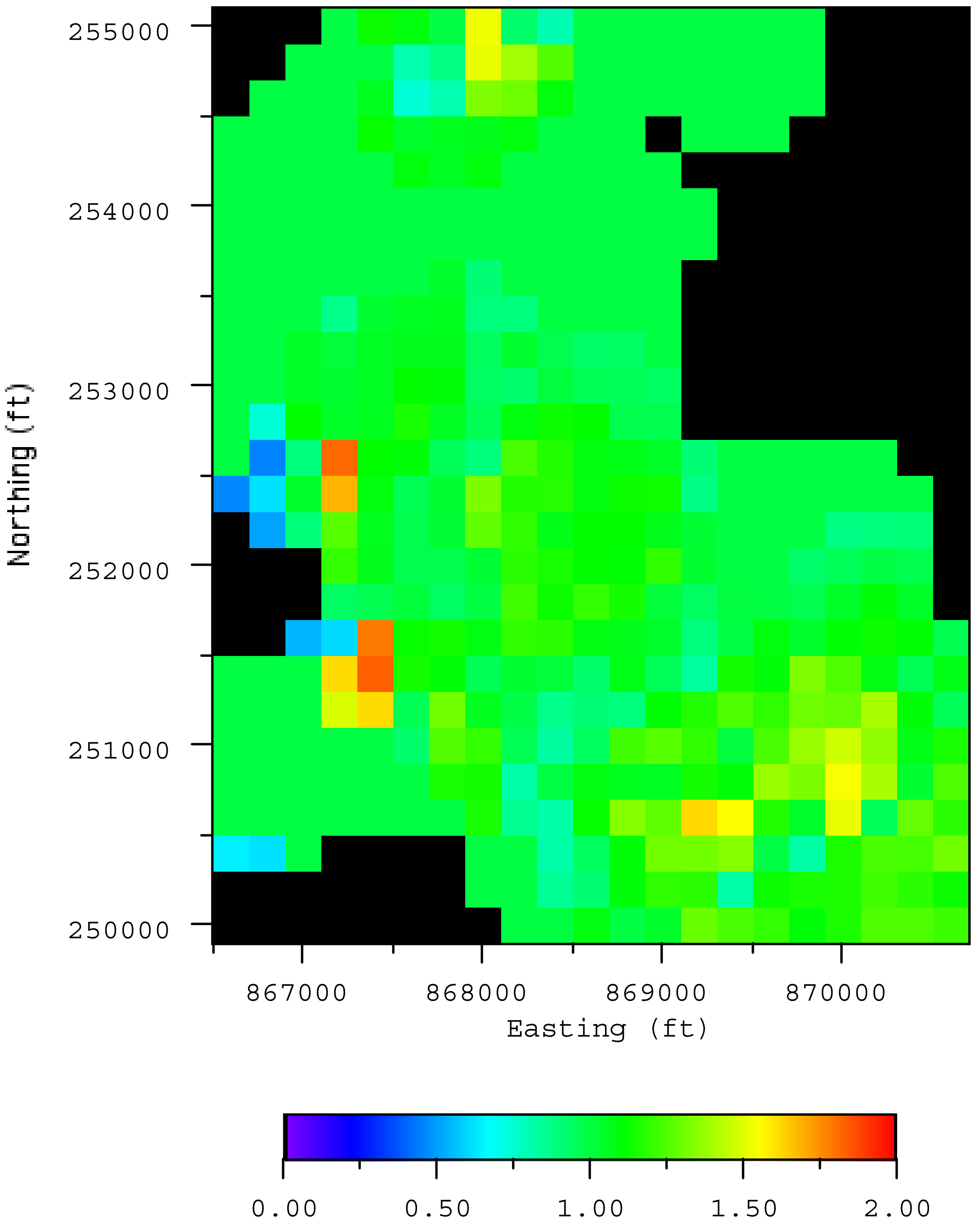

Figure 3-19. Benzene KV Ratios, First Threshold (FS-12)

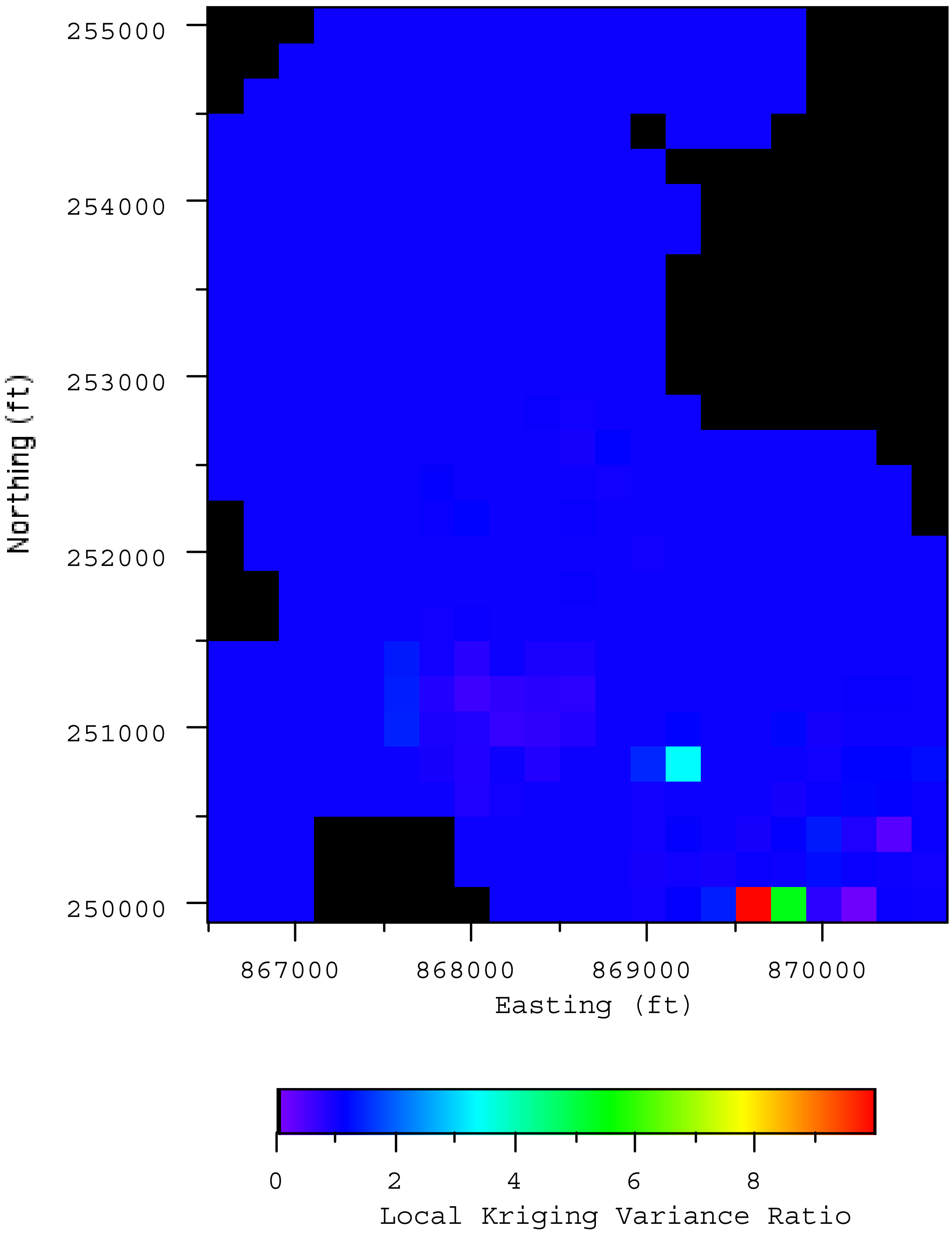

Figure 3-20. Benzene KV Ratios, Second Threshold (FS-12)

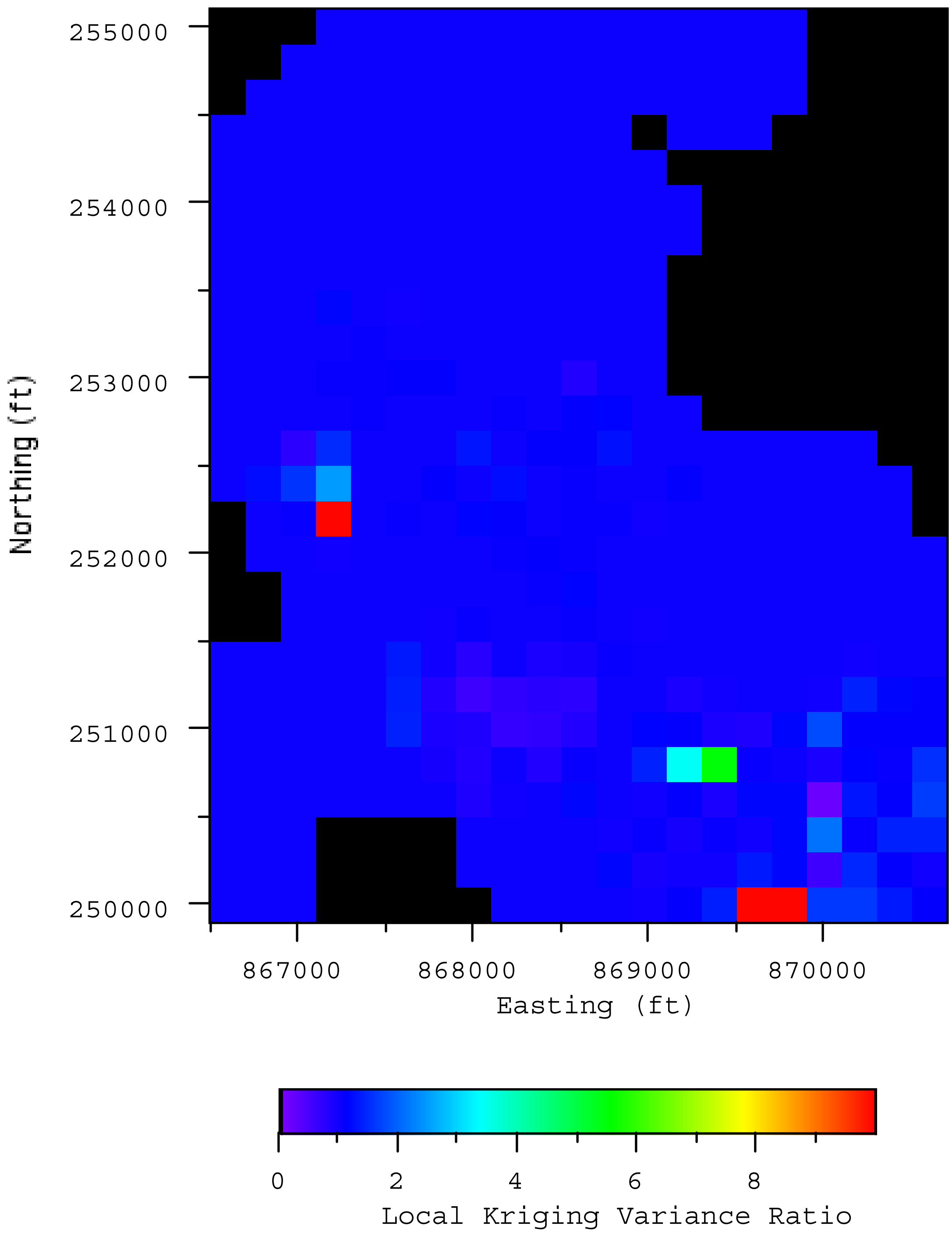

Figure 3-21. Benzene KV Ratios, Third Threshold (FS-12)

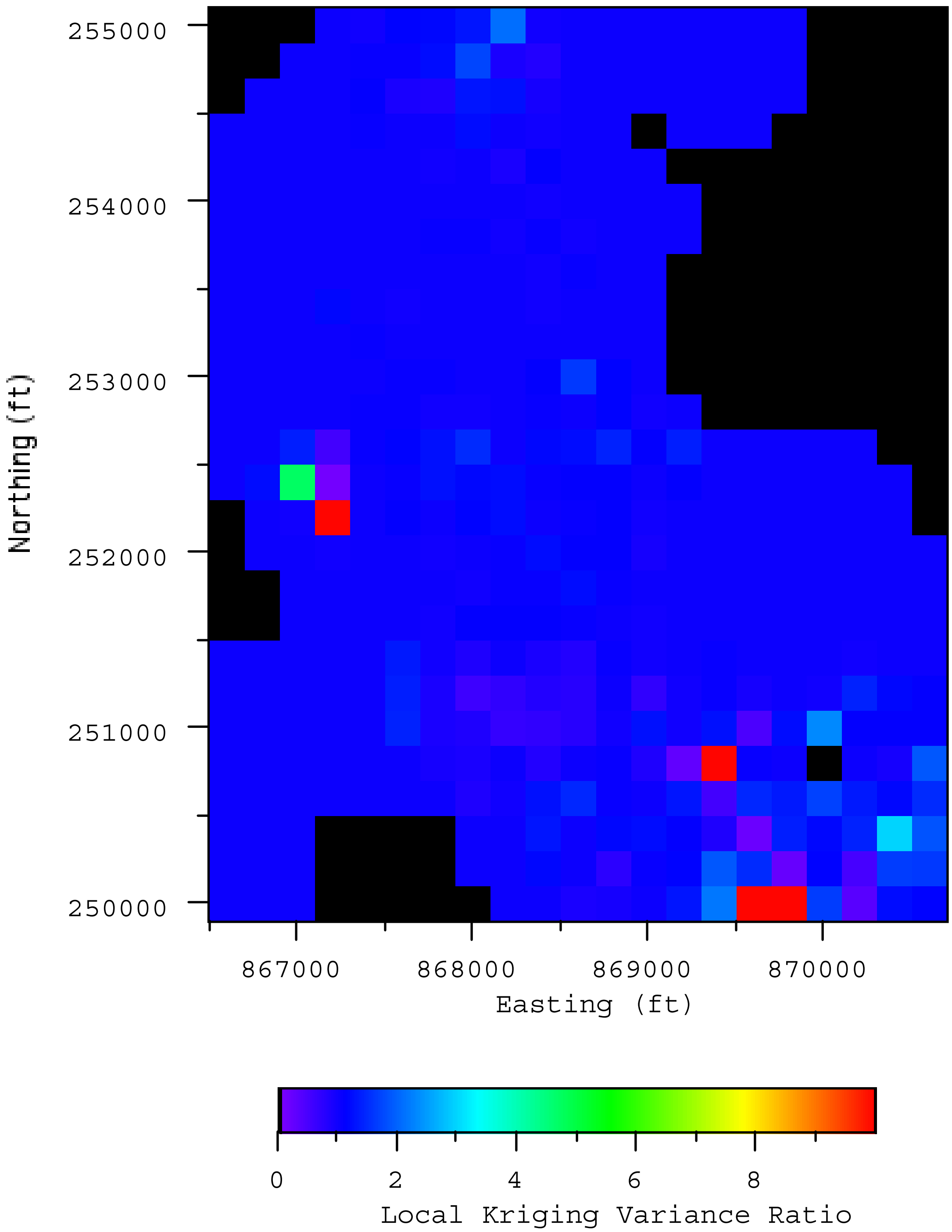

Figure 3-22. Benzene KV Ratios, Fourth Threshold (FS-12)

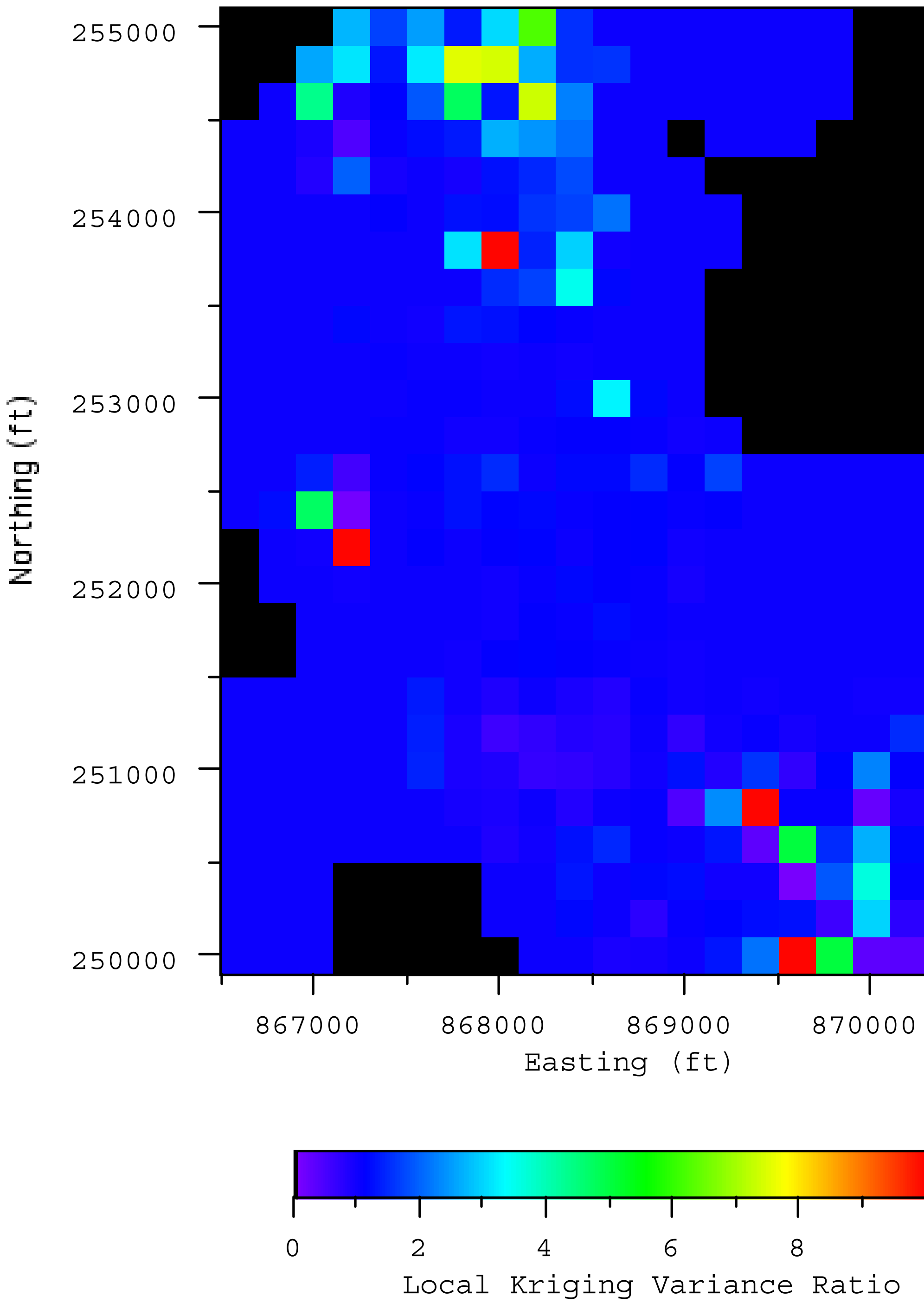

Figure 3-23. Benzene KV Ratios, Fifth Threshold (FS-12)

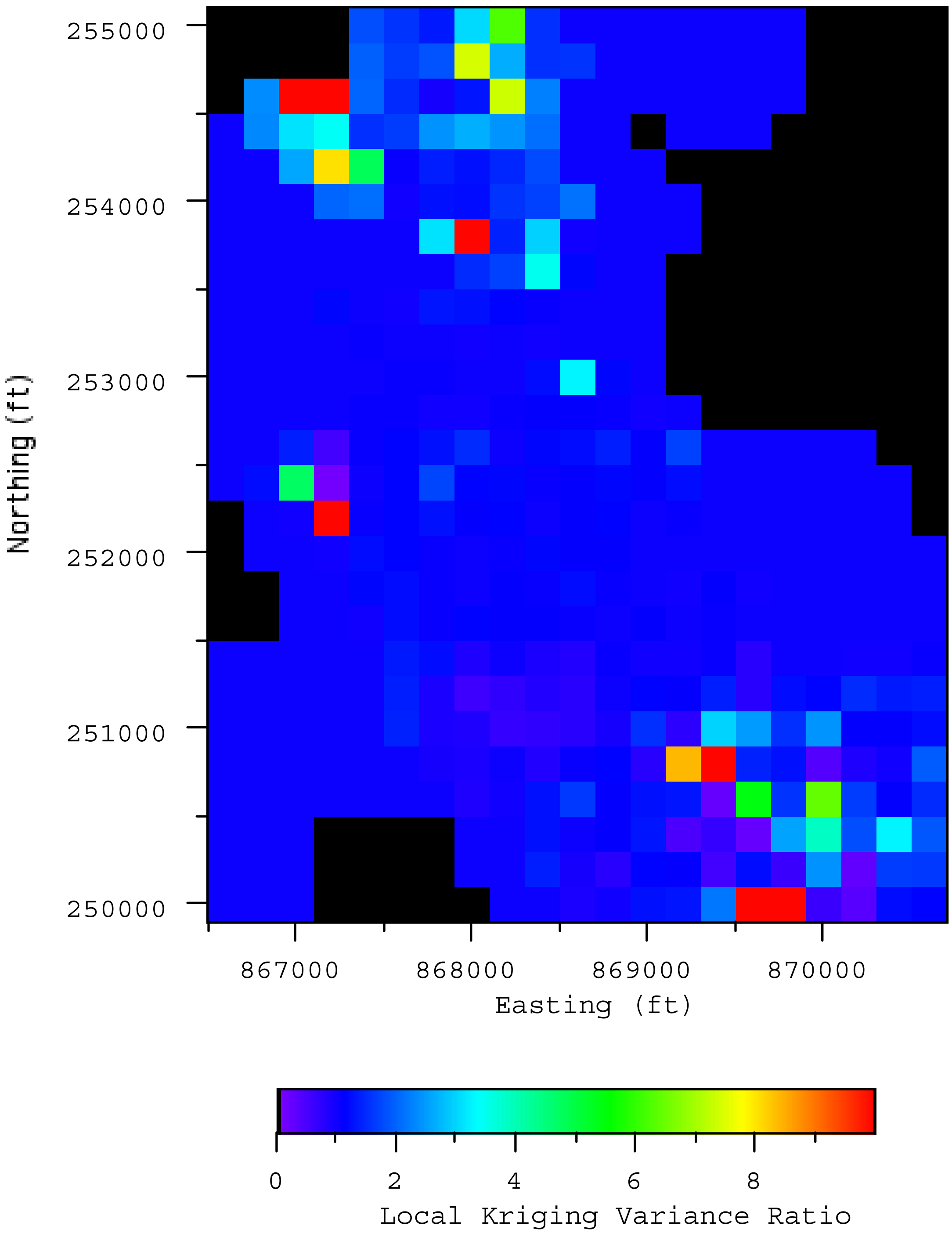

Figure 3-24. Benzene KV Ratios, Sixth Threshold (FS-12)

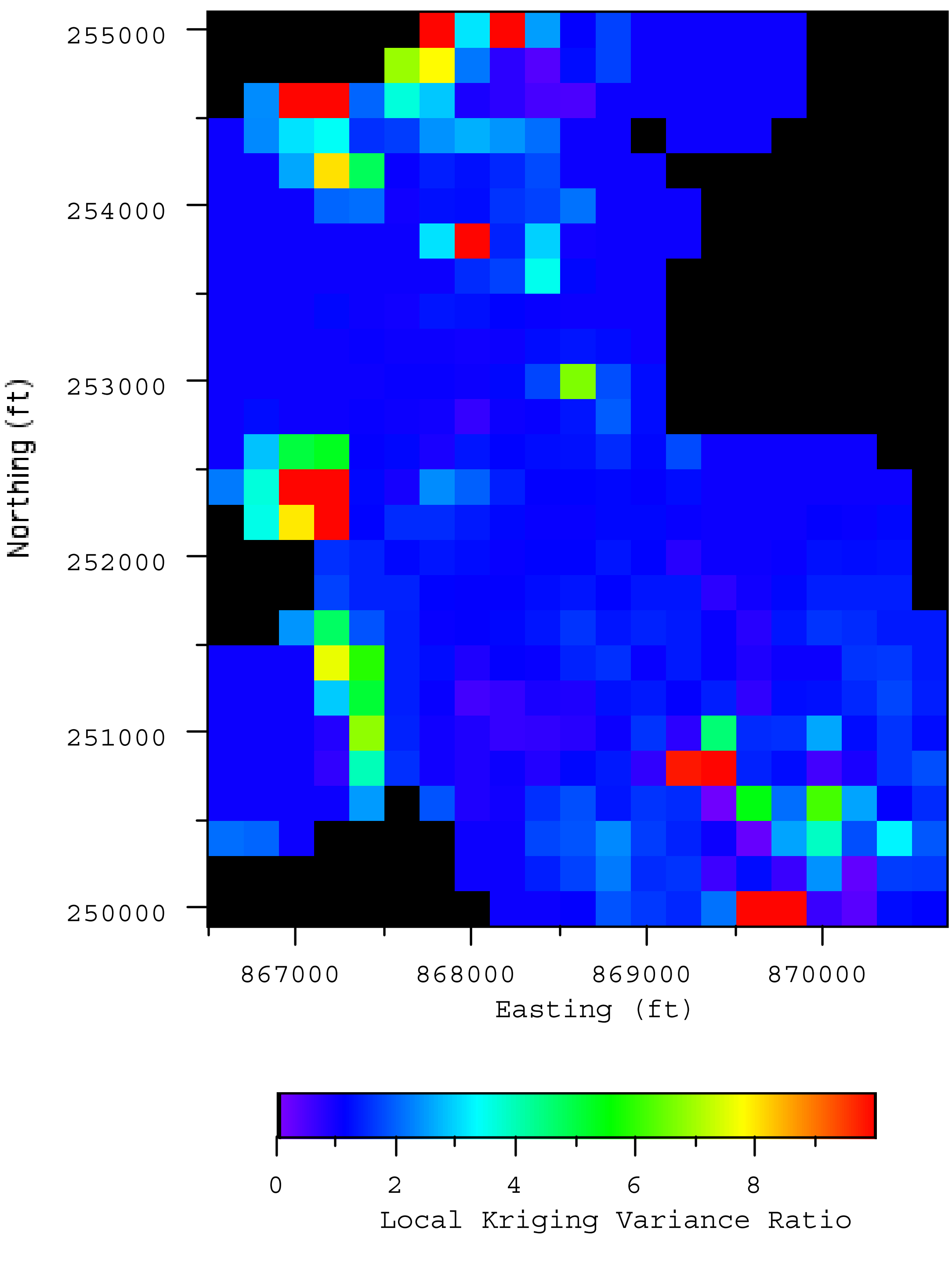

Figure 3-25. TCE KV Ratios, 1st Threshold (EBW)

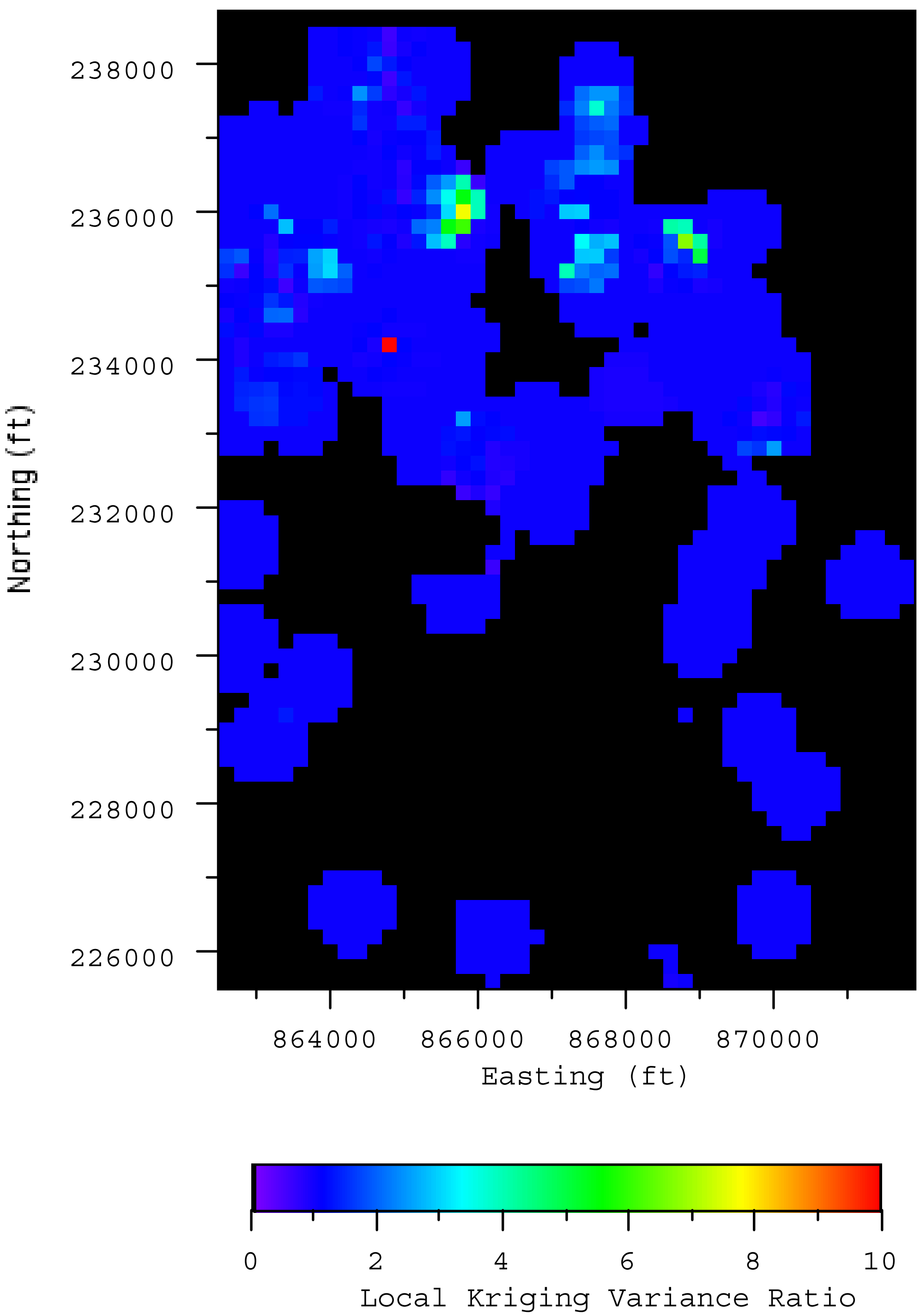

Figure 3-26. TCE KV Ratios, 2nd Threshold (EBW)

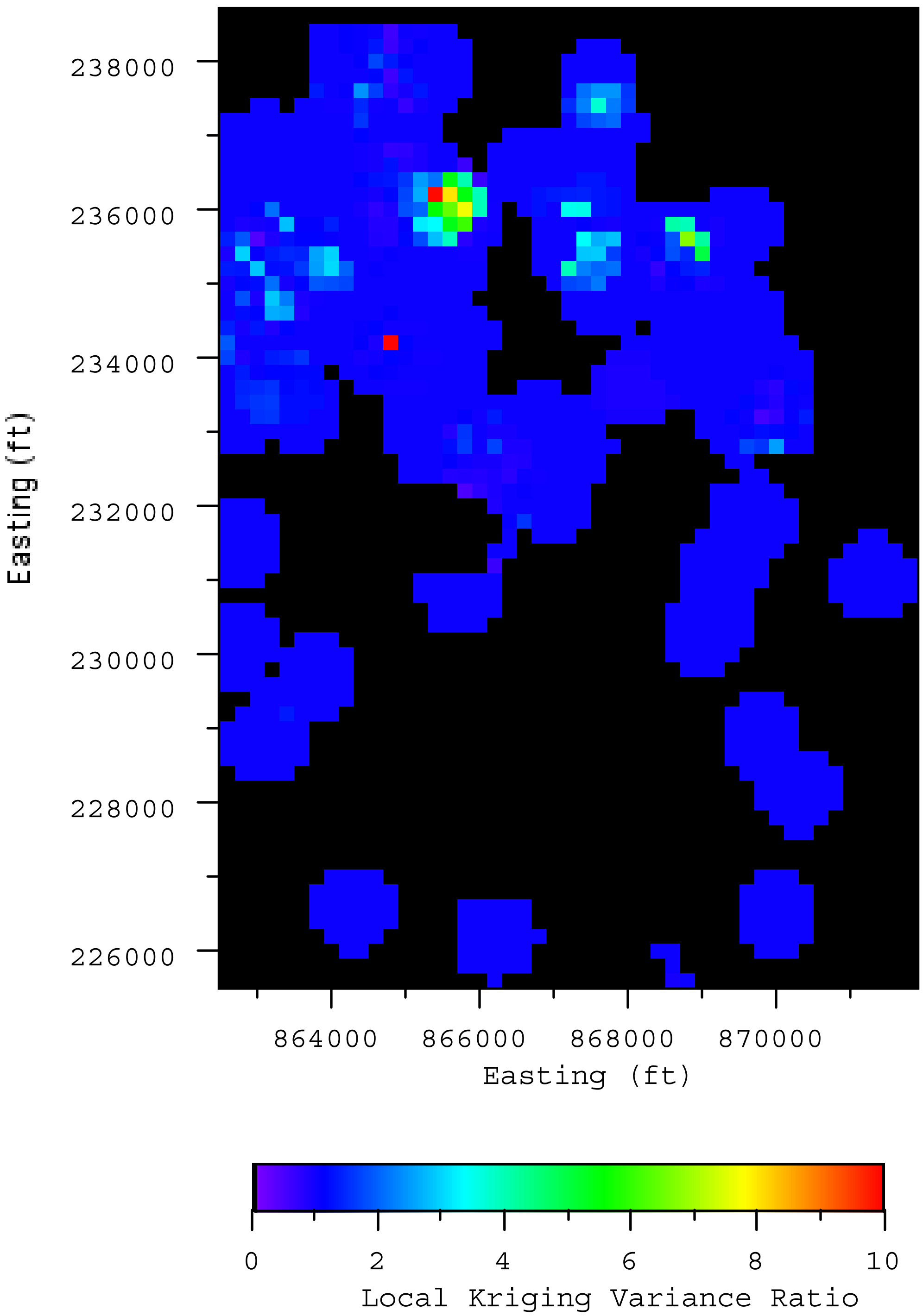

Figure 3-27. TCE KV Ratios, 3rd Threshold (EBW)

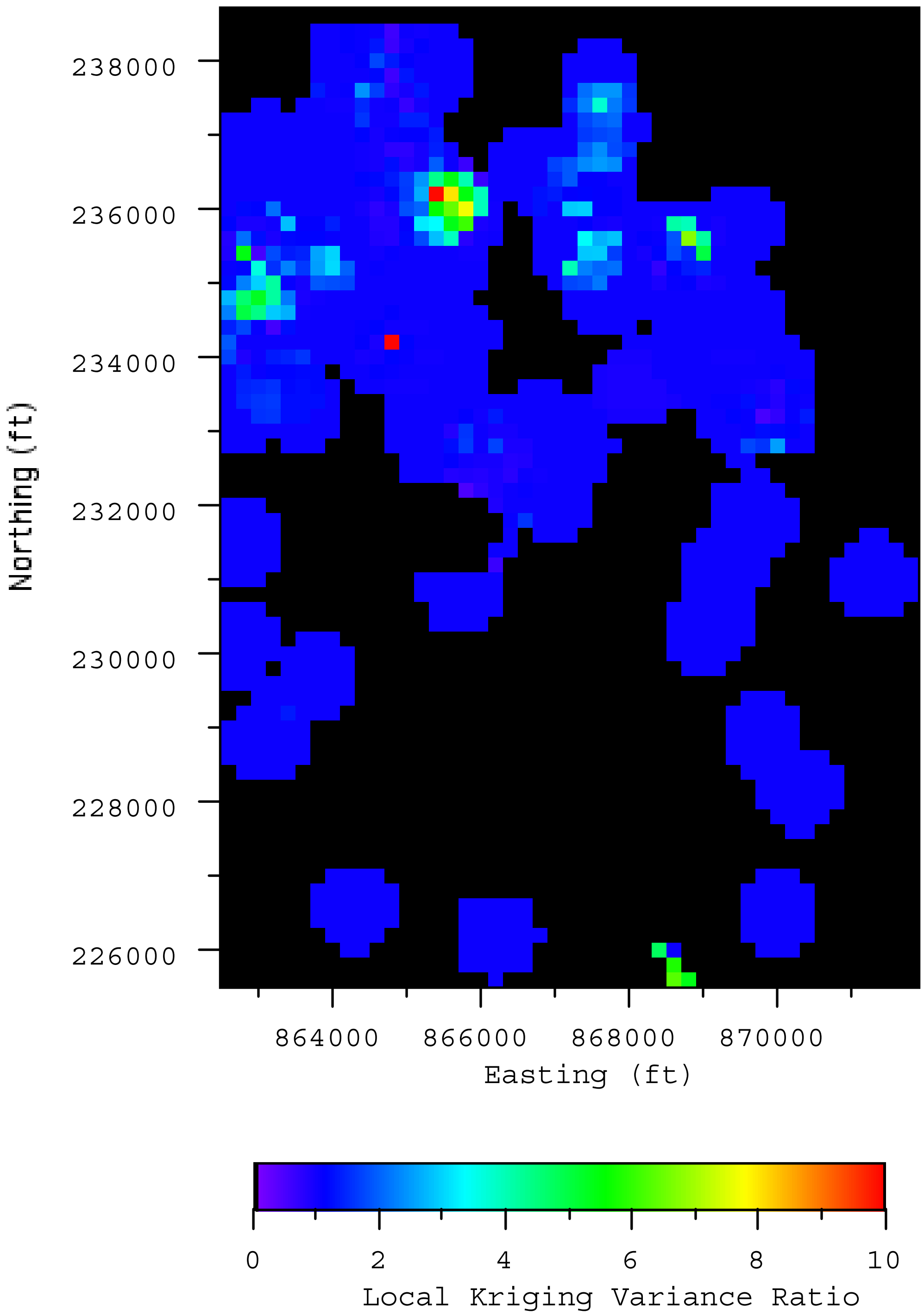

Figure 3-28. TCE KV Ratios, 4th Threshold (EBW)

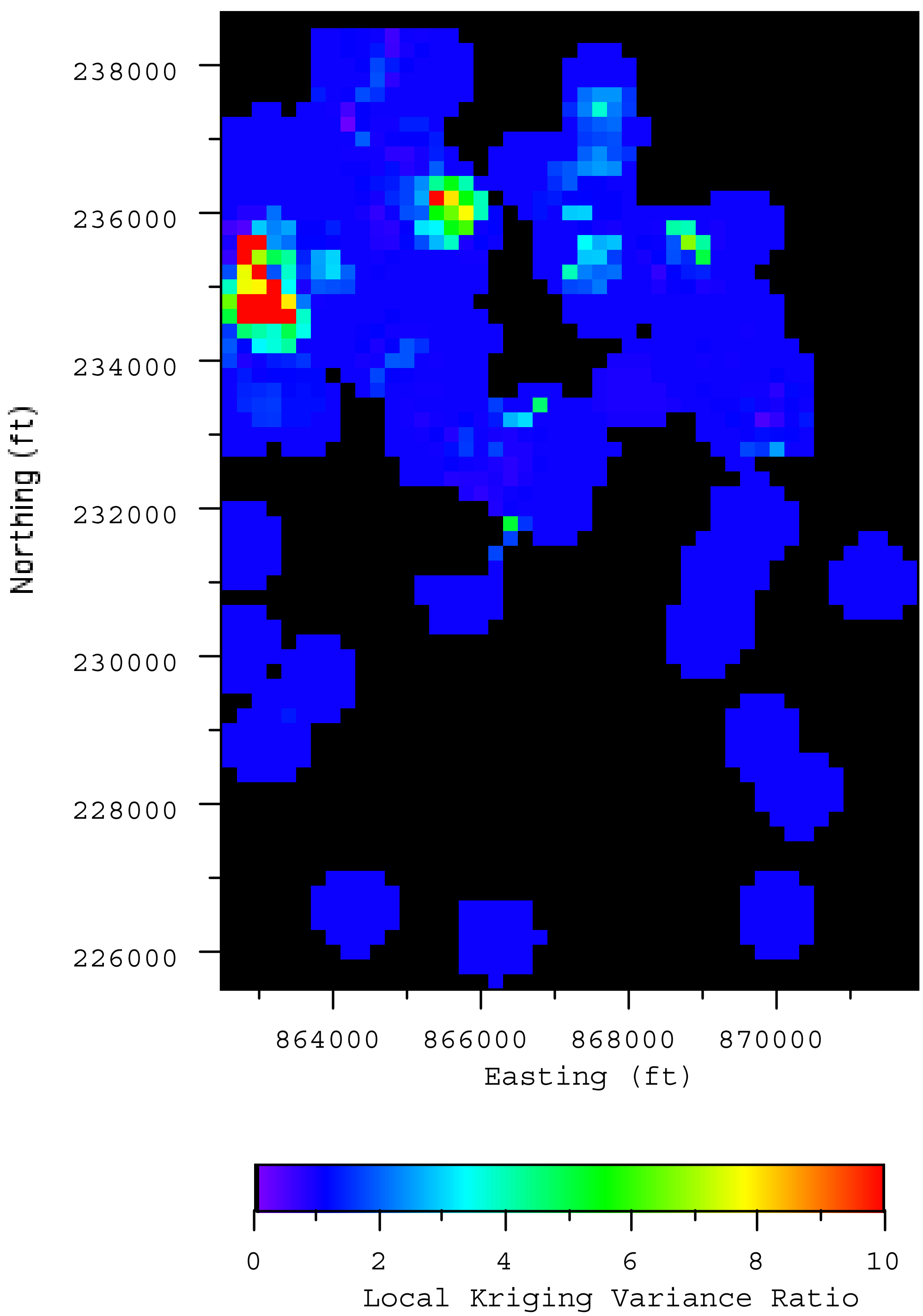

Figure 3-29. TCE KV Ratios, 5th Threshold (EBW)

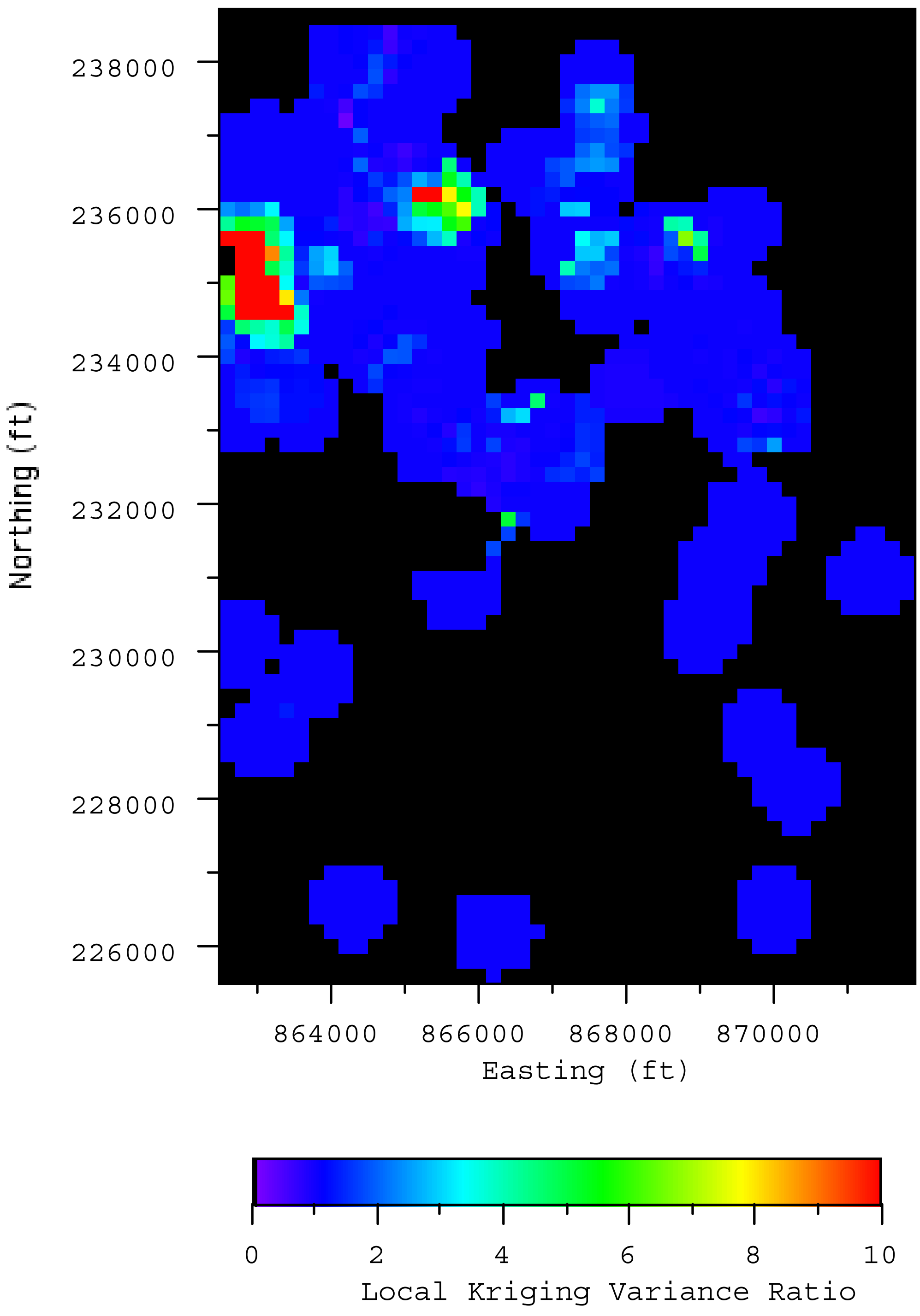

Figure 3-30. TCE KV Ratios, 6th Threshold (EBW)

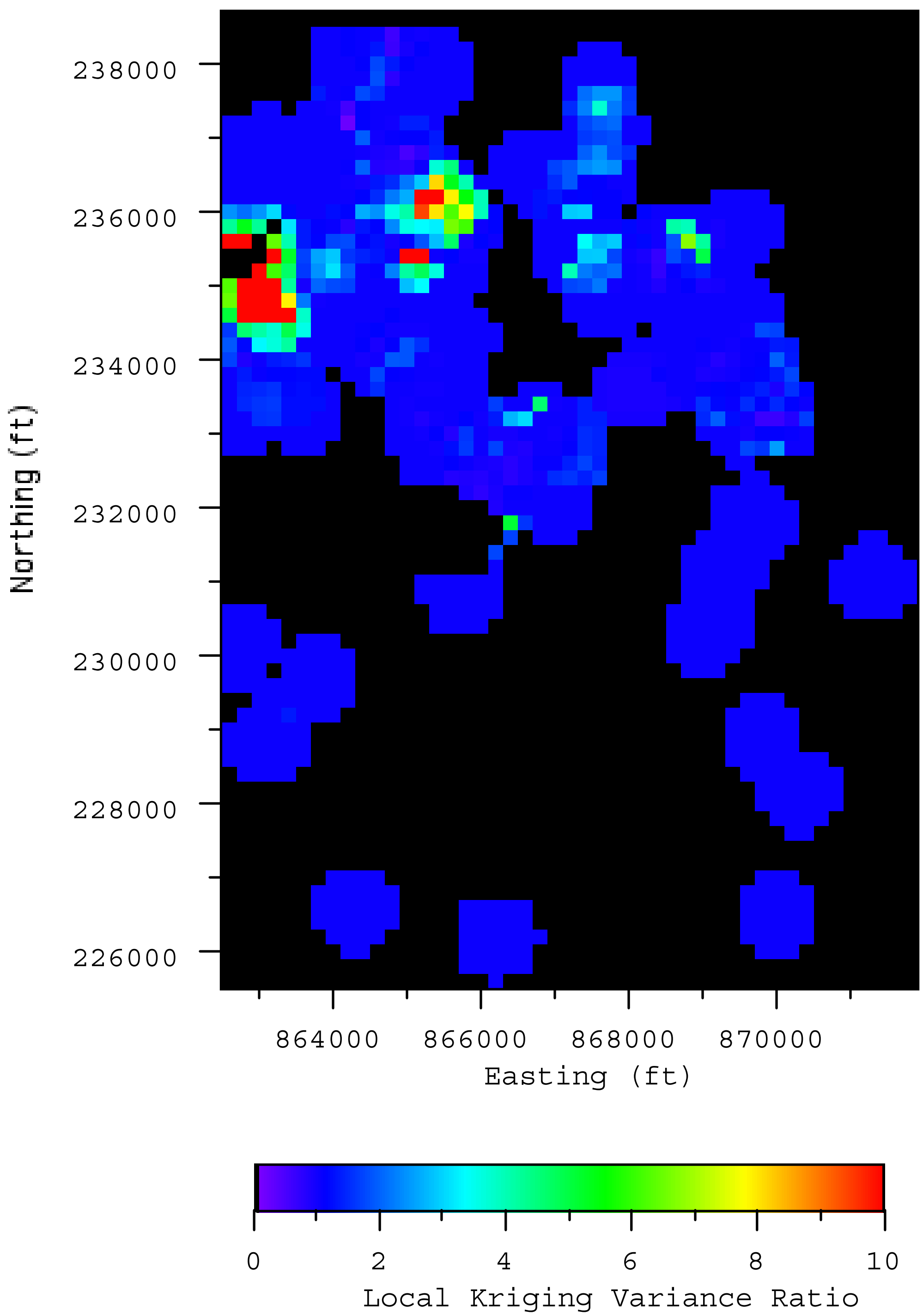

Figure 3-31. PCE KV Ratios, 1st Threshold (EBW)

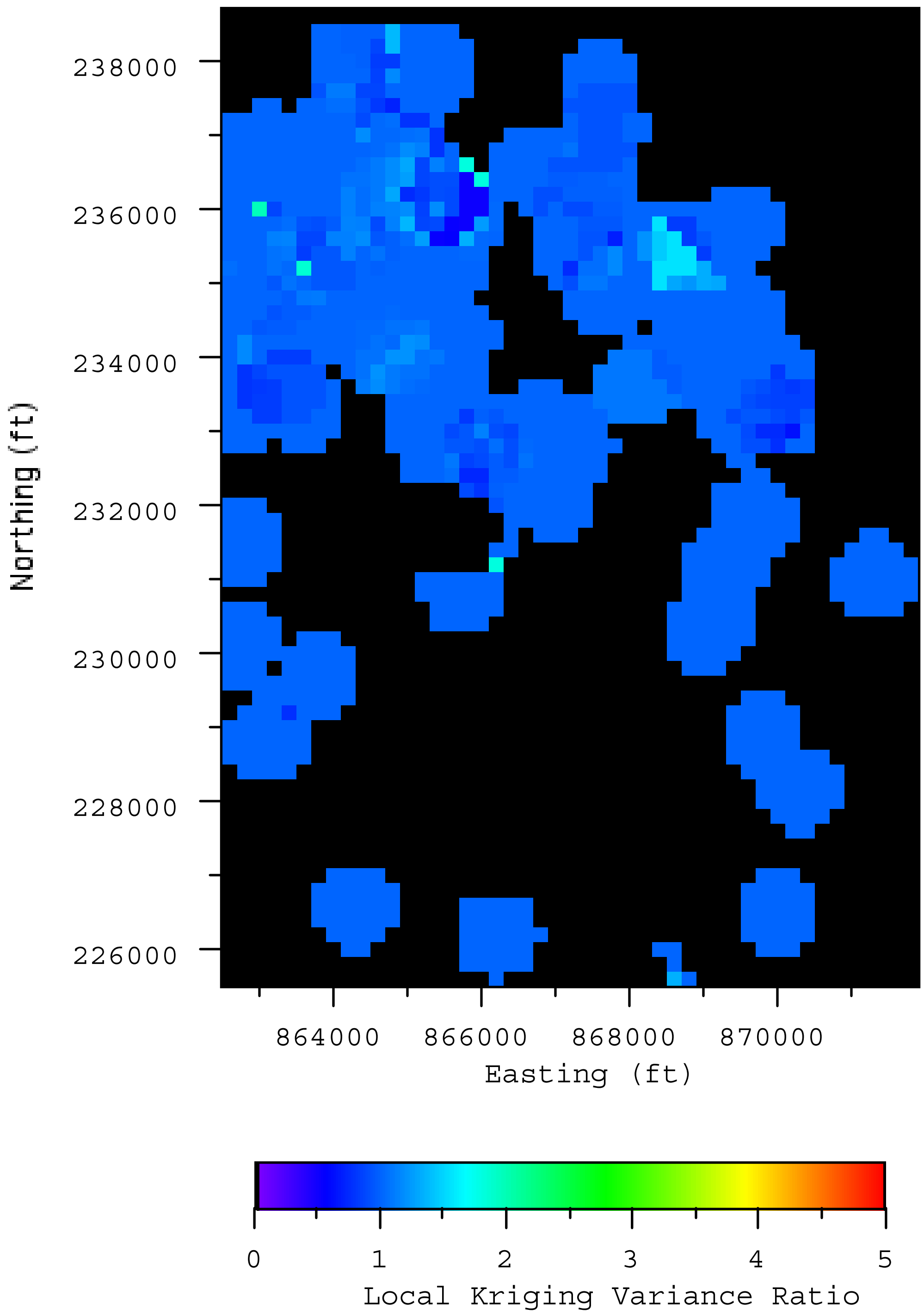

Figure 3-32. PCE KV Ratios, 2nd Threshold (EBW)

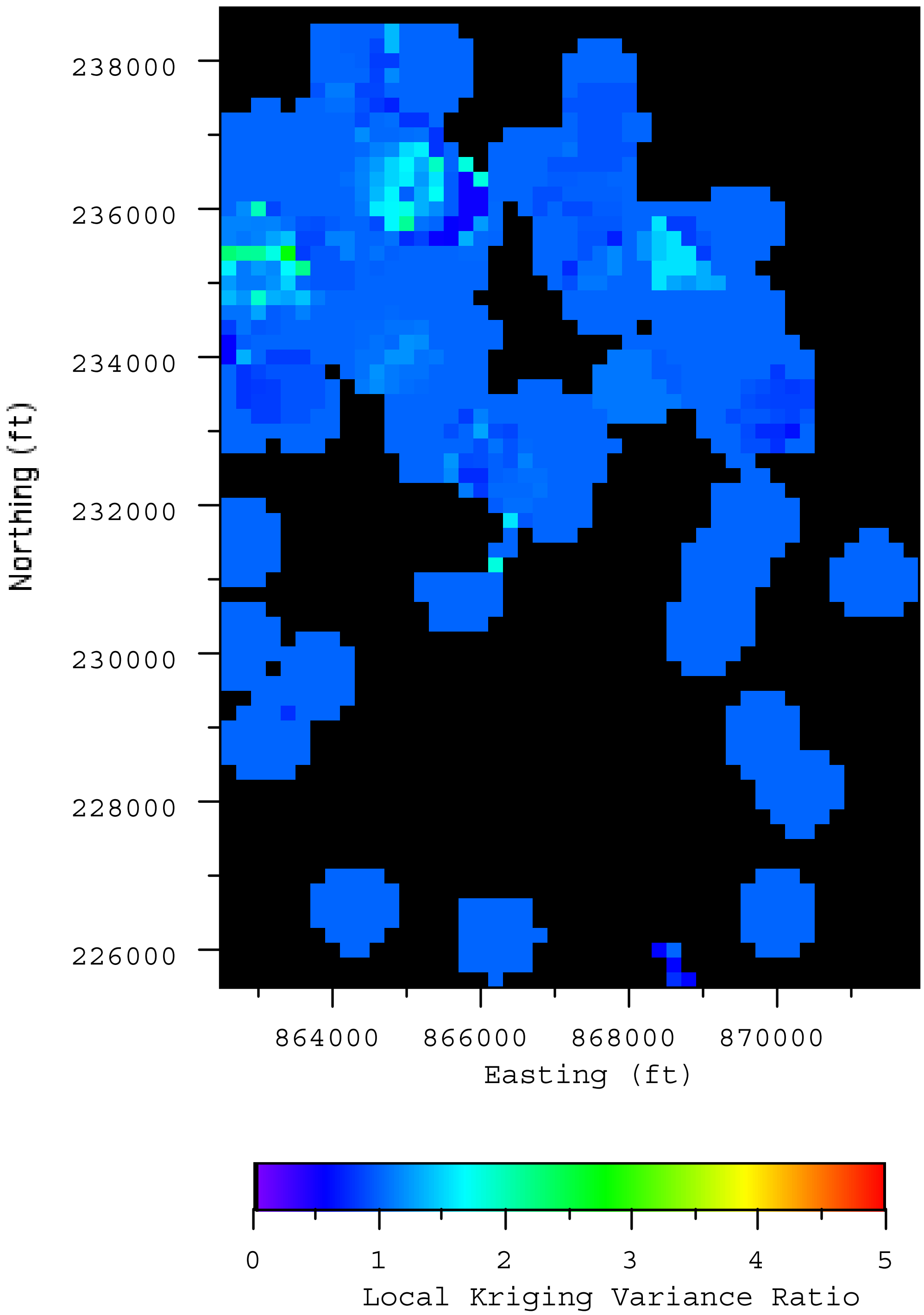

Figure 3-33. PCE KV Ratios, 3rd Threshold (EBW)

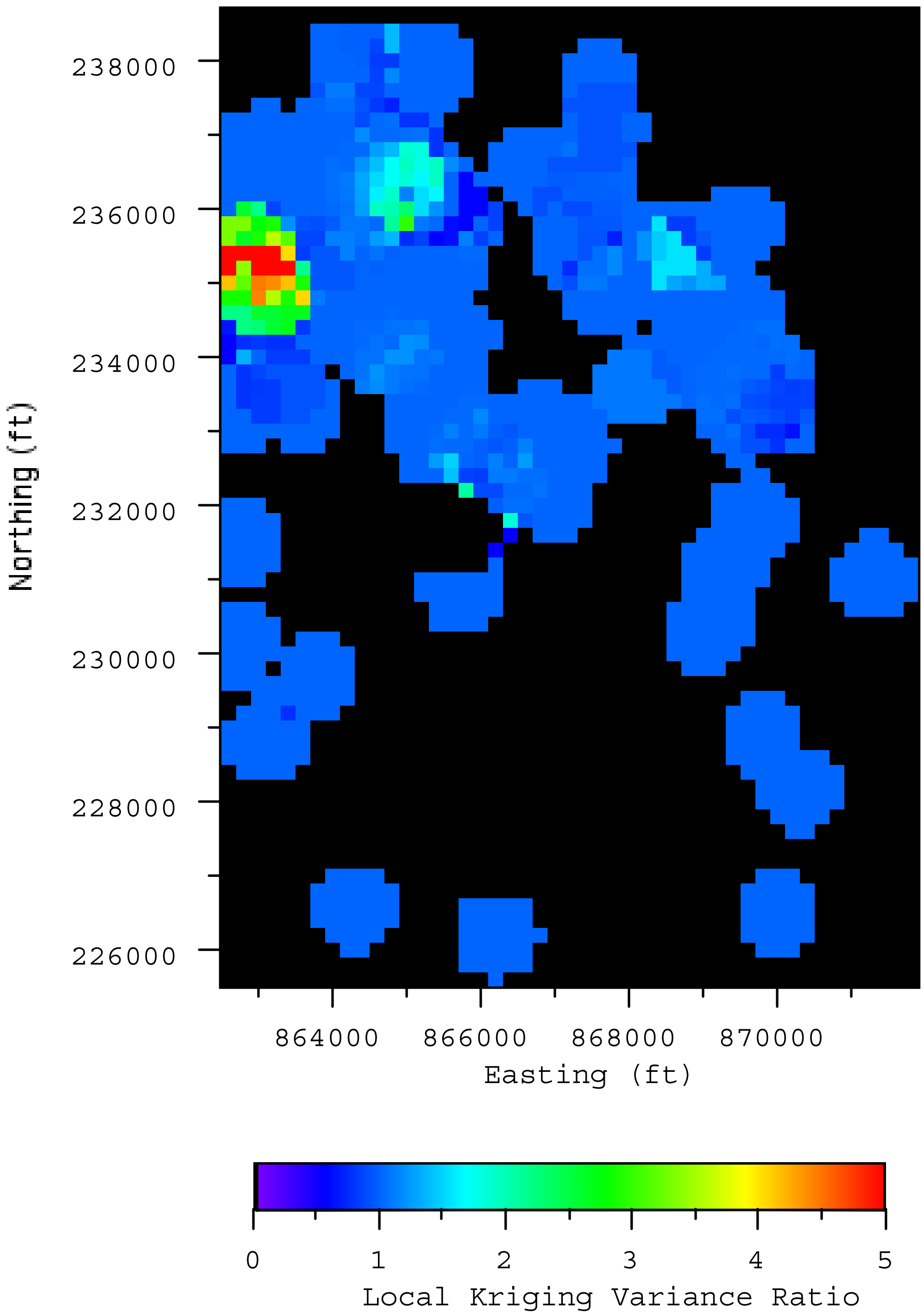

Figure 3-34. PCE KV Ratios, 4th Threshold (FS-12)

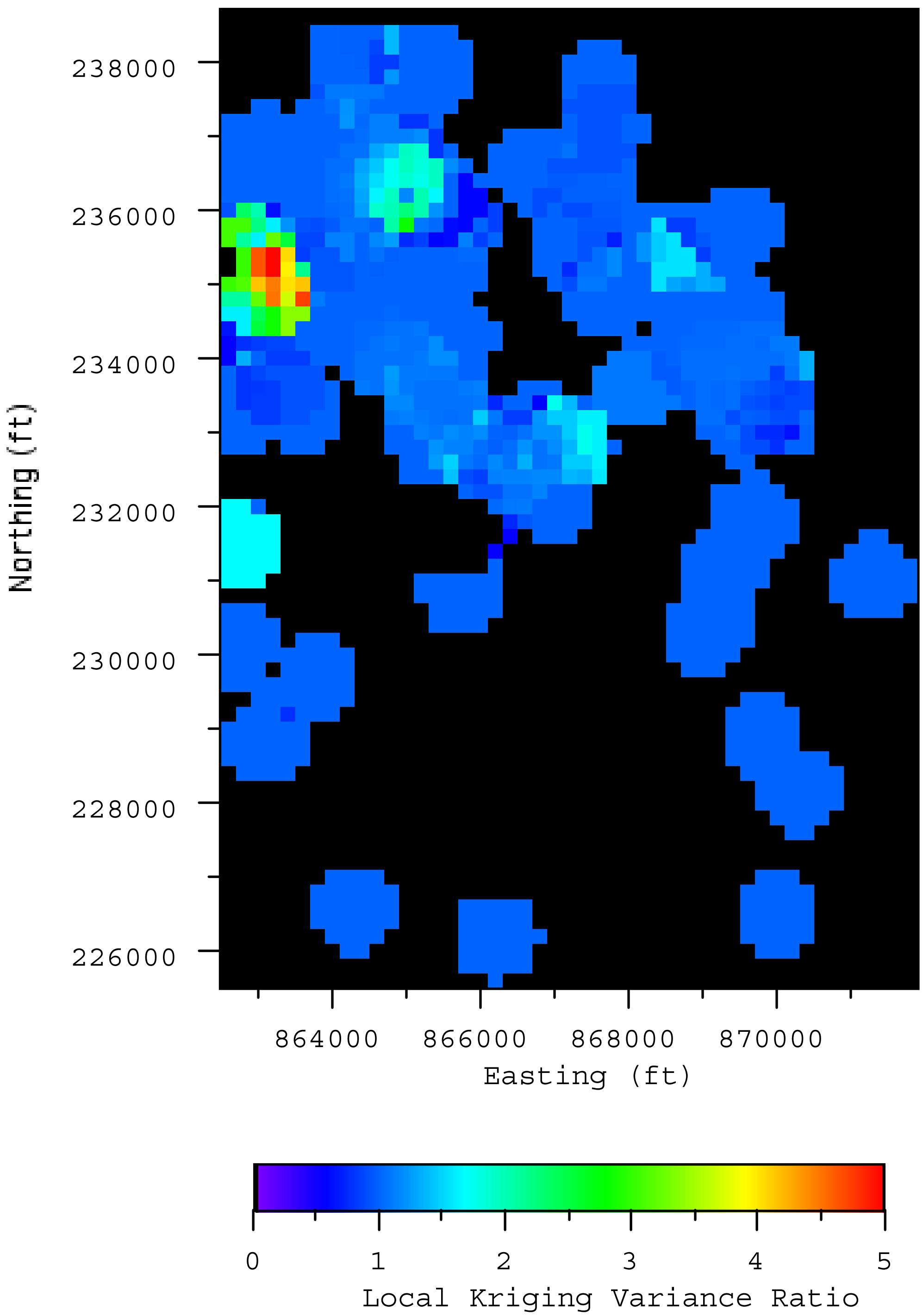

Figure 3-35. PCE KV Ratios, 5th Threshold (EBW)

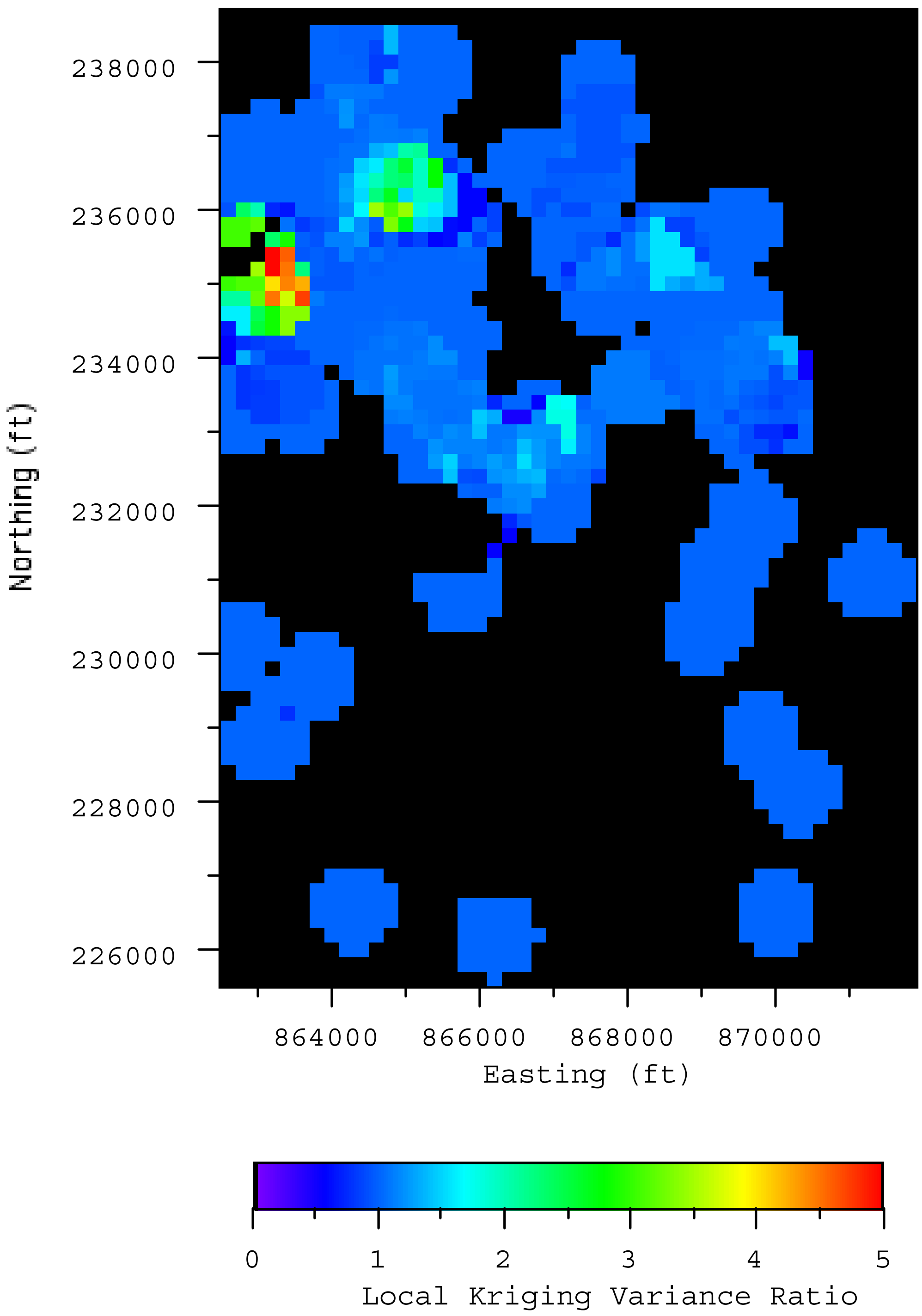

Figure 3-36. PCE KV Ratios, 6th Threshold (EBW)

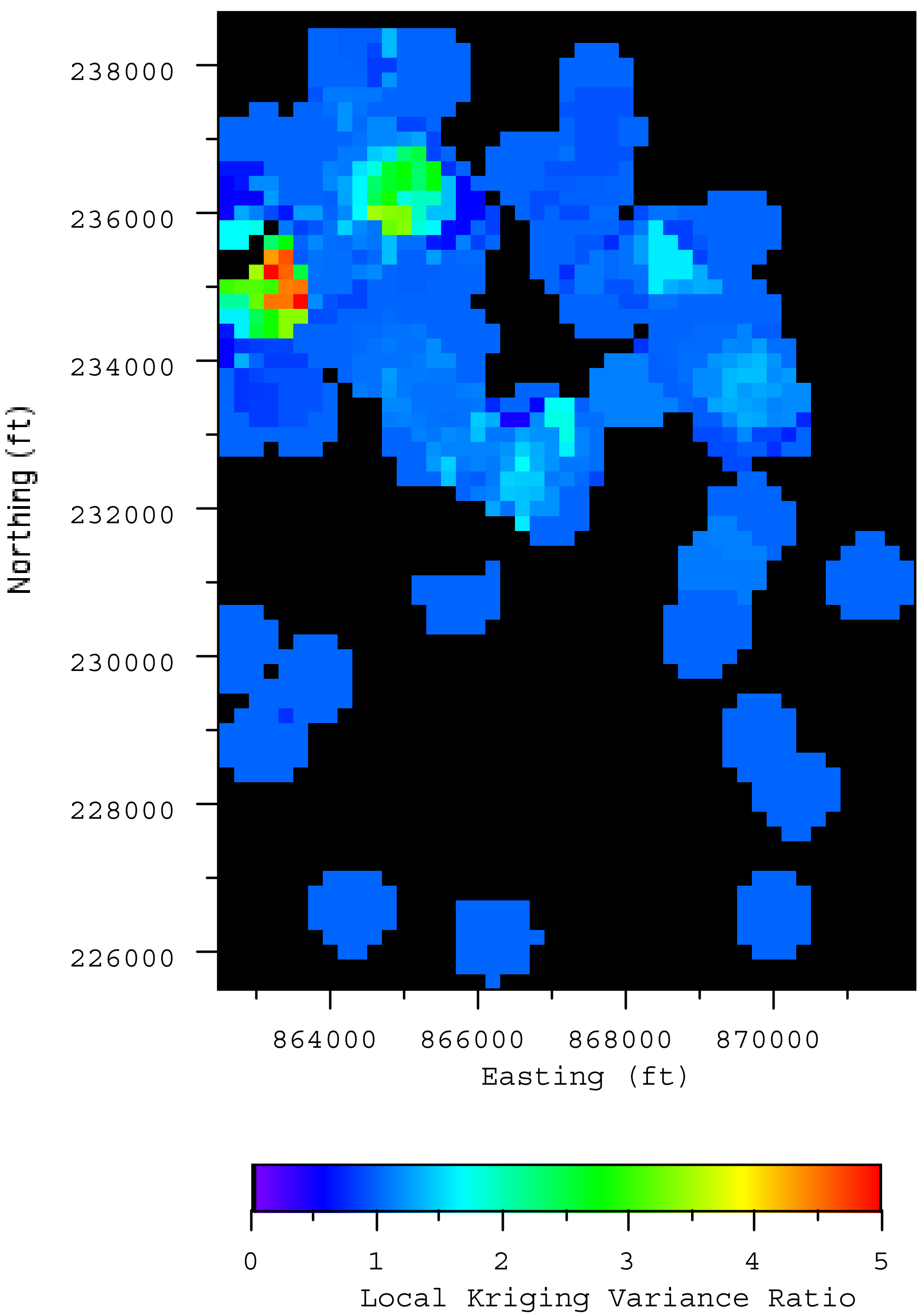

Figure 3-37. EDB IK Estimates, 1st Threshold, Q4 1998 (FS-12)

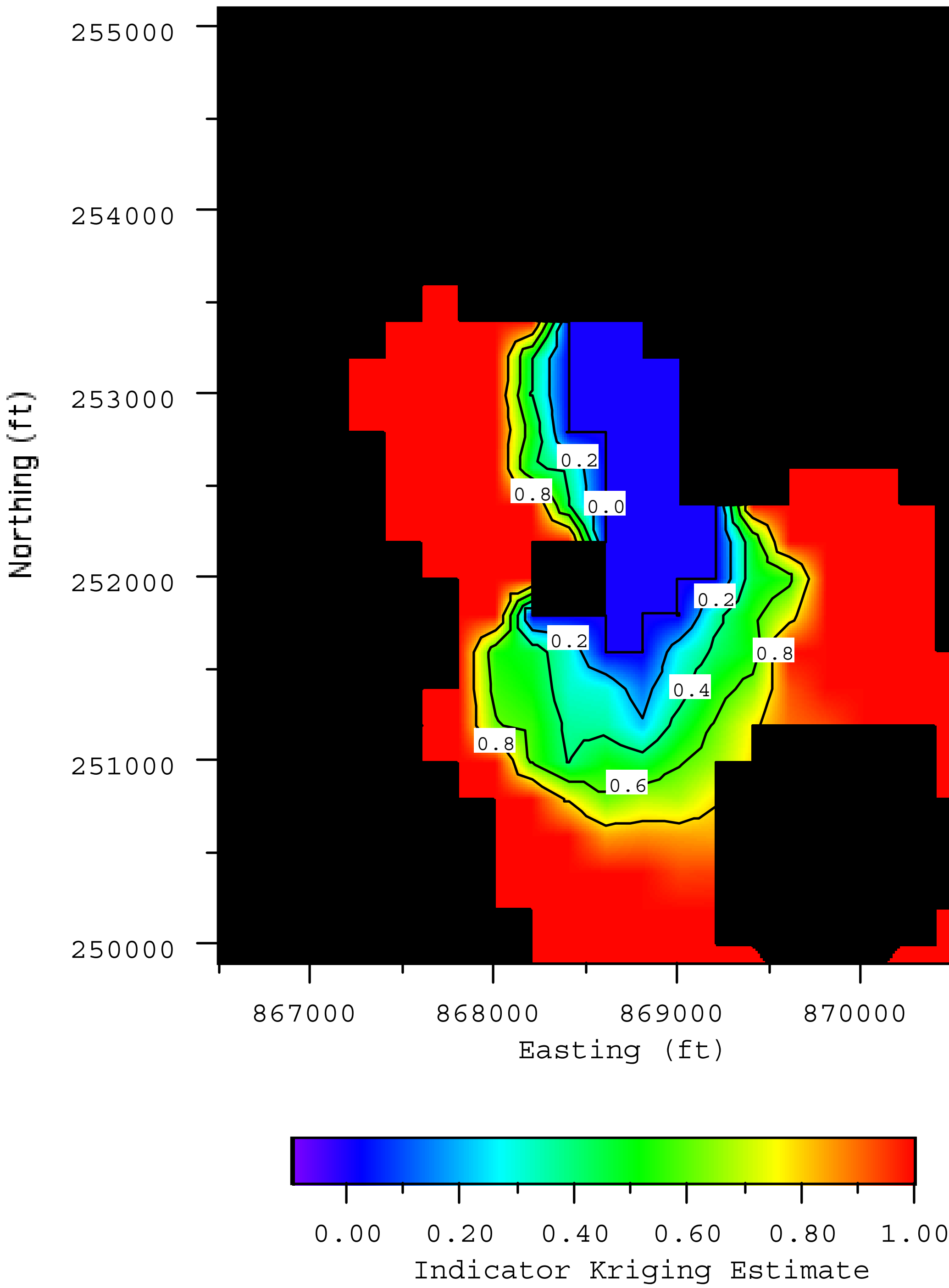

Figure 3-38. EDB IK Estimates, 2nd Threshold, Q4 1998 (FS-12)

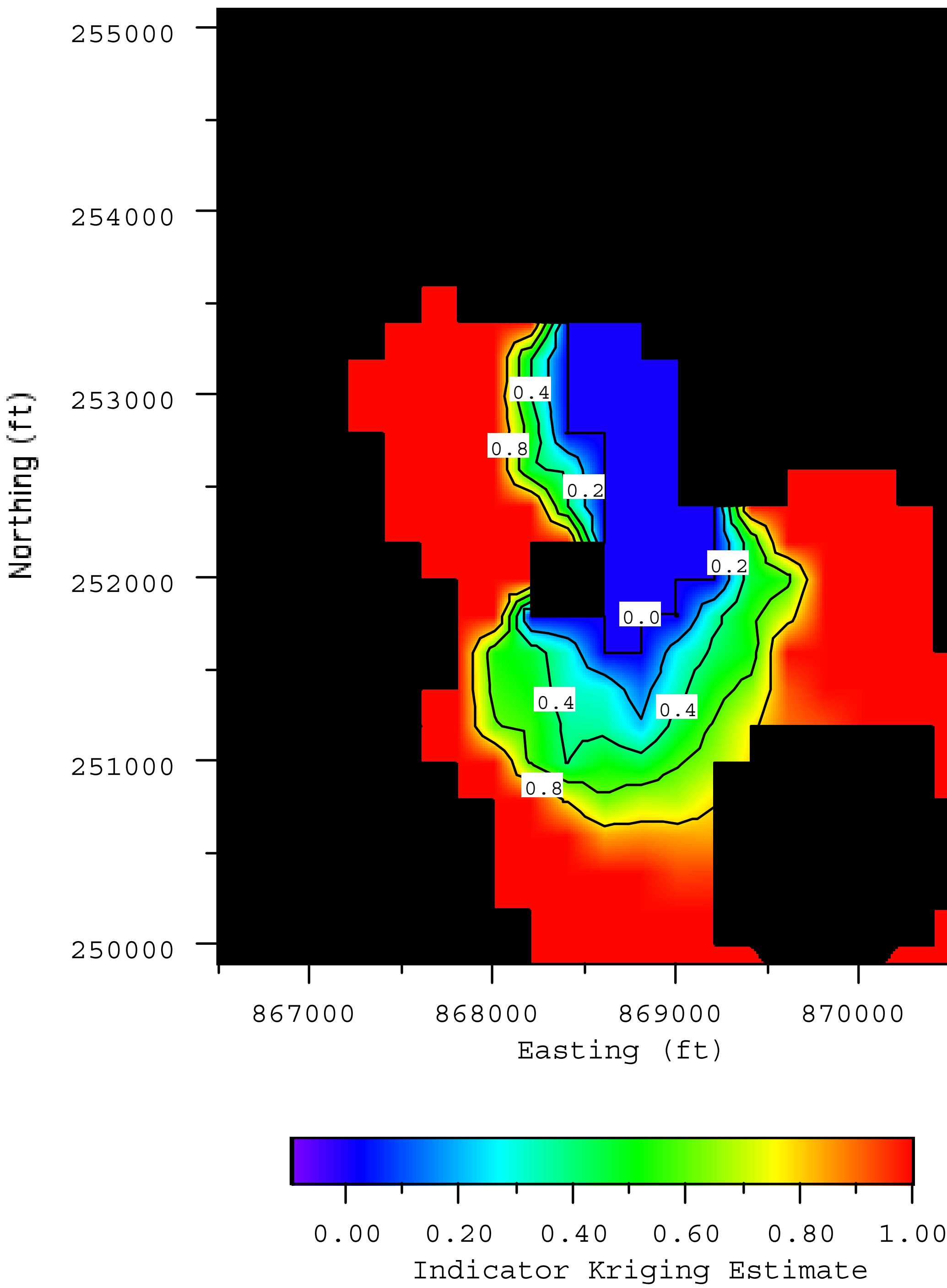

Figure 3-39. EDB IK Estimates, 3rd Threshold, Q4 1998 (FS-12)

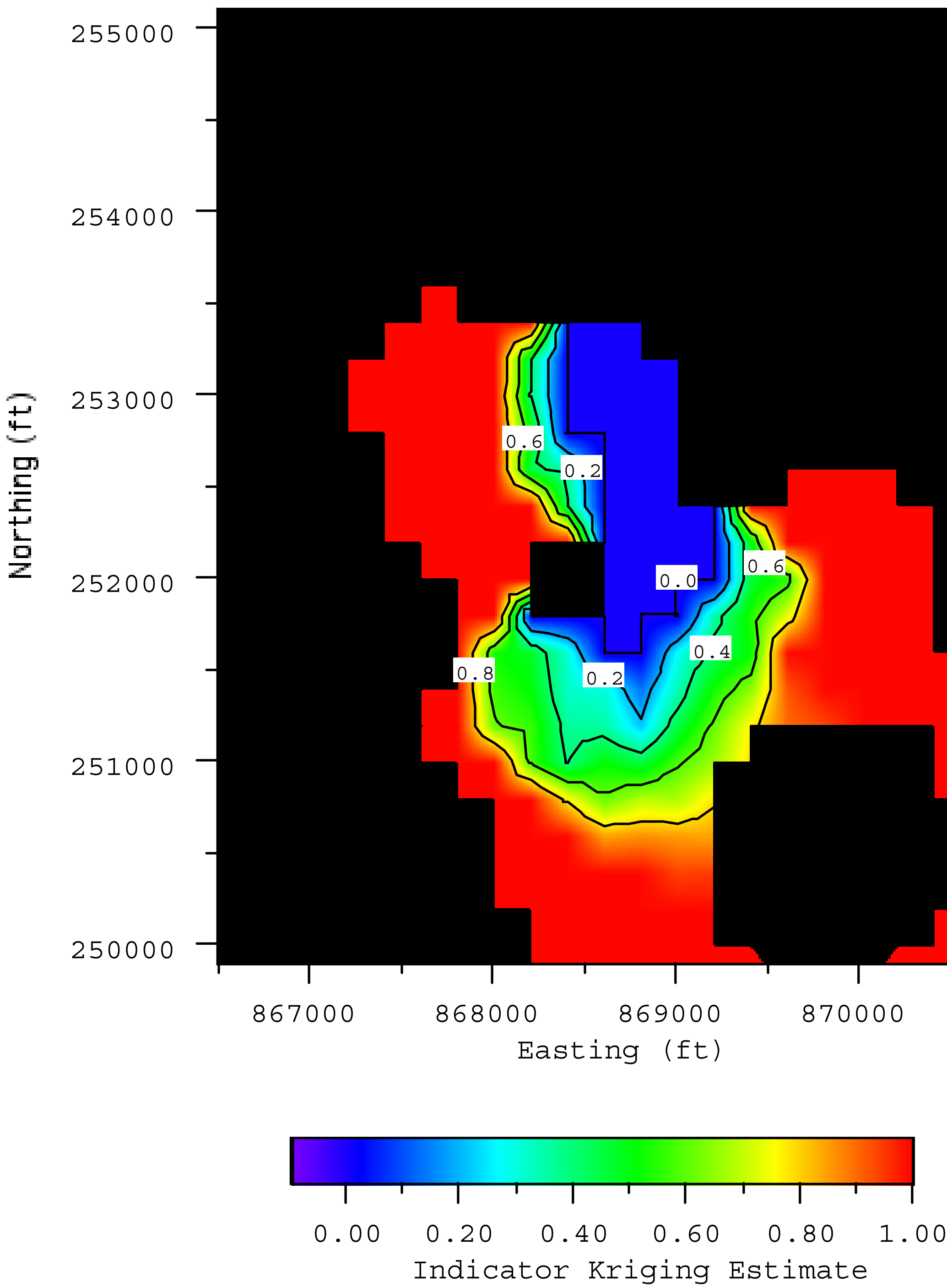

Figure 3-40. EDB IK Estimates, 4th Threshold, Q4 1998 (FS-12)

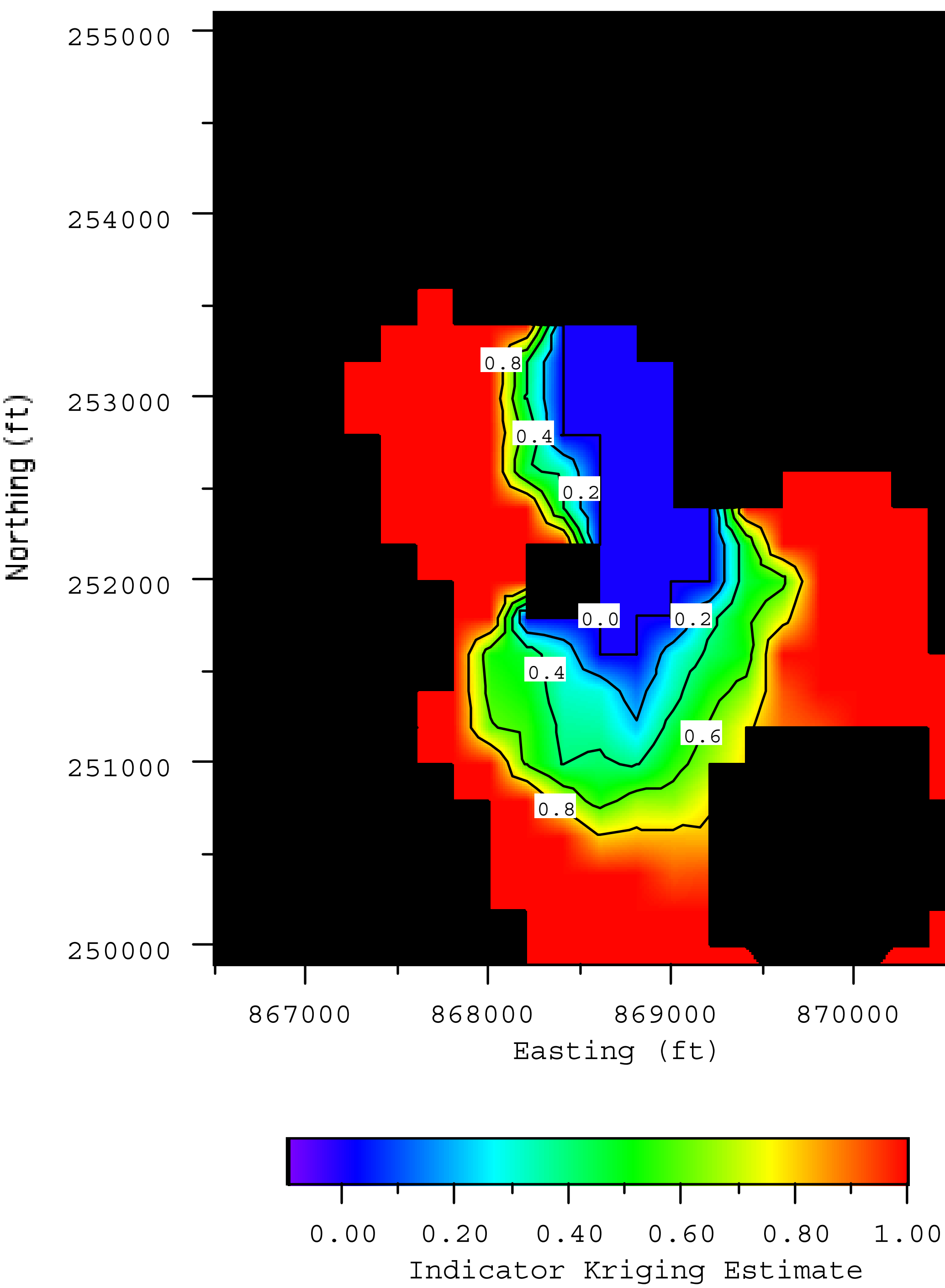

Figure 3-41. EDB IK Estimates, 5th Threshold, Q4 1998 (FS-12)

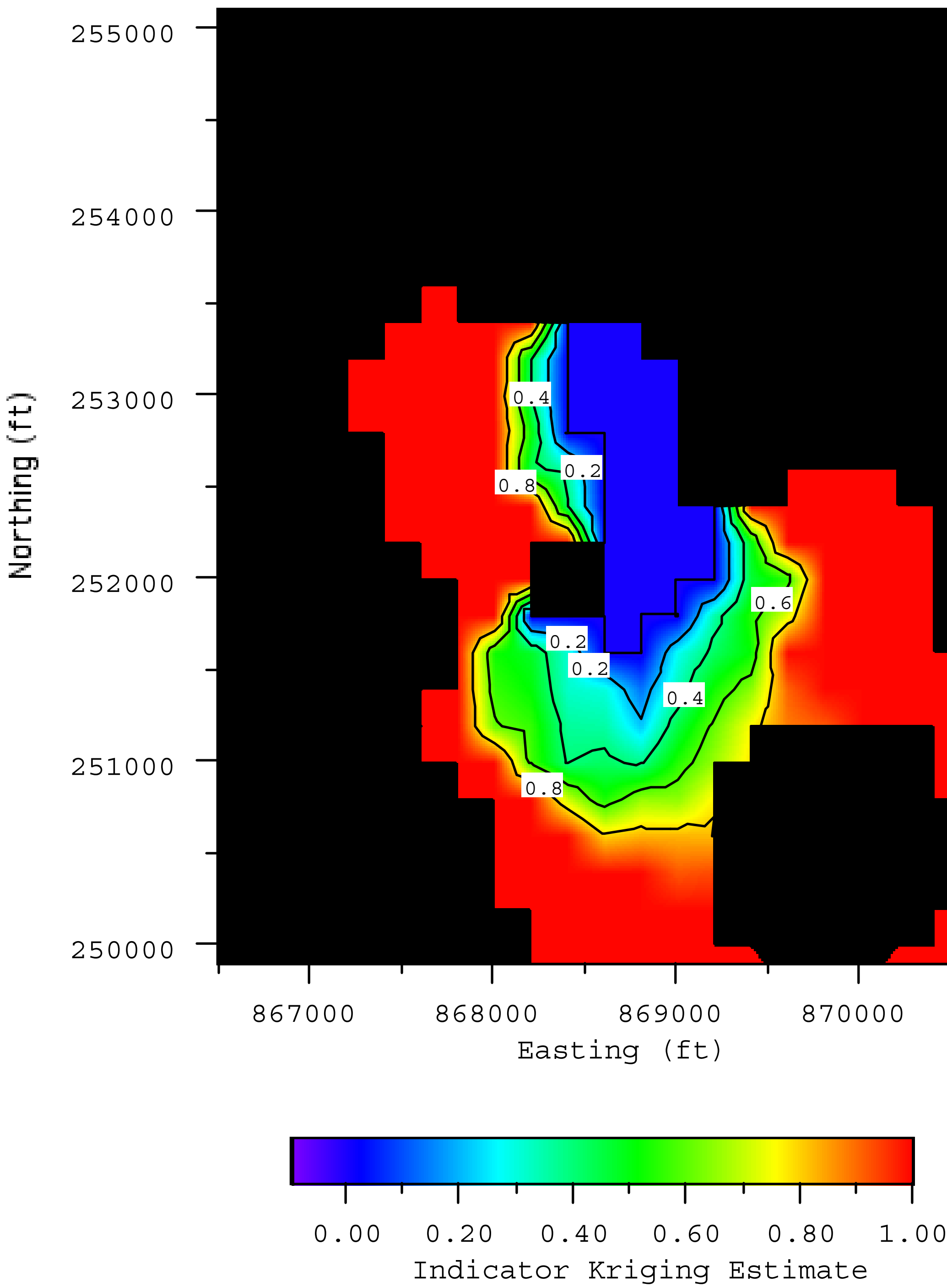

Figure 3-42. EDB IK Estimates, 6th Threshold, Q4 1998 (FS-12)

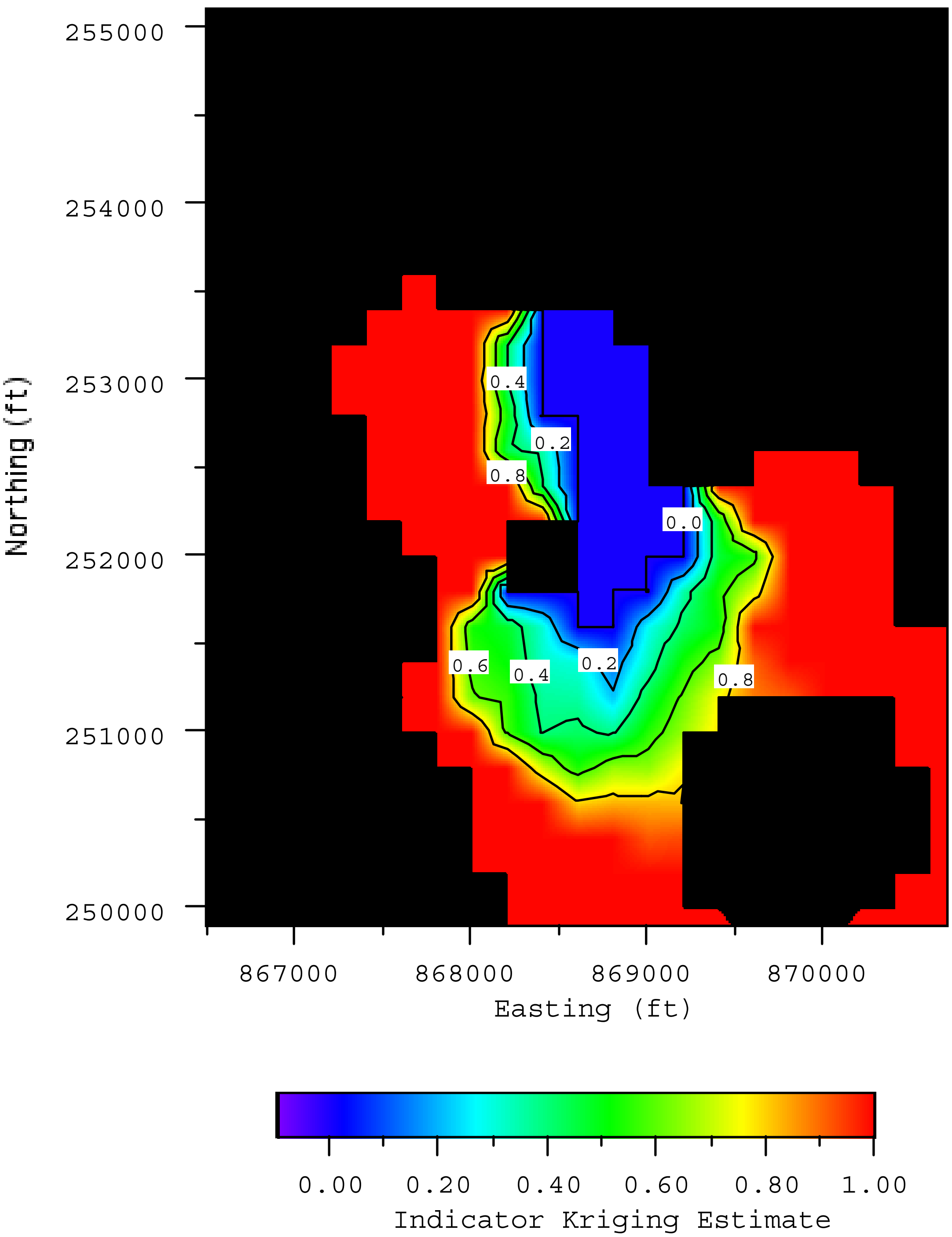

Figure 3-43. Benzene IK Estimates, 1st Threshold, Q4 1998 (FS-12)

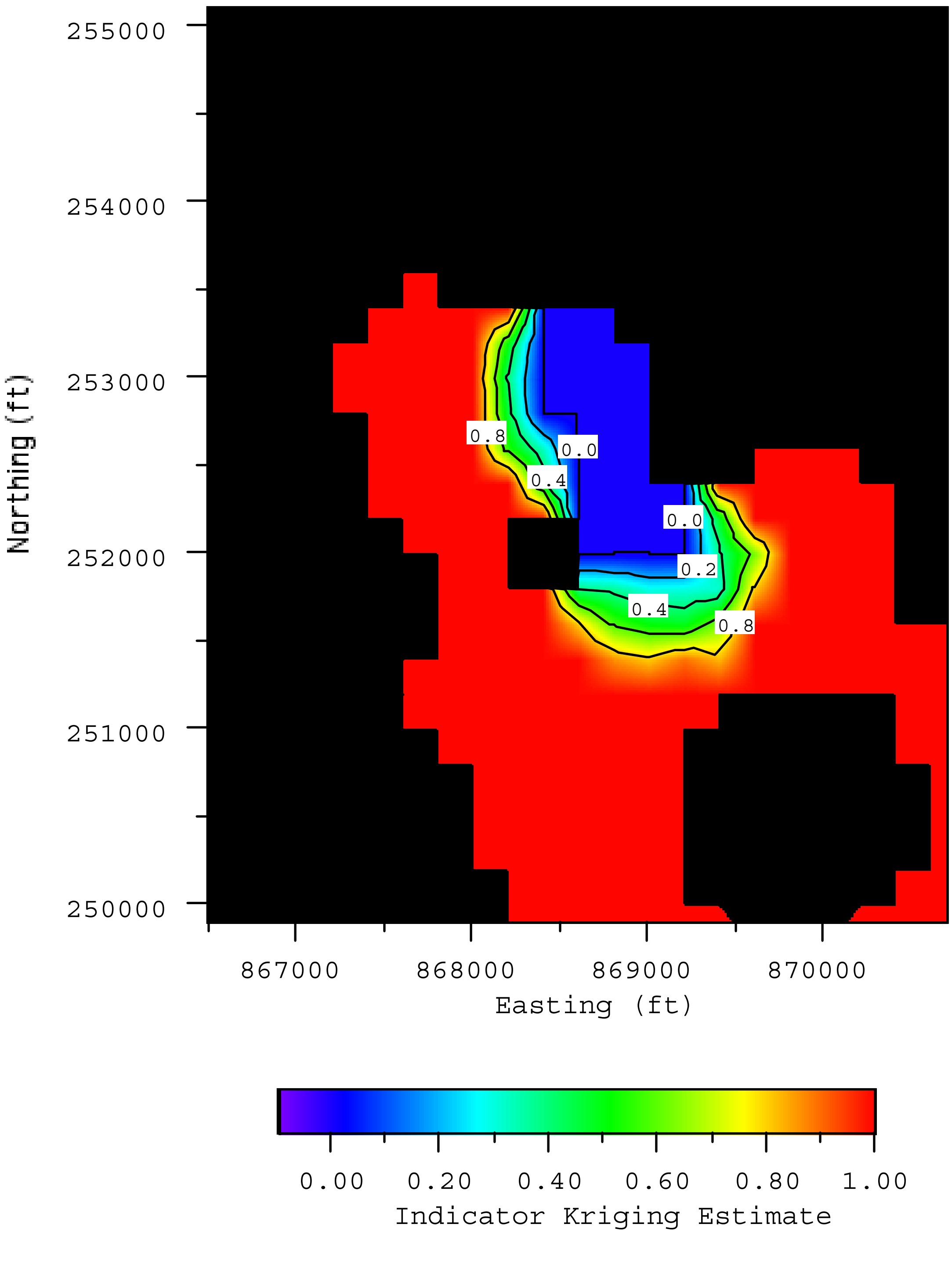

Figure 3-44. Benzene IK Estimates, 2nd Threshold, Q4 1998 (FS-12)

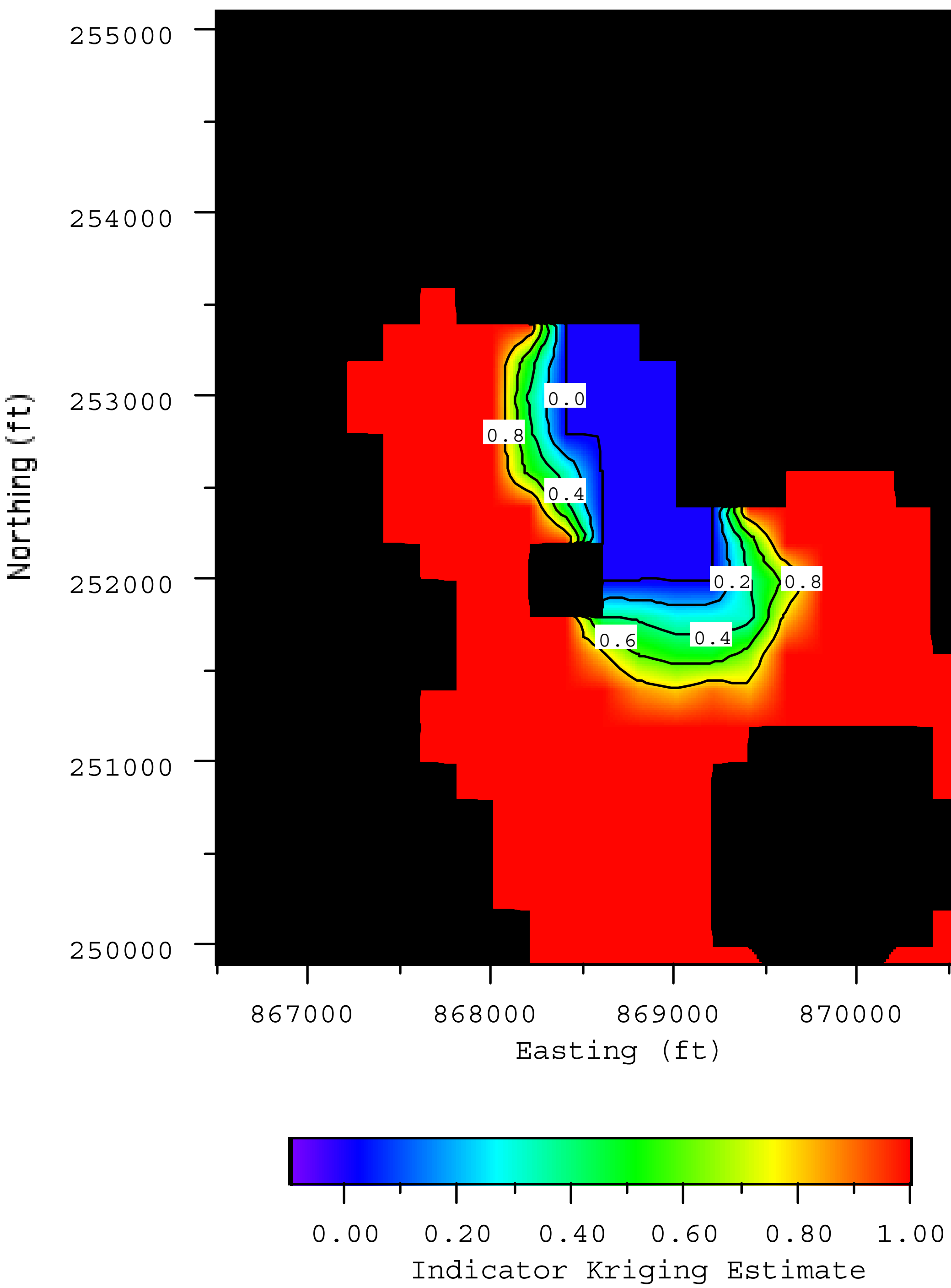

Figure 3-45. Benzene IK Estimates, 3rd Threshold, Q4 1998 (FS-12)

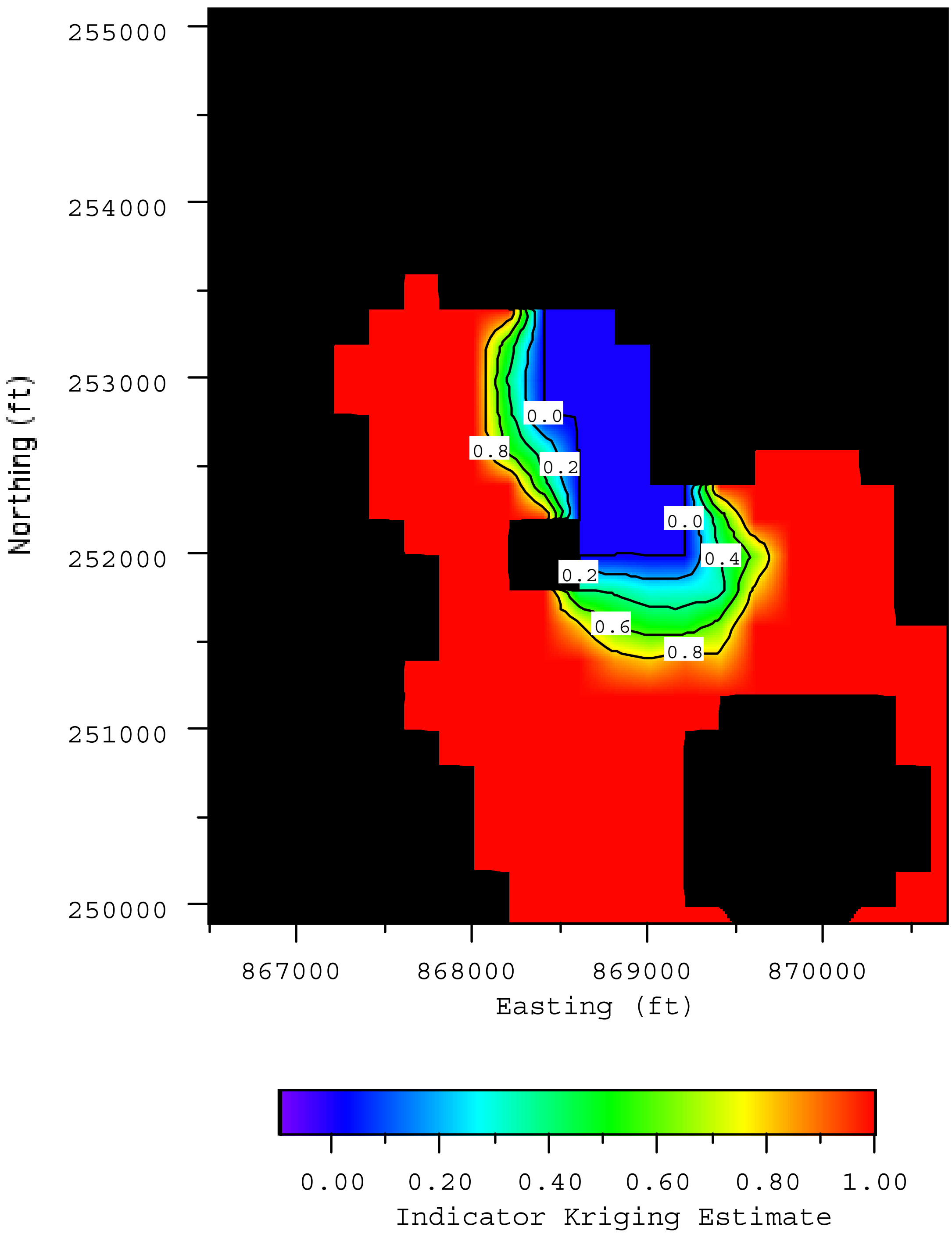

Figure 3-46. Benzene IK Estimates, 4th Threshold, Q4 1998 (FS-12)

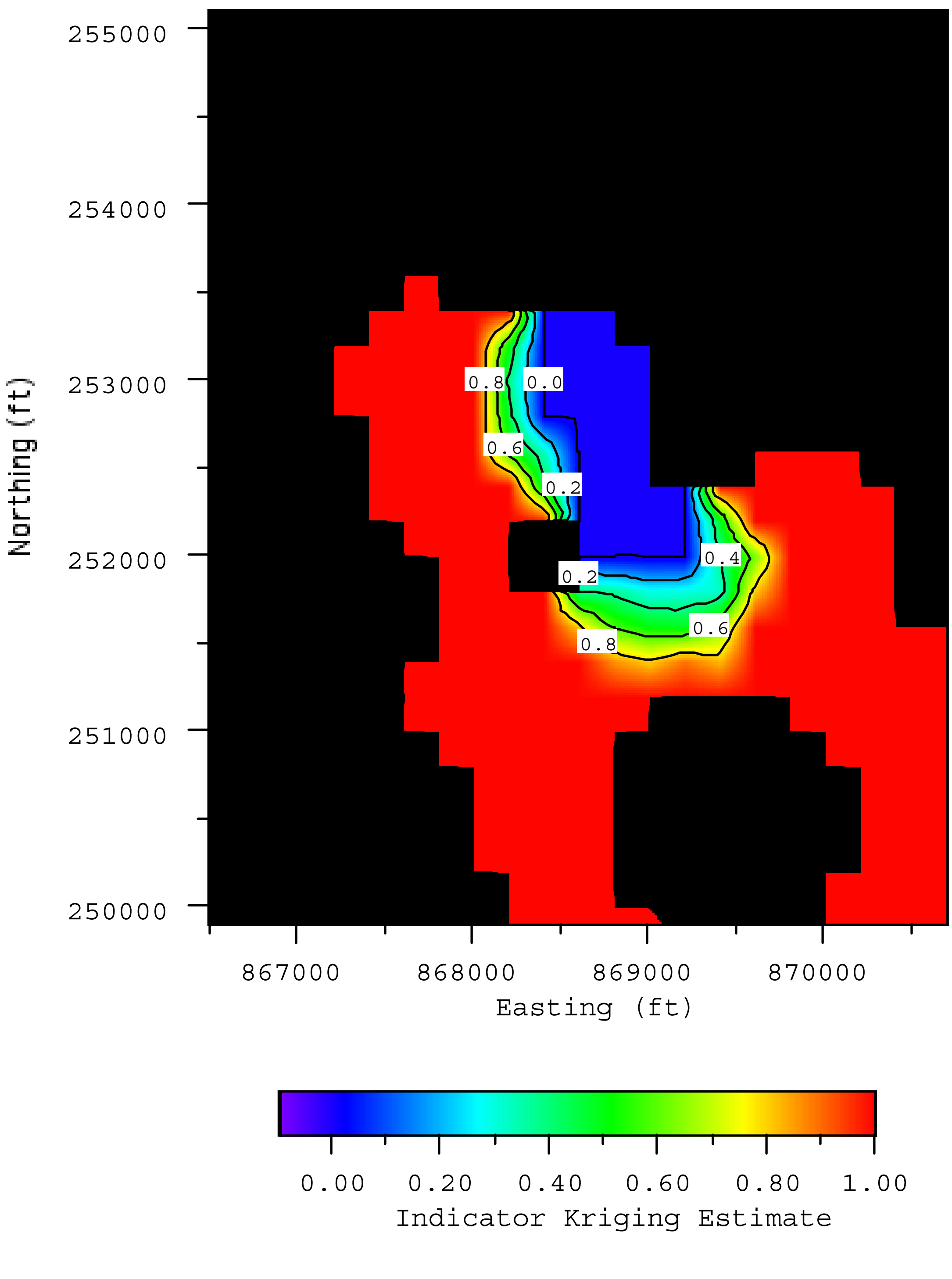

Figure 3-47. Benzene IK Estimates, 5th Threshold, Q4 1998 (FS-12)

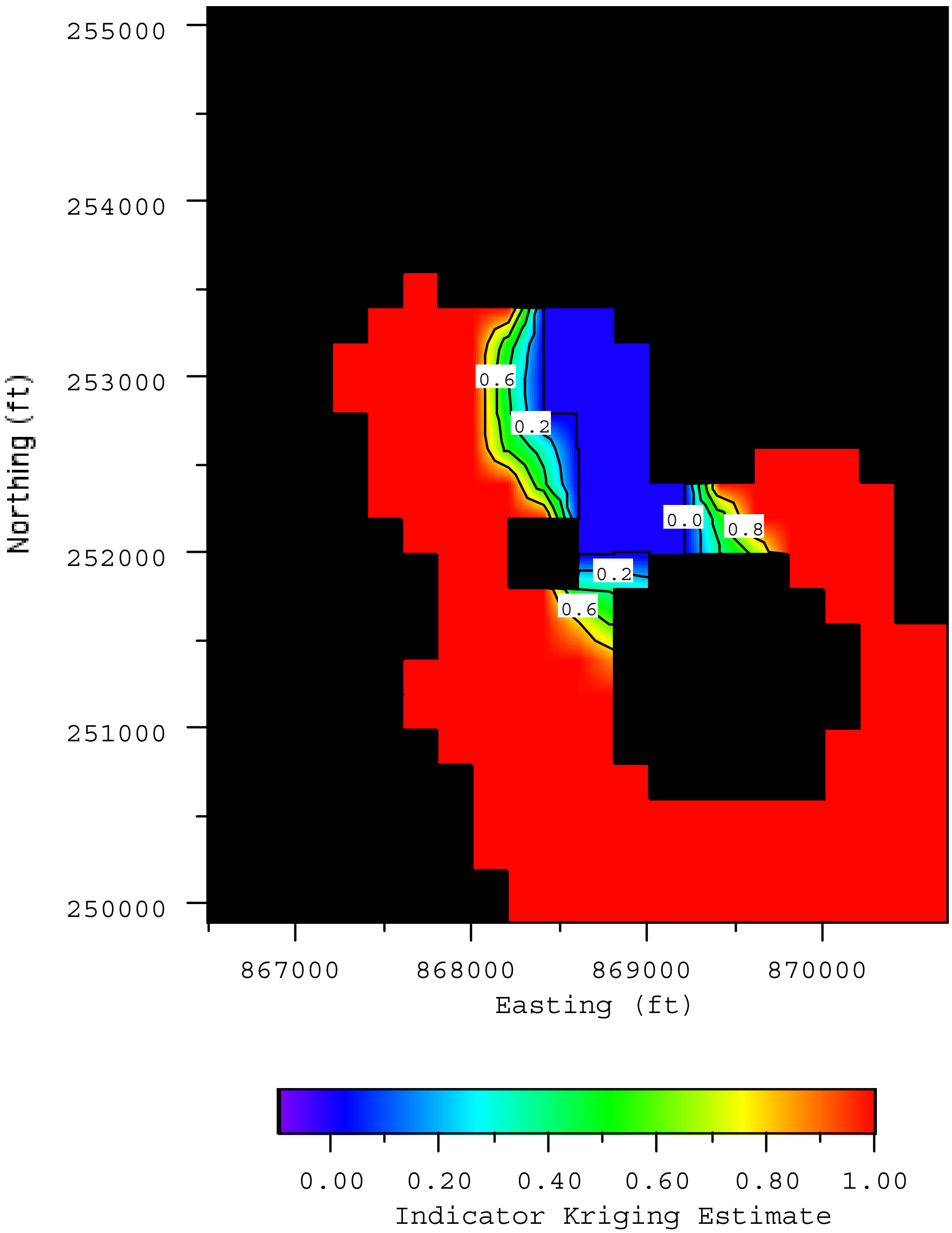

Figure 3-48. Benzene IK Estimates, 6th Threshold, Q4 1998 (FS-12)

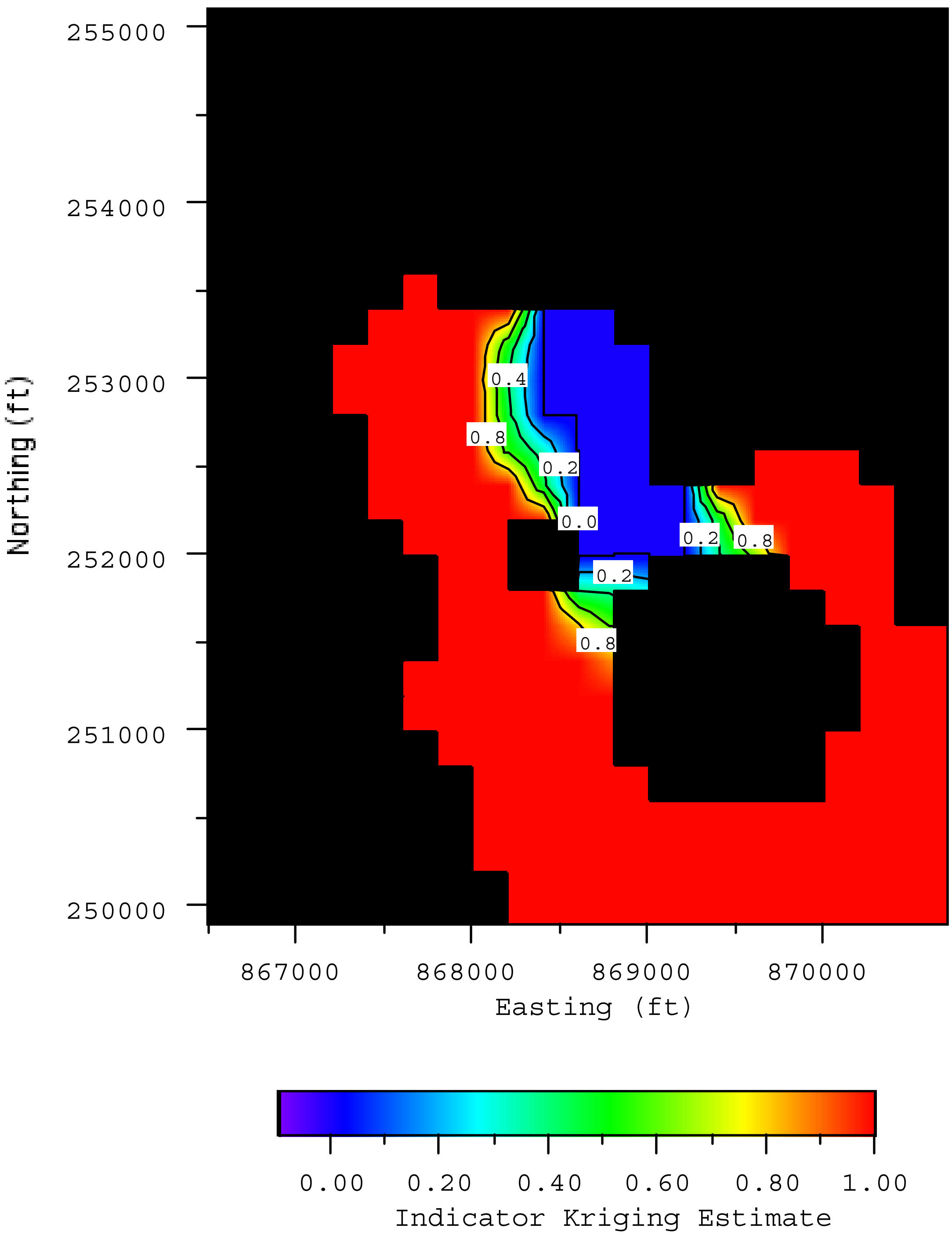

Figure 3-49. TCE IK Estimates, 1st Threshold, Q4 1998 (EBW)

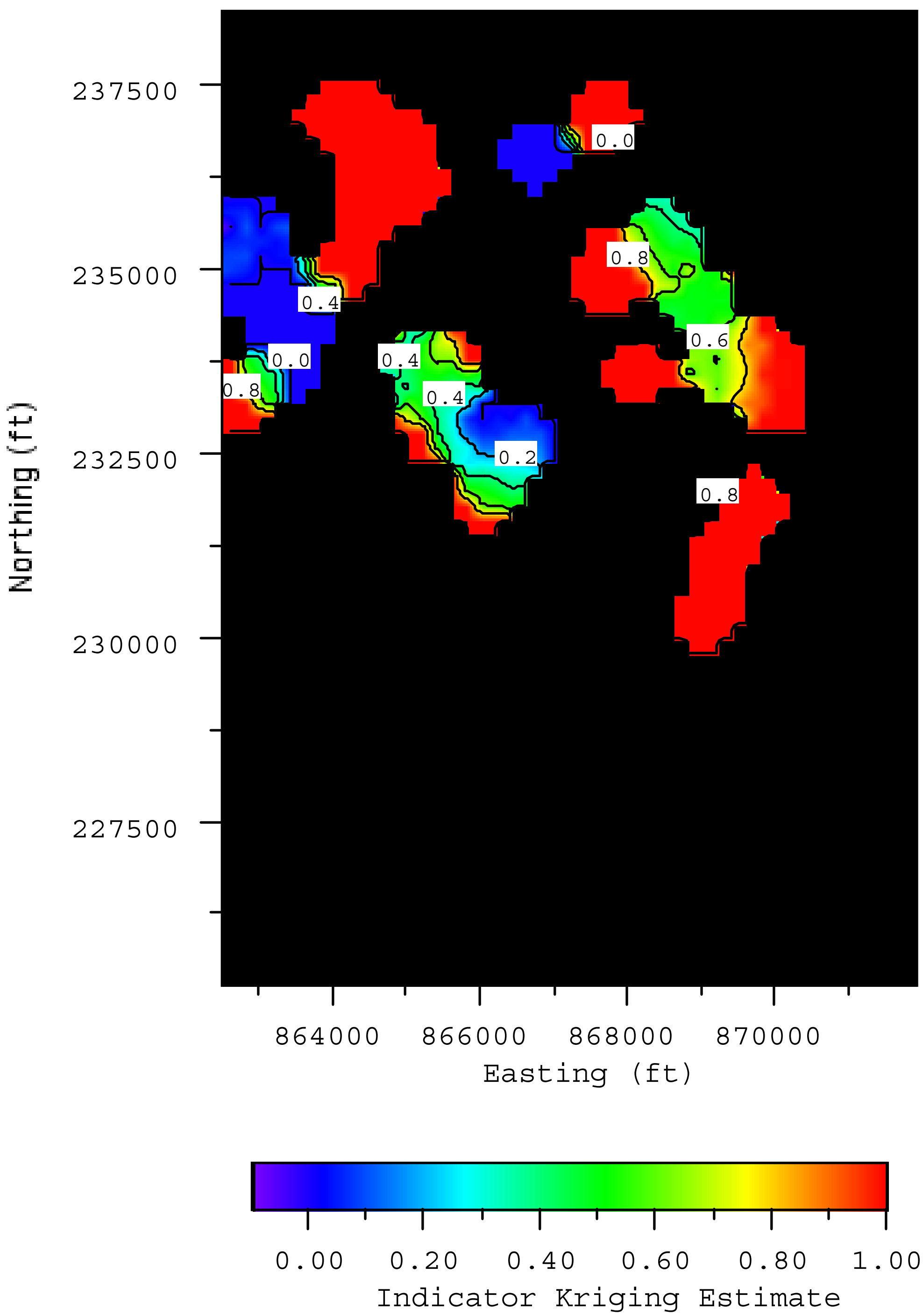

Figure 3-50. TCE IK Estimates, 2nd Threshold, Q4 1998 (EBW)

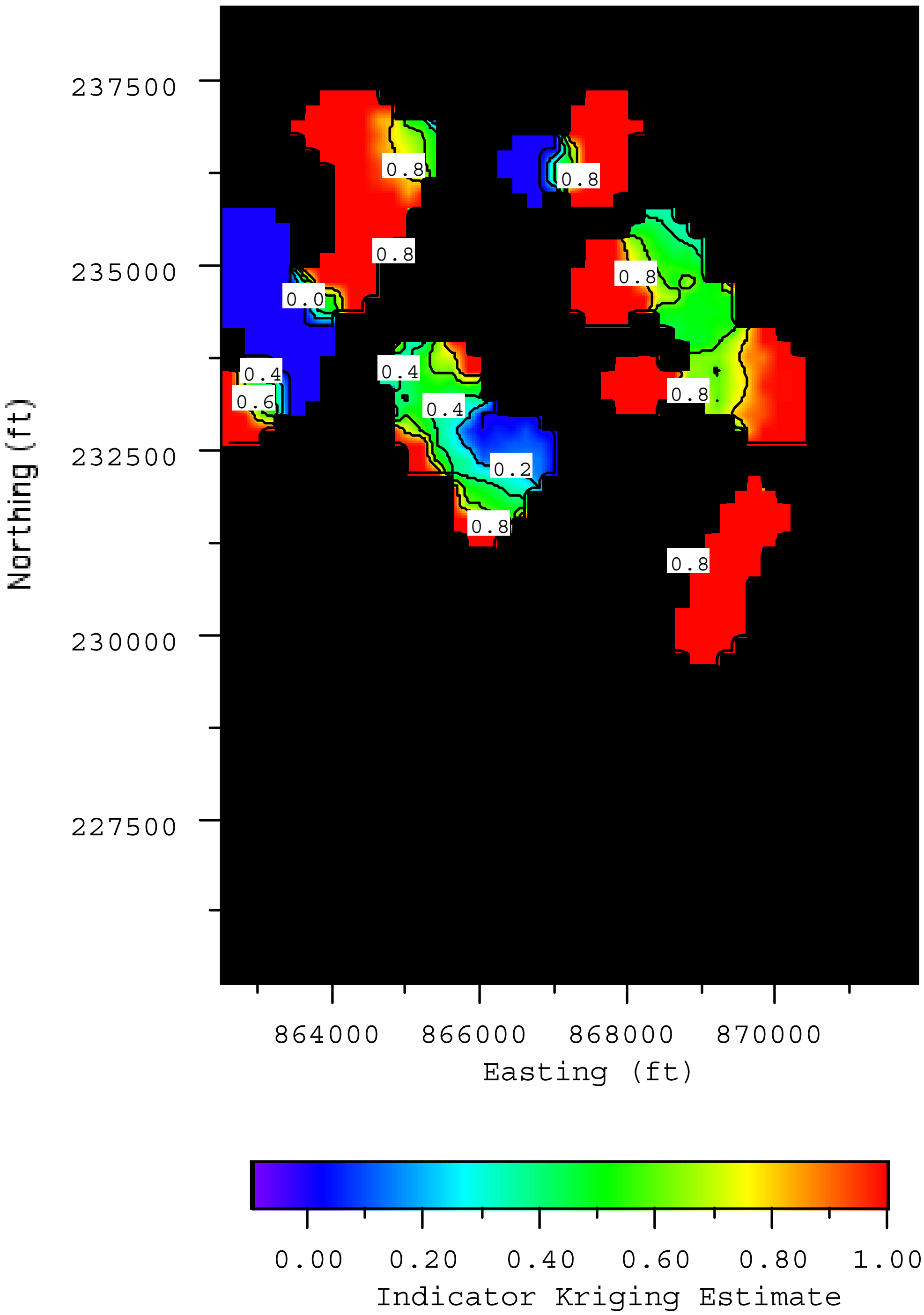

Figure 3-51. TCE IK Estimates, 3rd Threshold, Q4 1998 (EBW)

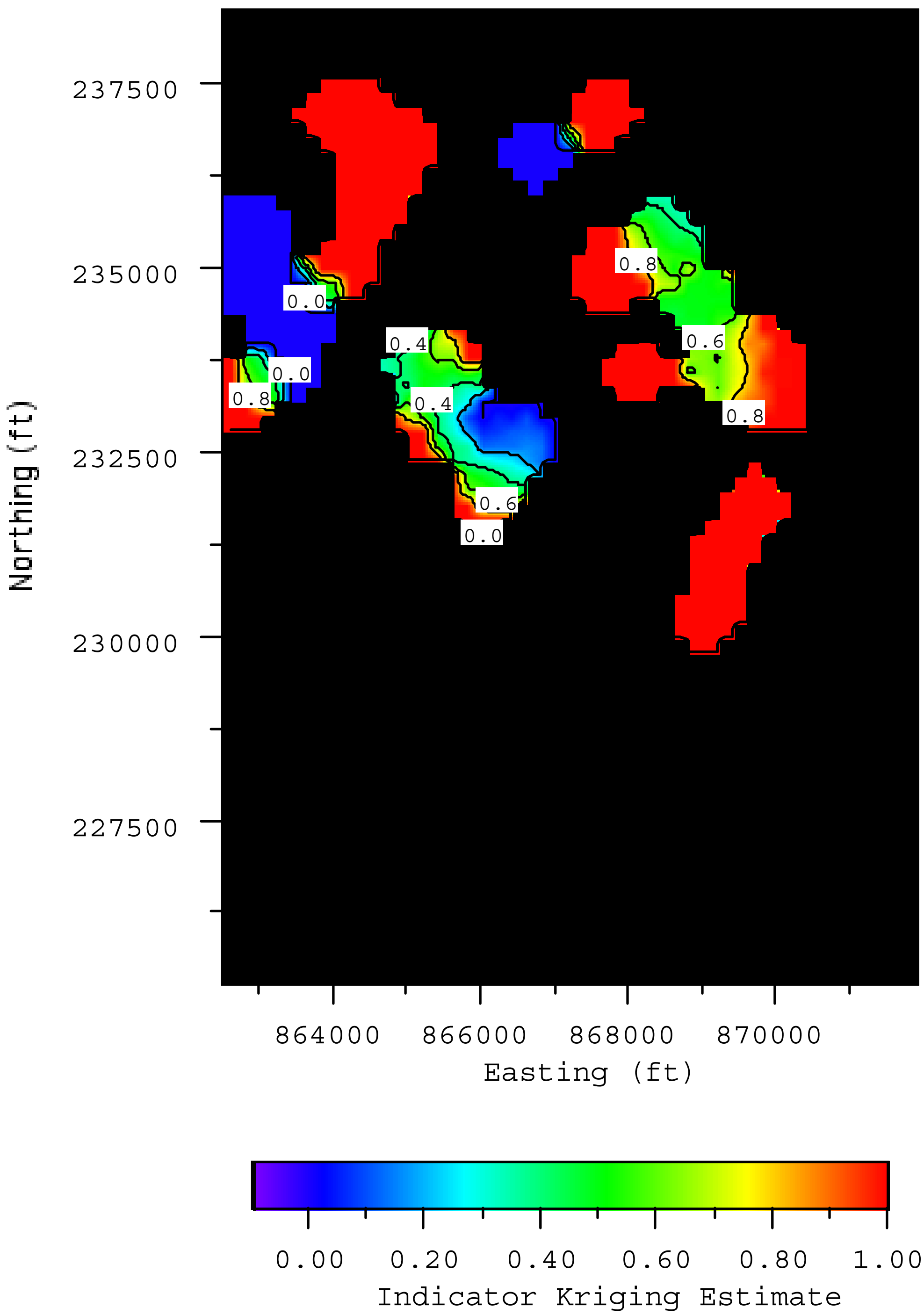

Figure 3-52. TCE IK Estimates, 4th Threshold, Q4 1998 (EBW)

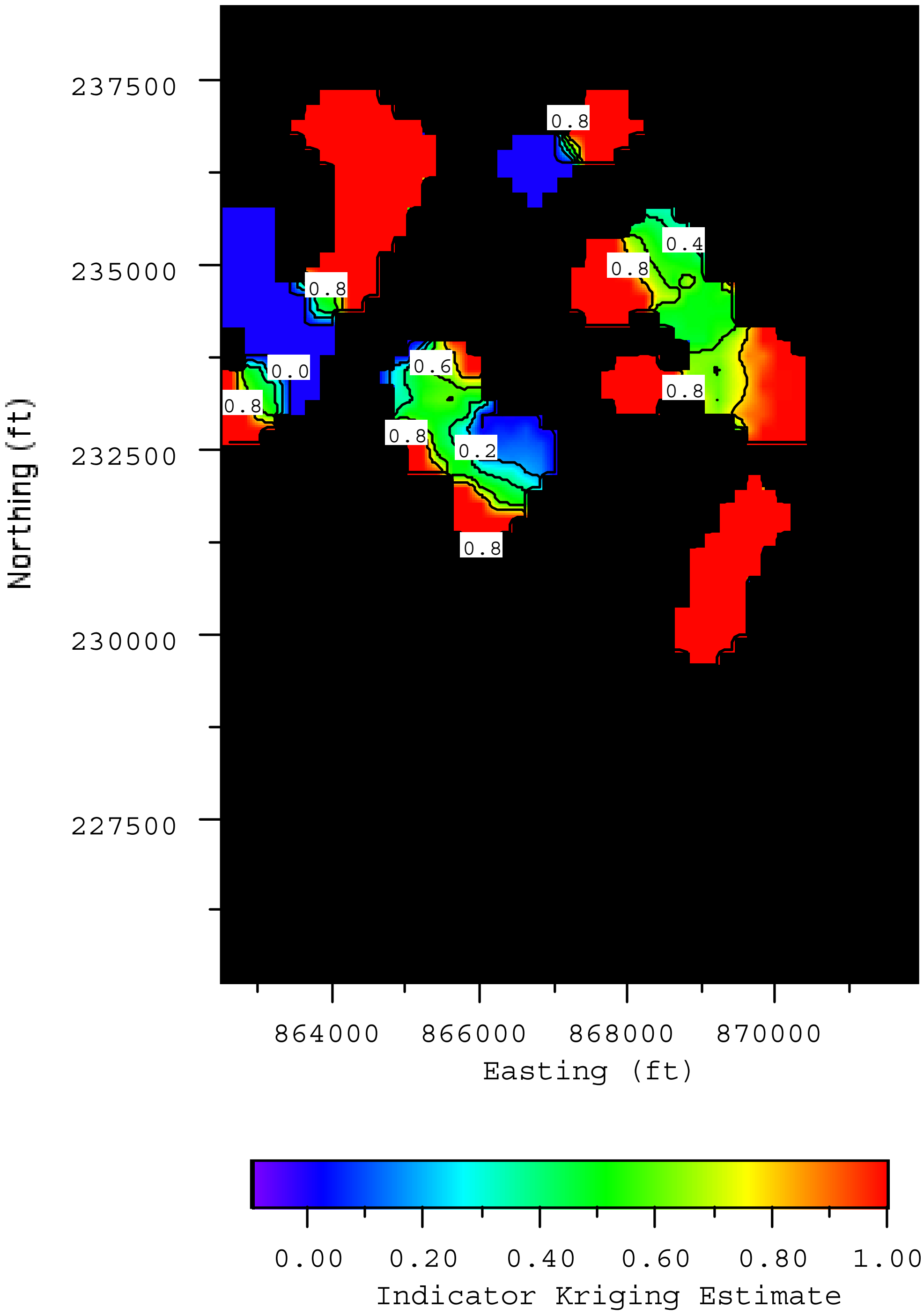

Figure 3-53. TCE IK Estimate, 5th Threshold, Q4 1998 (EBW)

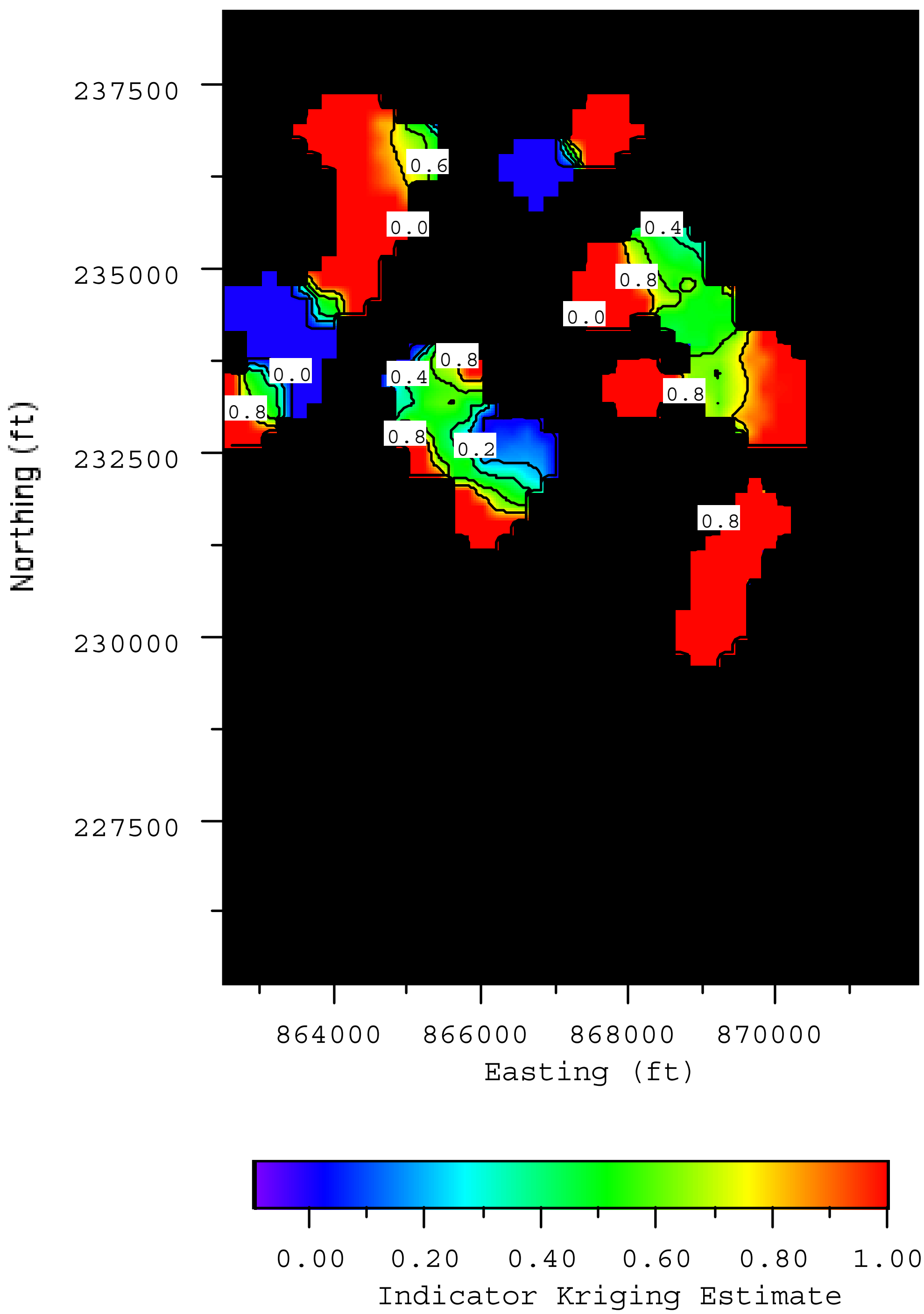

Figure 3-54. TCE IK Estimates, 6th Threshold, Q4 1998 (EBW)

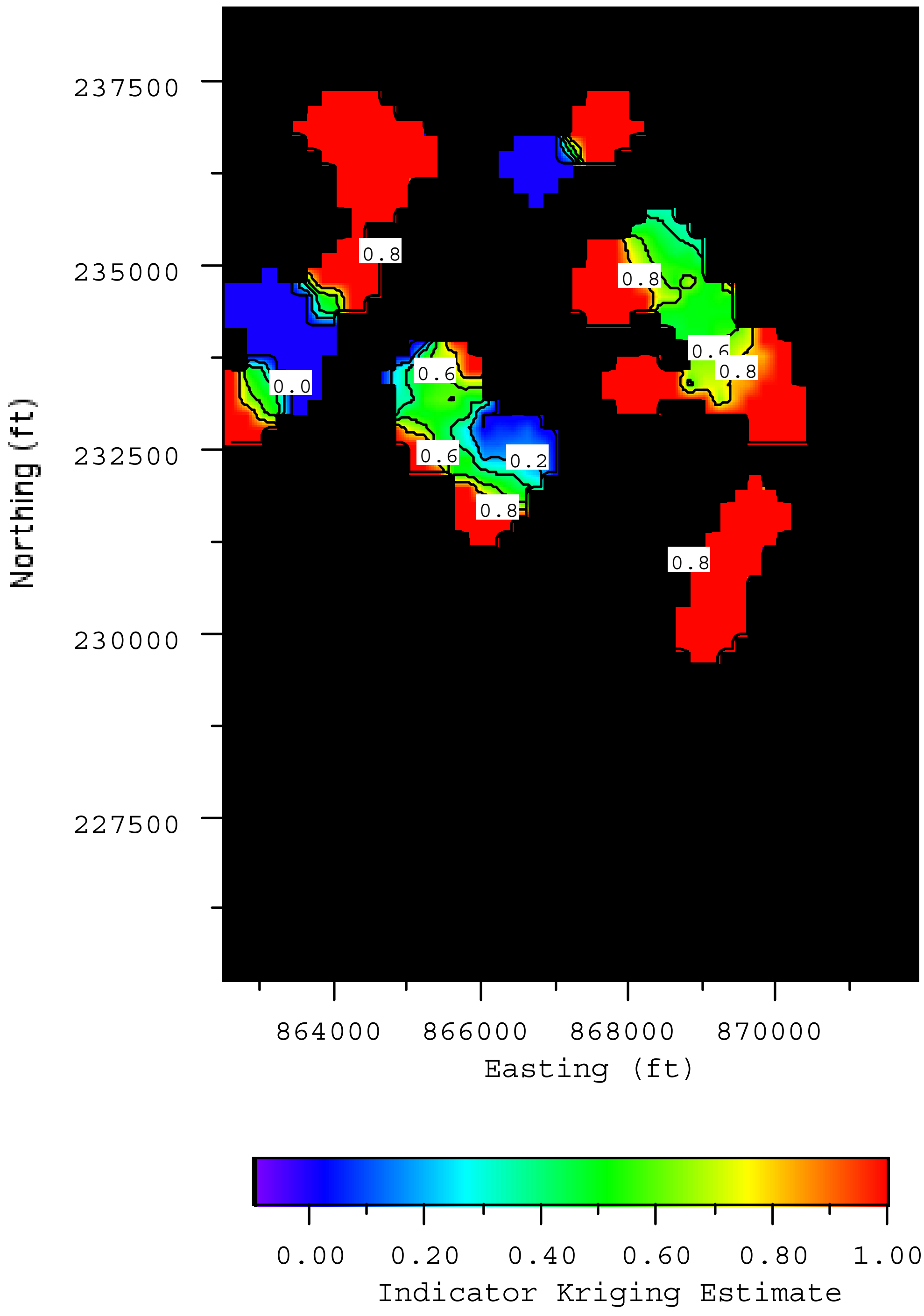

Figure 3-55. PCE IK Estimates, 1st Threshold, Q4 1998 (EBW)

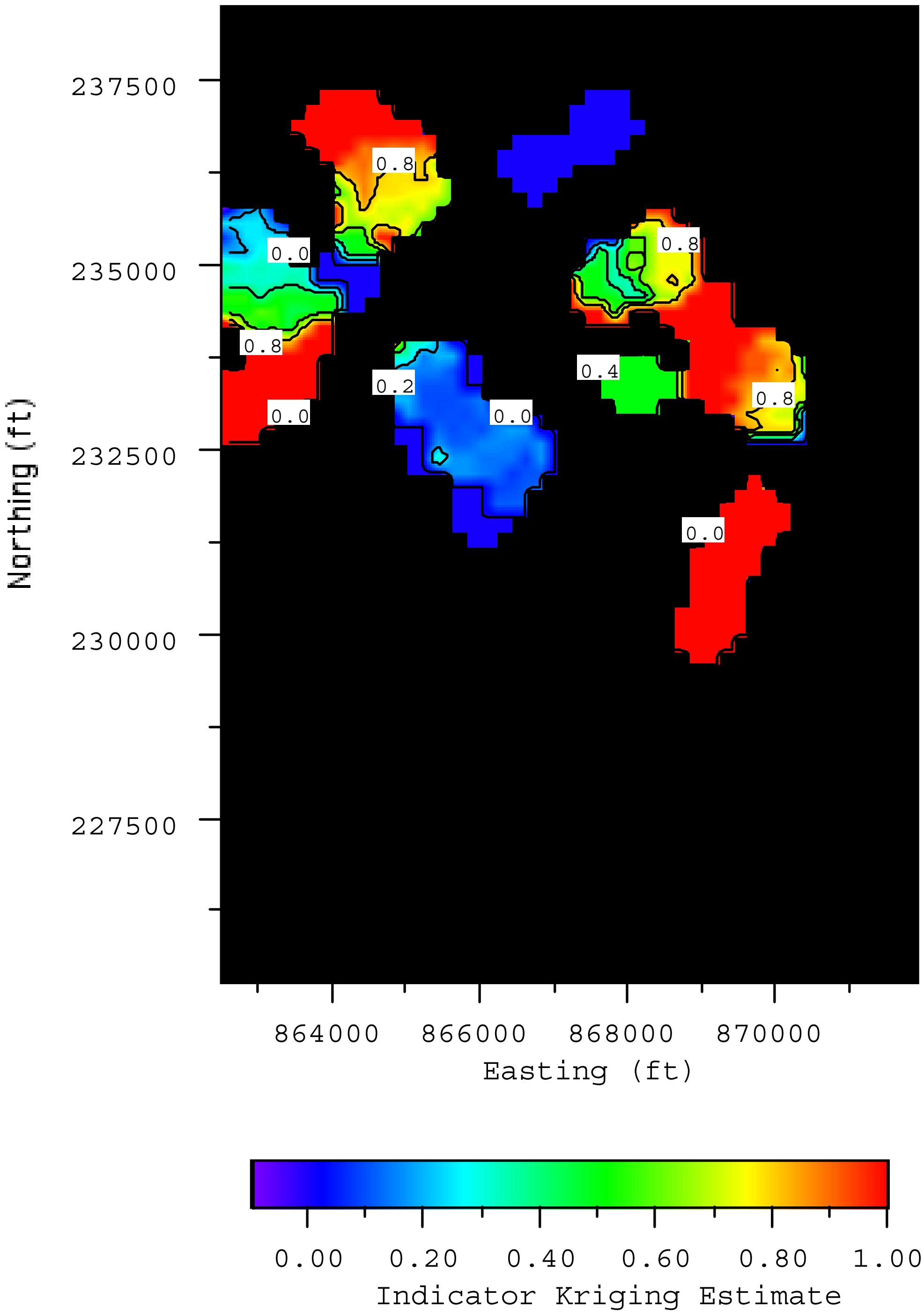

Figure 3-56. PCE IK Estimates, 2nd Threshold, Q4 1998 (EBW)

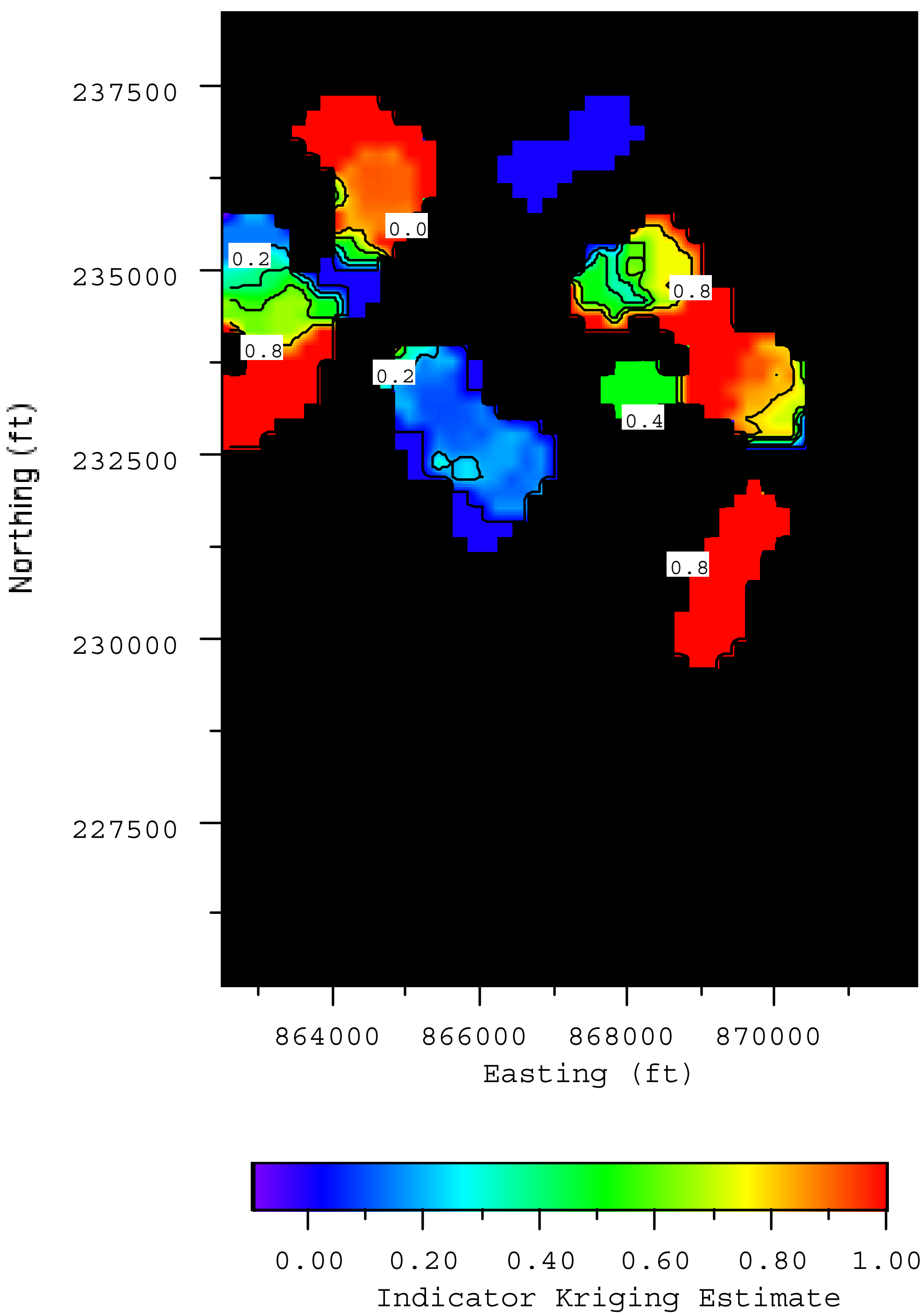

Figure 3-57. PCE IK Estimates, 3rd Threshold, Q4 1998 (EBW)

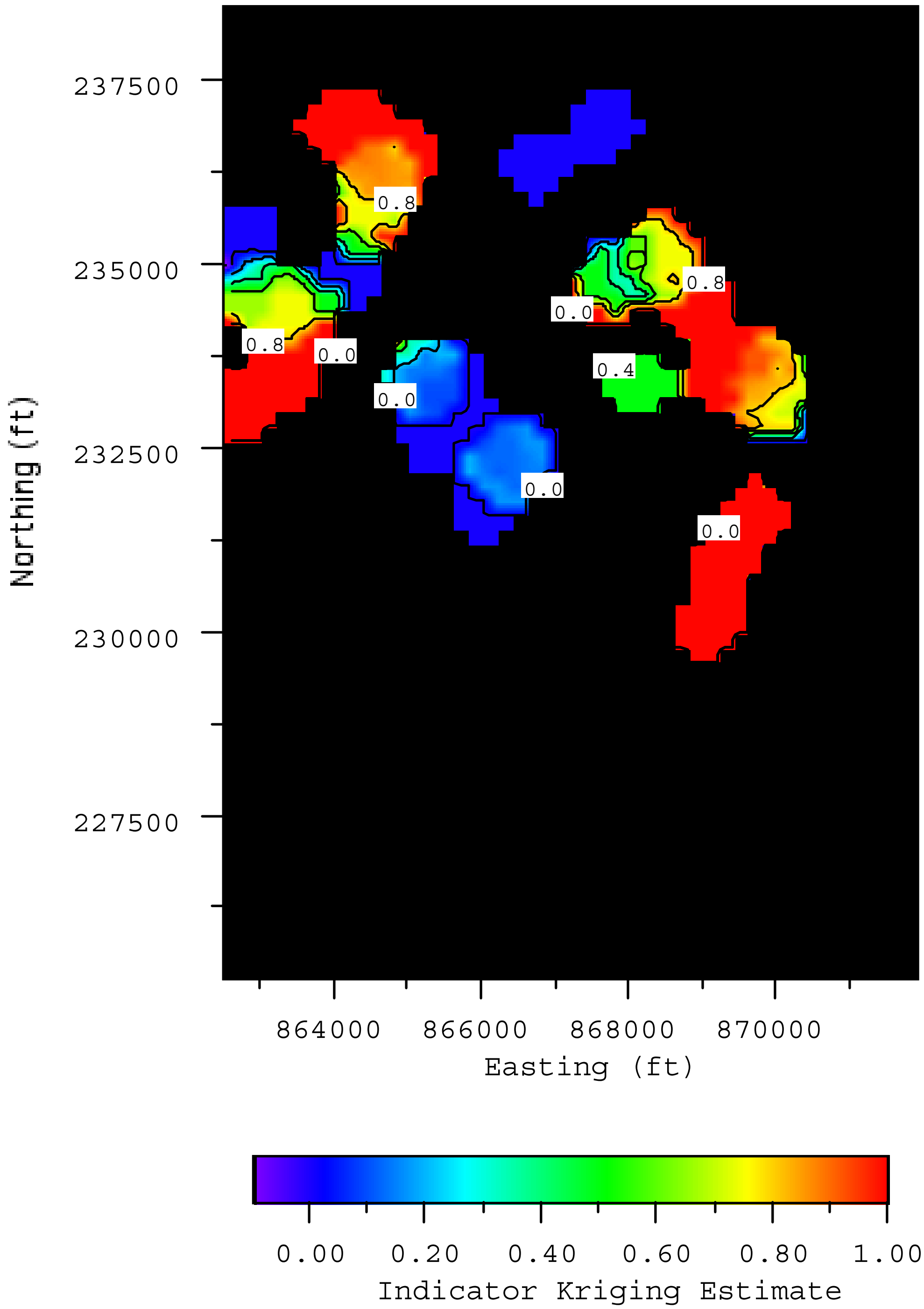

Figure 3-58. PCE IK Estimates, 4th Threshold, Q4 1998 (EBW)

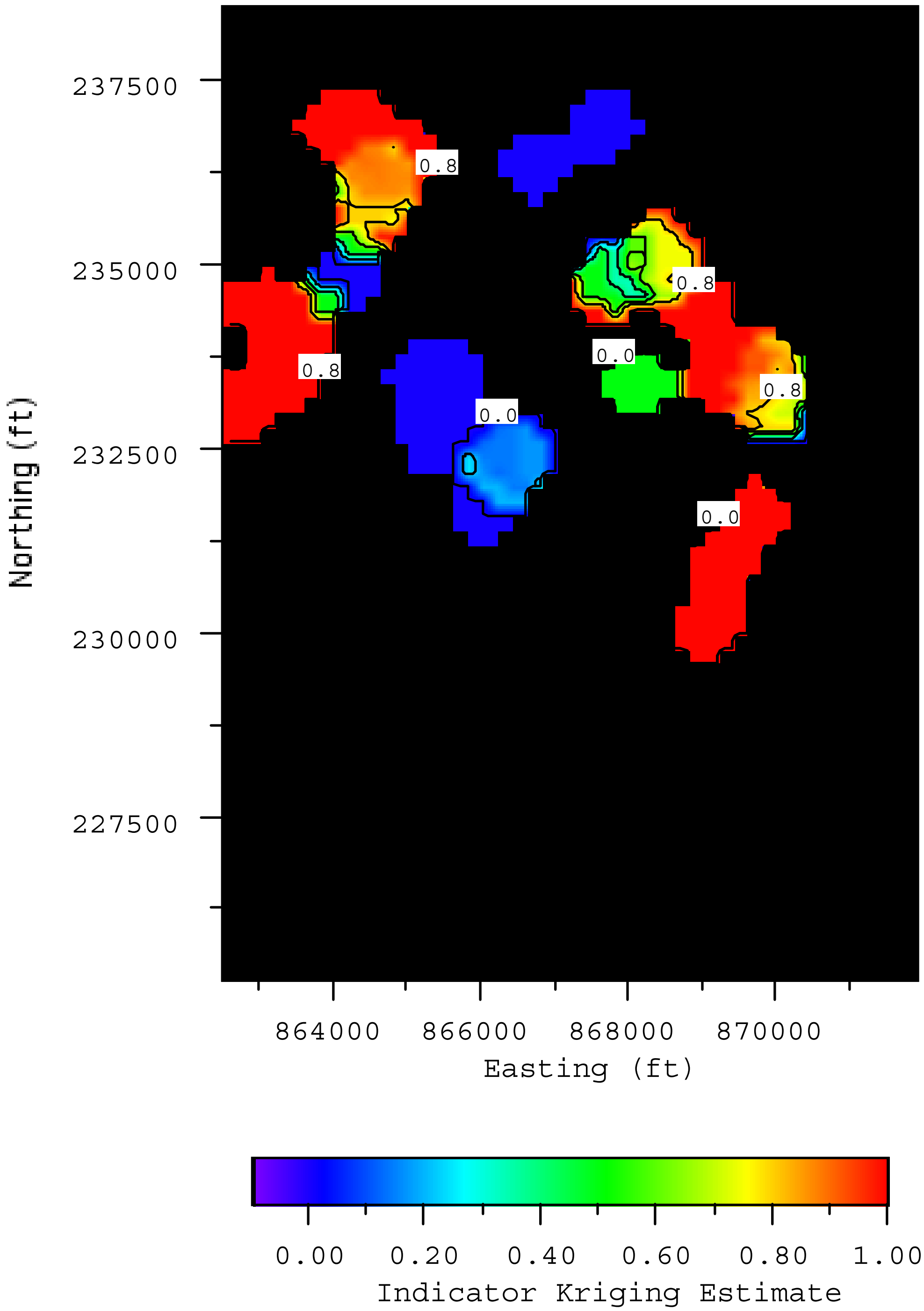

Figure 3-59. PCE IK Estimates, 5th Threshold, Q4 1998 (EBW)

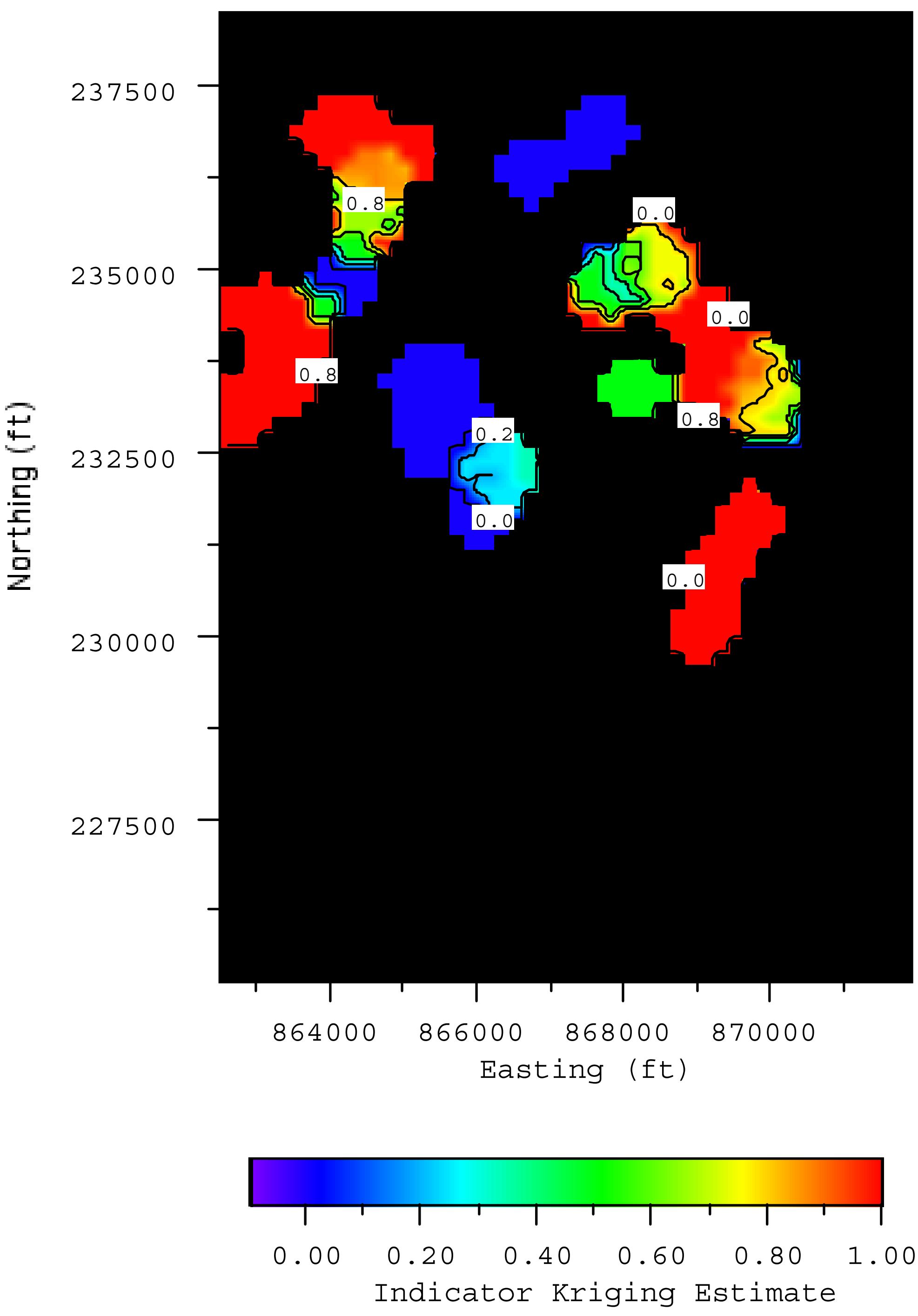

Figure 3-60. PCE IK Estimates, 6th Threshold, Q4 1998 (EBW)